**US Army Corps
of Engineers**
Waterways Experiment
Station

Theoretical Studies of Stress Wave Propagation in Laterally Confined Soils

by *Behzad Rohani*

Approved For Public Release; Distribution Is Unlimited

DTIC QUALITY INSPECTED 4

19990713 145

Prepared for   Defense Threat Reduction Agency

The contents of this report are not to be used for advertising, publication, or promotional purposes. Citation of trade names does not constitute an official endorsement or approval of the use of such commercial products.

The findings of this report are not to be construed as an official Department of the Army position, unless so designated by other authorized documents.

# THEORETICAL STUDIES OF STRESS WAVE PROPAGATION IN LATERALLY CONFINED SOILS

by

B. Rohani

August 1968

U. S. Army Engineer Waterways Experiment Station

CORPS OF ENGINEERS
Vicksburg, Mississippi

US Army Corps
of Engineers
Waterways Experiment
Station

INFORMATION TECHNOLOGY LABORATORY

HEADQUARTERS BUILDING

MAIN ENTRANCE

COASTAL & HYDRAULICS LABORATORY

GEOTECHNICAL LABORATORY

ENVIRONMENTAL LABORATORY

STRUCTURES LABORATORY

FOR INFORMATION CONTACT:
PUBLIC AFFAIRS OFFICE
U.S. ARMY ENGINEER
WATERWAYS EXPERIMENT STATION
3909 HALLS FERRY ROAD
VICKSBURG, MISSISSIPPI 39180-6199
PHONE: (601) 634-2502

SCALE
500   0   500 m

AREA OF RESERVATION : 2.7 sq km

TABLE OF CONTENTS

TABLE OF CONTENTS

PREFACE

The investigations reported herein comprise a collection of pertinent literature applicable to one-dimensional stress wave propagation in soils. The work was performed in connection with research on propagation of ground shock through earth media being conducted by personnel of the Soils Division, WES, for DASA.

The work was accomplished during the period February 1968 through August 1968 under the supervision of Dr. J. S. Zelasko and the general direction of Messrs. W. J. Turnbull, A. A. Maxwell, R. W. Cunny, and J. G. Jackson, Jr., of the Soils Division.

This report was prepared by Mr. B. Rohani and the material contained herein was submitted as a technical paper in partial fulfillment of the requirements administrated in a Civil Engineering graduate course at Texas A&M University, College Station, Texas.

COL John R. Oswalt, Jr., CE, and COL Levi A. Brown, CE, were Directors of the WES during this investigation. Mr. J. B. Tiffany was Technical Director.

This 1999 report is a reprint of a technical paper prepared by the author in 1968 in partial fulfillment of the requirements in a graduate course offered by the Department of Civil Engineering, Texas A&M University, College Station, Texas. The work was performed in connection with research on propagation of ground shock through earth media conducted by members of the staff of the Structures Laboratory (SL), U.S. Army Engineer Waterways Experiment Station (WES), Vicksburg, MS, a complex of five laboratories of the Engineer Research and Development Center (ERDC), for the Defense Threat Reduction Agency, Alexandria, VA.

The work was accomplished by Dr. Behzad Rohani, Geomechanics and Explosion Effects Division (GEED), SL, WES, during February through August 1968 under the supervision of Dr. J. S. Zelasko and the general direction of Messrs. W. J. Turnbull, A. A. Maxwell, R. W. Cunny, and Dr. J. G. Jackson, Jr., GEED. Dr. Bryant Mather was Director, SL, during the publication of this report.

The purpose of the study was to assemble pertinent theoretical literature applicable to one-dimensional stress wave propagation in soils, rewrite the mathematics in detail using consistent notations and terminology, computerize each solution, prepare instructions for each computer program, and to make comparative studies with the various mathematical models for a wave propagation problem. The theoretical developments were documented in a format that can be used for engineering training and self-study and are published for such purposes. The computer programs, based on the technology of the 1960's, are published here for historical and reference purposes.

Commander of ERDC during the publication of this report was COL Robin R. Cababa, EN. This report was published at the WES complex of ERDC.

I

Introduction

A. Background

The first major research concerning the behavior of soils under transient loadings was sponsored by the United States Army Corps of Engineers to aid in the design of underground protective structures. The work was carried out at the Massachusetts Institute of Technology (MIT) under the directions of D. W. Taylor and R. V. Whitman. A brief summary of this work was published by Whitman (1) in 1957; it states

> A hydraulic apparatus and special instrumentation were constructed to test triaxial soil samples. Failure was achieved in times as short as 0.001 second. Curves of compressive strength versus strain rate (rapidity of loading) were determined for cohesive soils, dry sand, and saturated sands. Transient pore-water pressures were recorded during tests on saturated sands.

> Another apparatus was constructed to study wave propagation. Soil samples, 2 in. in diameter and 32 in. long, were struck at one end by a ram. Results for a dry sand were compared with theoretical solutions for the wave propagation problem.

> Other tests were devised to study creep and relaxation phenomena in dry sand, and to study the permeability of saturated sands to pressure gradients applied suddenly.

Whitman compared the results of the wave propagation experiments with the one-dimensional rate-independent plastic wave propagation theory developed by Von Karman and Duwez (see Chapter II, Section -D). The theory did not predict the initial peak stress or spike at the impact end of the sand column (fig. I-1) and he concluded that lateral inertia effects were responsible for the occurrence of the stress peak. In 1961, B. R. Parkin (2) developed a rate-dependent elastic-plastic theory to study

1

one-dimensional stress wave propagation in sand. This theory predicted the occurrence of the impact stress peak of the MIT experiments without considering lateral inertia effects (fig. I-1). Parkin concluded that the initial peak stress was due entirely to interaction of strain-rate sensitivity and static stress-strain properties of the medium with the elastic compliance of the impacting stress gage. Parkin's conclusion aroused much interest and resulted in a symposium (3) on impact waves in sand.

The subject of wave propagation in soils was given much attention after Parkin's work. New advances in nuclear technology and space ventures, in particular, provided considerable impetus towards this effort. Presently (1968) a number of research organizations are working on different phases of the problem with an overall objective of predicting wave propagation phenomena in an in situ soil mass.

B. The problem

The problem to be considered in wave propagation in soils is that of predicting the form and the effect of an input wave after it has propagated through the soil, at a specified point in space and time. In particular, the attenuation of peak stress and particle velocity with depth is of interest. The solution of this problem, like any other boundary value problem, requires a knowledge of:

  a. the equations governing the motion of the soil mass,

  b. the equation of continuity which expresses the conservation of mass,

  c. the constitutive equations which relate stress to strain and strain rate, and

  d. the boundary and initial conditions.

2
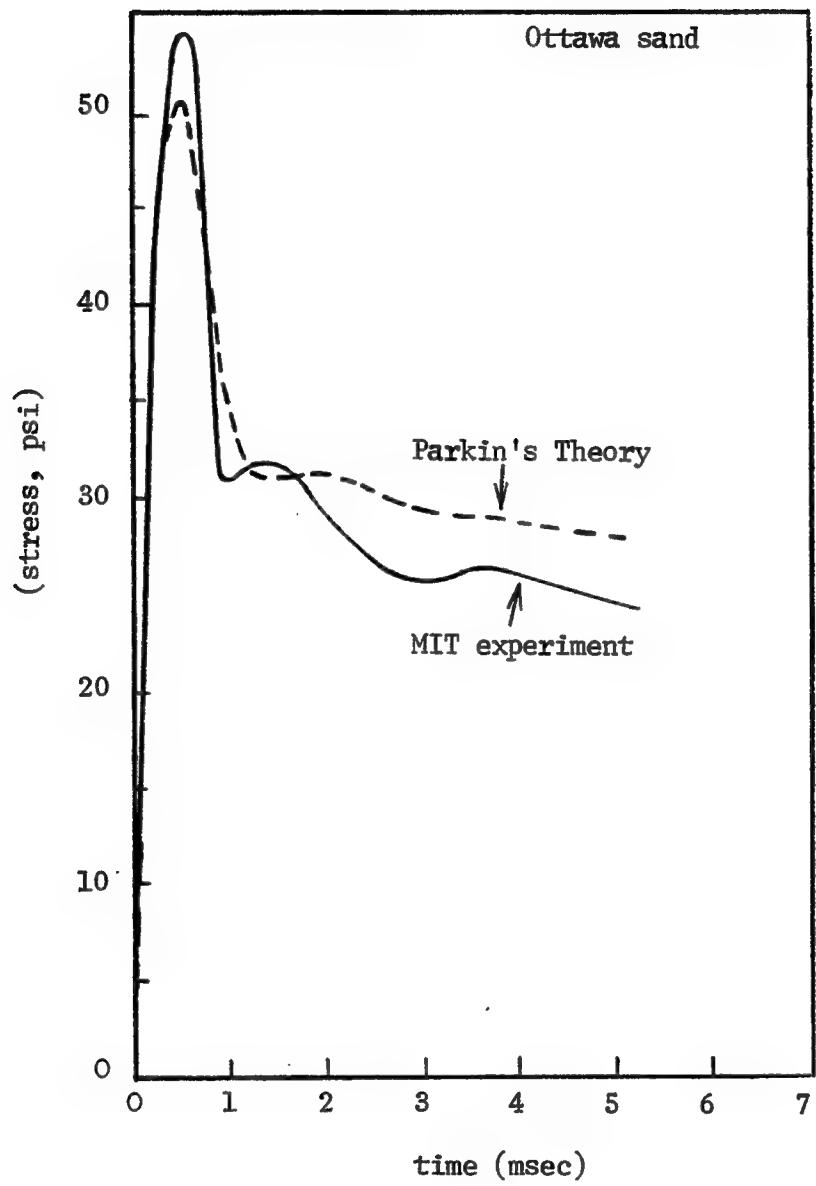
Fig. I-1. Impact stress-time history for Ottawa sand.

3

The solution of the equations of motion with specified boundary and initial conditions and constitutive equations is the solution to the problem. Major difficulties arise when attempts are made to solve such problems for soils. The fact that the stress-strain relations for soils are highly non-linear, hysteretic and rate-dependent makes the task of obtaining an analytical solution a difficult one. The problem becomes even more complicated when one considers the inhomogeneity of in situ soil masses and the fact that a soil medium is not strictly a continuum.

C. Equations of motions and continuity

The equations of motion expressing the equality of applied force and time-rate of change of momentum, neglecting body forces, are given as

$$\rho \frac{\partial \dot{u}_x}{\partial t} = \frac{\partial \sigma_{xx}}{\partial x} + \frac{\partial \sigma_{xy}}{\partial y} + \frac{\partial \sigma_{xz}}{\partial z}$$

$$\rho \frac{\partial \dot{u}_y}{\partial t} = \frac{\partial \sigma_{yx}}{\partial x} + \frac{\partial \sigma_{yy}}{\partial y} + \frac{\partial \sigma_{yz}}{\partial z} \qquad\qquad \text{I-1}$$

$$\rho \frac{\partial \dot{u}_z}{\partial t} = \frac{\partial \sigma_{zx}}{\partial x} + \frac{\partial \sigma_{zy}}{\partial y} + \frac{\partial \sigma_{zz}}{\partial z}$$

where

ρ is the mass density of the material,

$\dot{u}_x$, $\dot{u}_y$, $\dot{u}_z$ are the velocity components in the x , y , and z Cartesian directions respectively, and

σ_{xx} , σ_{xy} , σ_{xz} , σ_{yx} , etc., are components of the stress tensor in Cartesian coordinates.

These equations of motion will hold, irregardless of the stress-strain behavior of the medium.

4

The equation of continuity expressing the conservation of mass in Cartesian coordinates is given by

$$\frac{d\rho}{dt} + \rho\left(\frac{\partial \dot{u}_x}{\partial x} + \frac{\partial \dot{u}_y}{\partial y} + \frac{\partial \dot{u}_z}{\partial z}\right) = 0 \qquad \text{I-2}$$

Equations I-1 and I-2 are 4 equations in 10 unknowns (6 stress components, 3 velocity components, and the mass density of the medium). To solve Equations I-1 and I-2 six additional equations are needed. These additional equations must be obtained from the constitutive relations of the material.

D. Constitutive relations

Constitutive relations are equations which relate in some manner the respective components of the stress and strain tensors. These relations must be determined from property tests conducted on samples of the material of interest to measure the appropriate material properties. For a linearly elastic, isotropic and homogeneous material only two constants are needed to completely formulate the constitutive equations. These constants can be determined by performing appropriate property tests. The most conventional property test is the simple tension test from which both Young's modulus of elasticity, E, and Poisson's ratio, ν, can be obtained. These constants are related to other elastic material parameters as follows:

$$M = \frac{E(1 - \nu)}{(1 + \nu)(1 - 2\nu)} = \frac{3K(1 - \nu)}{(1 + \nu)} = \frac{2G(1 - \nu)}{(1 - 2\nu)} \qquad \text{I-3}$$

where

   M is the constrained modulus of elasticity

5

K is the bulk modulus of elasticity

G is the shear modulus

The constitutive equations for a linearly elastic, isotropic and homogeneous material can be written in terms of any two of these elastic constants. In terms of Young's modulus and Poisson's ratio, these equations are given by

$$\sigma_{xx} = \frac{E}{(1 - 2\nu)(1 + \nu)} \left[(1 - \nu)\ \epsilon_{xx} + \nu\ (\epsilon_{yy} + \epsilon_{zz})\right]$$

$$\sigma_{yy} = \frac{E}{(1 - 2\nu)(1 + \nu)} \left[(1 - \nu)\ \epsilon_{yy} + \nu\ (\epsilon_{xx} + \epsilon_{zz})\right]$$

$$\sigma_{zz} = \frac{E}{(1 - 2\nu)\ (1 + \nu)} \left[(1 - \nu)\ \epsilon_{zz} + \nu\ (\epsilon_{xx} + \epsilon_{yy})\right]$$

$$\sigma_{xy} = \frac{E}{2(1 + \nu)}\ \epsilon_{xy}$$

$$\sigma_{xz} = \frac{E}{2(1 + \nu)}\ \epsilon_{xz}$$

$$\sigma_{yz} = \frac{E}{2(1 + \nu)}\ \epsilon_{yz}$$

I-4

where

ϵ_{xx} , ϵ_{xy} , ϵ_{xz} , ϵ_{yx} , etc., are components of the strain tensor in Cartesian coordinates.

Stress-strain relations for soils are not unique and in general they assume a variety of forms depending upon many factors such as state of stress, previous stress history, rate of loading, degree of saturation, etc. Unlike the linear elastic material, each property test for soils will yield a highly non-linear relation between the appropriate stress and strain components. There are no representative equations that can

6

completely relate these components in a rigorous manner as is done in the classical theory of linear elasticity (equation I-4).

In order to minimize rate effects, soil property tests for dynamic problems should be conducted at rates appropriate to the type of dynamic problem investigated. Two types of dynamic soil property tests currently in use are the uniaxial strain test (fig. I-2) and the triaxial compression test (fig. I-3). Radial symmetry is established in both of these tests. The slope of the uniaxial strain test defines the constrained modulus M while the slope of the triaxial compression test curve defines the shear modulus G where radial strain is known. The complexity of formulating constitutive equations for soils is illustrated by the diverse nature property test results.

E. <u>Boundary loads</u>

The dynamic boundary loads which are of interest in wave propagation studies in soils are shown in fig. I-4. These loads may be generated by explosions or vibrating machinery. Fig. I-4a depicts a typical overpressure-distance curve resulting from a nuclear explosion. This type of loading is probably the most complicated boundary load that has to be dealt with in solving a dynamic problem. The fact that the velocity of the traveling shock wave changes as it moves away from ground zero is a major component of the complexity of this problem.

Fig. I-4b shows a single pulse characterized by a peak stress at the shock front and an exponentially decaying behavior thereafter. This type of loading may be generated by a single charge explosion.

A steady-state type input generated by vibrating machinery is shown
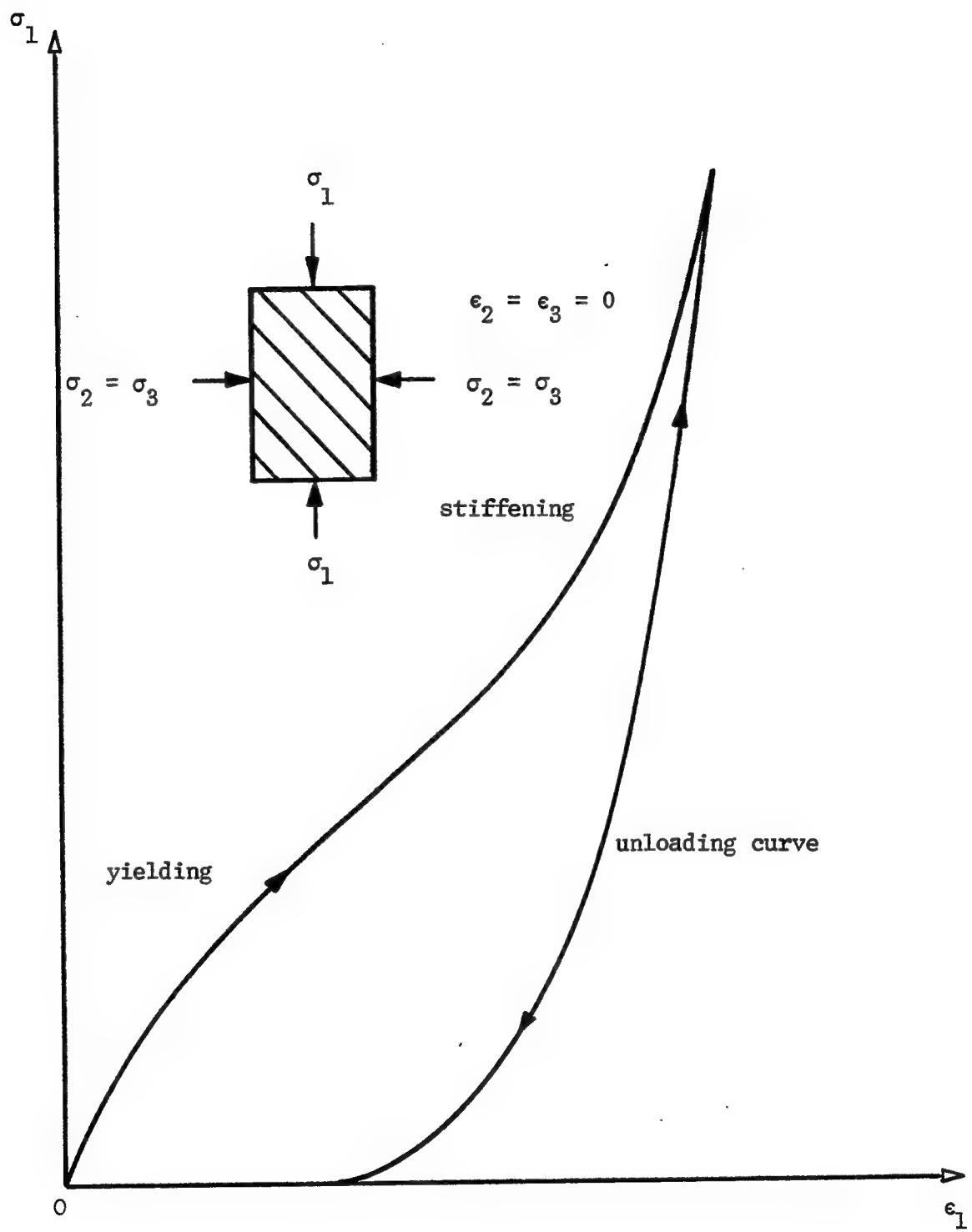
Fig. I-2. Typical load-unload stress-strain curve for soils in uniaxial strain.
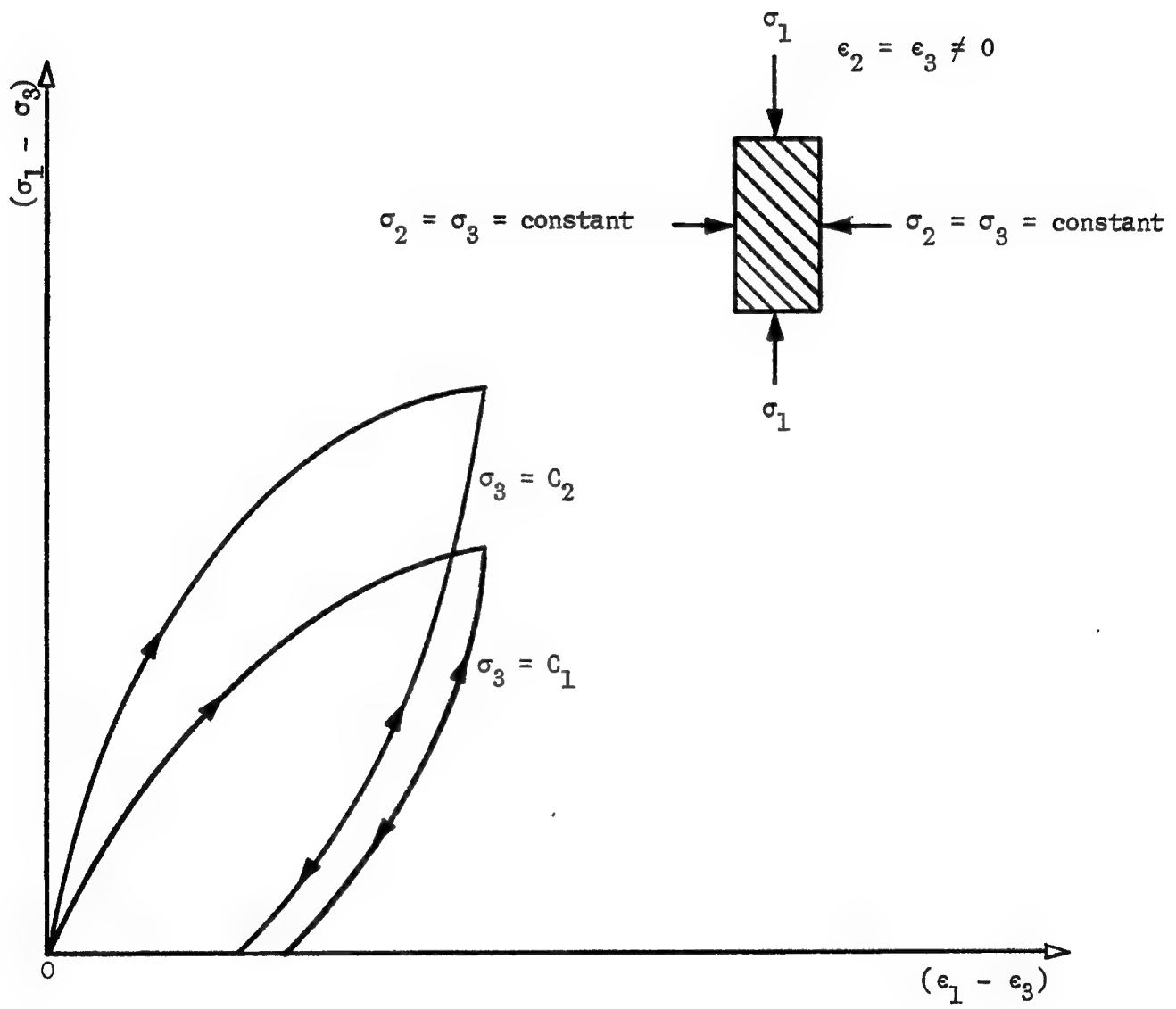
Fig. I-3. Typical load-unload stress-strain curves for soils in triaxial compression.

Envelope of peak
overpressure–distance

Ground
Zero

distance

(a) Traveling shock waves due to nuclear detonation

Peak overpressure

time

(b) Single pulse loading

Pressure

time

(c) Steady-state pressure on a vibrating foundation
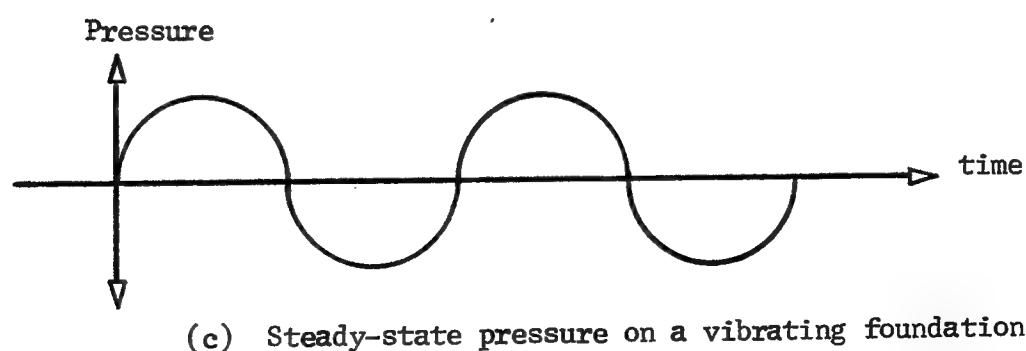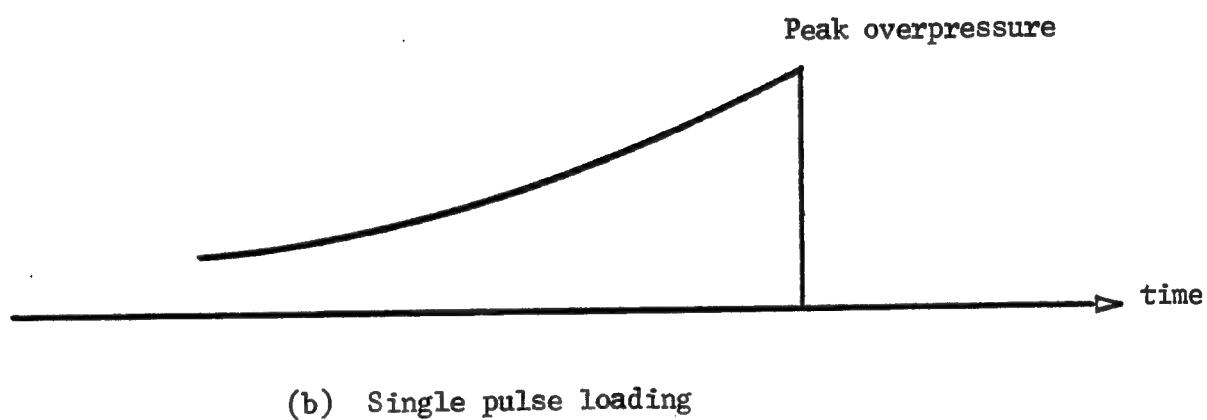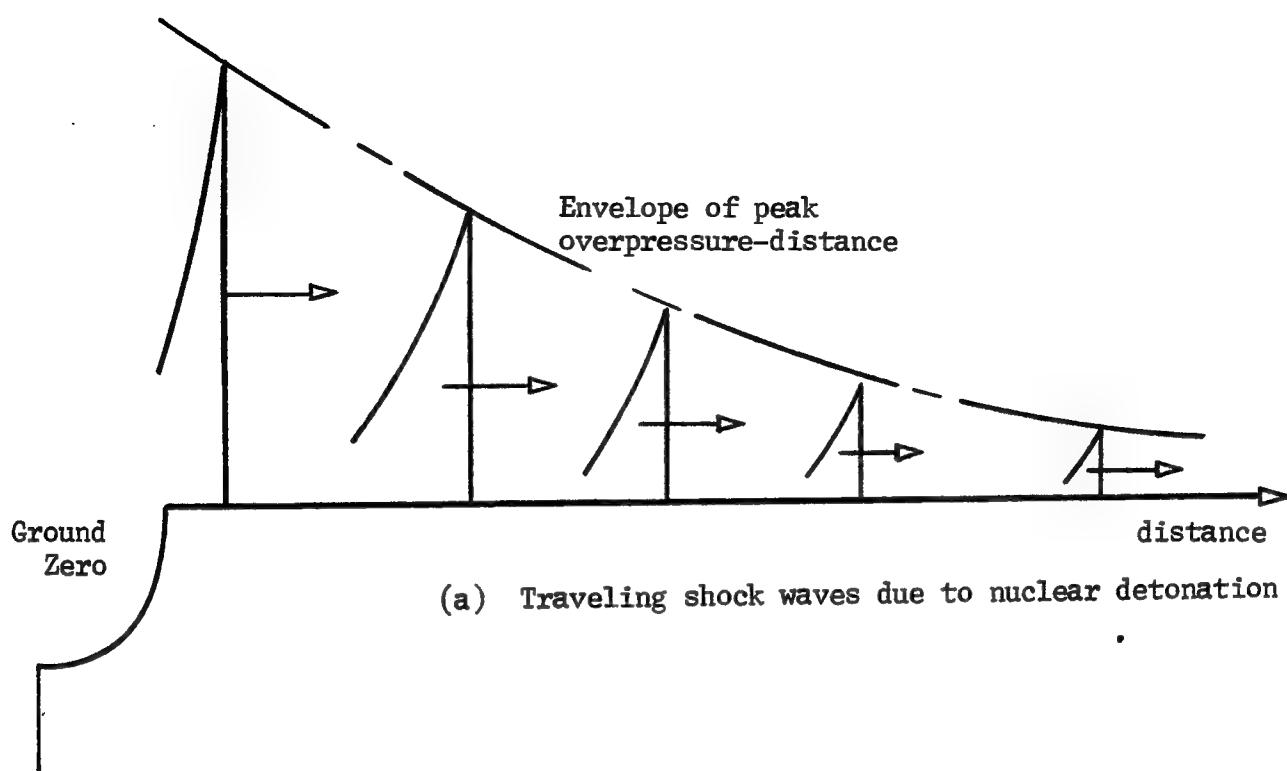
Fig. I-4. Typical boundary loads.

in fig. I-4c. This type of loading is usually of low amplitude and relatively long duration.

F. Scope of the present study

In this study, the response of a semi-infinite homogeneous body of soil due to a time-dependent pressure wave applied at the free surface of the medium is to be studied. The loading is assumed to be applied uniformly over the entire surface of the medium. Under this assumption, one-dimensional geometry is obtained, i.e., there are no lateral deformations and the equations of motion (equation I-1) and continuity (equation I-2) simplify as follows:

$$\rho \frac{\partial \dot{u}}{\partial t} = \frac{\partial \sigma}{\partial z} \qquad\qquad \text{I-5}$$

$$\frac{d\rho}{dt} + \rho \frac{\partial \dot{u}}{\partial z} = 0 \qquad\qquad \text{I-6}$$

The subscripts have been dropped since only vertical components are to be considered.

The stress-strain relation required by the one-dimensional geometry is the uniaxial strain relation (fig. I-2). This relation is not unique and there are a number of regions in this curve in which different types of material behavior are dominate. For example, for dry cohesionless materials, during the early stages of loading, the stress-strain curve may be concave downward reflecting a rearrangement of particles. As the load is increased the particles begin to lock together and the strains that take place are due primarily to the deformation of the particles at the points of contact. As the stress continues to increase, the contact forces become so large that the particles begin to crush. As the stress is

11

further increased, the particles lock again and the curve becomes concave
to the stress axis with the particles smaller and more angular than
before resulting in a progressively higher modulus. During unloading,
the curve exhibits a higher modulus than the loading curve and permanent
strain occurs. For cohesive soils, rate-dependency is also a factor to
be considered in utilizing the stress-strain relation of fig. I-2.

To overcome the mathematical difficulties in the solution to these
problems, real soil stress-strain response may be idealized by various
linear and/or nonlinear hysteretic approximations as shown in fig. I-5.
A considerable body of scientific literature on one-dimensional stress
wave propagation for such models has been published in recent years by
various researchers both in the United States and abroad. It was the aim
of this study to assemble all pertinent literature applicable to wave
propagation in soils, rewrite the mathematics in detail, computerize each
solution, prepare operating instructions for each computer program, and to
make comparative studies with the various models for a wave propagation
problem. In Chapter II, the elements of elastic, plastic, visco-elastic
and shock-wave propagation are reviewed in detail as a background for the
remainder of the report.
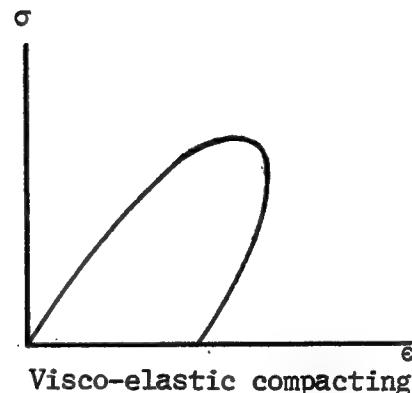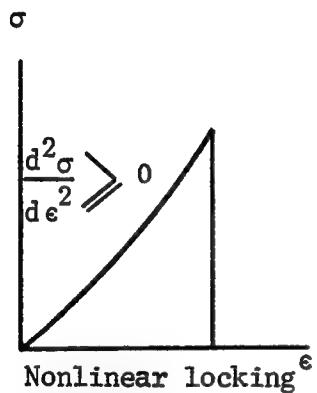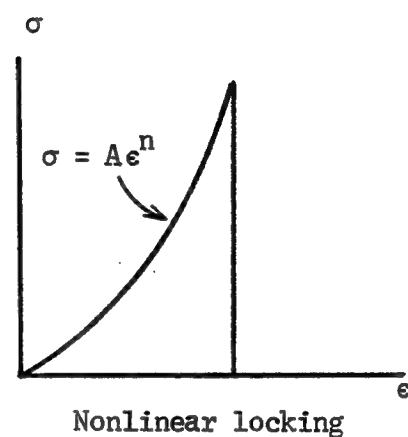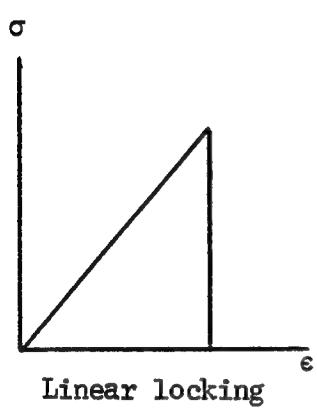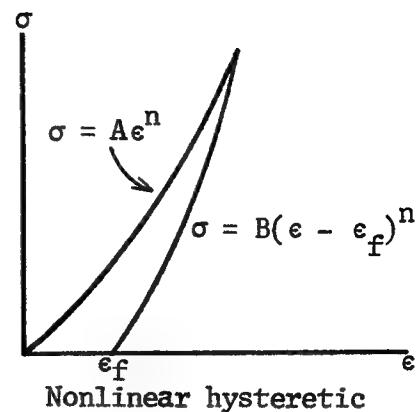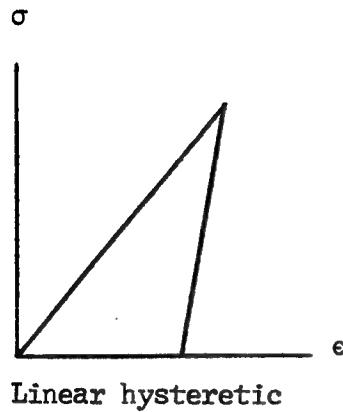
Fig. I-5. Idealized stress-strain curves for soils
in uniaxial state of strain.

13

Elements of One-Dimensional
Stress Wave Propagation

A. Historical background

Interest in the theory of propagation of longitudinal waves dates
from the 17th century when Newton attempted to solve the problem of sound
wave propagations, a solution finally completed by Lord Rayleigh in the
19th century (4). Much of the theory in this period was developed for
materials with highly idealized stress-strain relations. The theory of
propagation of longitudinal waves in elastic bars is presented in a
number of publications (5). The solution for this case is virtually
complete if the lateral inertial forces are negligible. Pochhammer solved
the problem considering lateral inertia for a cylindrical bar (6). Stress
wave propagation in visco-elastic materials has been studied by Kolsky (5)
and Morrison (7) for linear visco-elastic materials. An excellent summary
of one-dimensional wave propagation theory for standard models of visco-
elasticity as well as three and four parameters models is given by Kolsky
(1963). The first development of plastic wave propagation theory is
credited to Donnell (8). He suggested that if the stress-strain curve for
a plastic material could be approximated by two straight lines, then the
time history of a wave propagating through that material can be deduced by
superposition of the time histories of the two elastic waves. The com-
plete theory of one-dimensional plastic wave propagation was developed
during the Second World War. Solutions were obtained independently by
Von Karman (9), Taylor (10), and Rokhmatulin (11). The theory was later
extended by White and Griffis (12) to handle both plastic and shock wave

propagation and by Malvern to handle materials which exhibit strain rate
effects (13).

B. Longitudinal elastic waves

In the simple theory of longitudinal wave propagation (no lateral
strain) it is assumed that plane cross sections remain plane; only axial
stresses are considered, being uniformly distributed over the cross section
(fig. II-1). The cross-sectional area of the element is denoted by A ,
the thickness by dz and the mass density by ρ . The displacement of the
element in z direction is given by u . Newton's second law of motion
for the element of fig. II-1 gives

$$-\rho \; A \; dz \; \frac{\partial^2 u}{\partial t^2} = - A \; \sigma + A\left(\sigma + \frac{\partial \sigma}{\partial z} \; dz\right) \qquad \text{II-1}$$

or

$$\rho \; \frac{\partial^2 u}{\partial t^2} = - \frac{\partial \sigma}{\partial z} \qquad \text{II-2}$$

where σ is the axial compressive stress. For infinitesimal strain, the
equation of continuity in the one-dimensional case reduces to the defini-
tion of strain

$$\epsilon = - \frac{\partial u}{\partial z} \qquad \text{II-3}$$

where ϵ is the axial compressive strain. The constitutive relation for
an elastic medium with no lateral motion allowed is given by

$$\sigma = M_o \; \epsilon \qquad \text{II-4}$$

where M_o is the constrained modulus of elasticity. M_o is related to

P(t)

σ

dz

$\sigma + \frac{\partial \sigma}{\partial z} dz$

z

Stresses on an
element of the
medium

Medium property

M_o, ρ
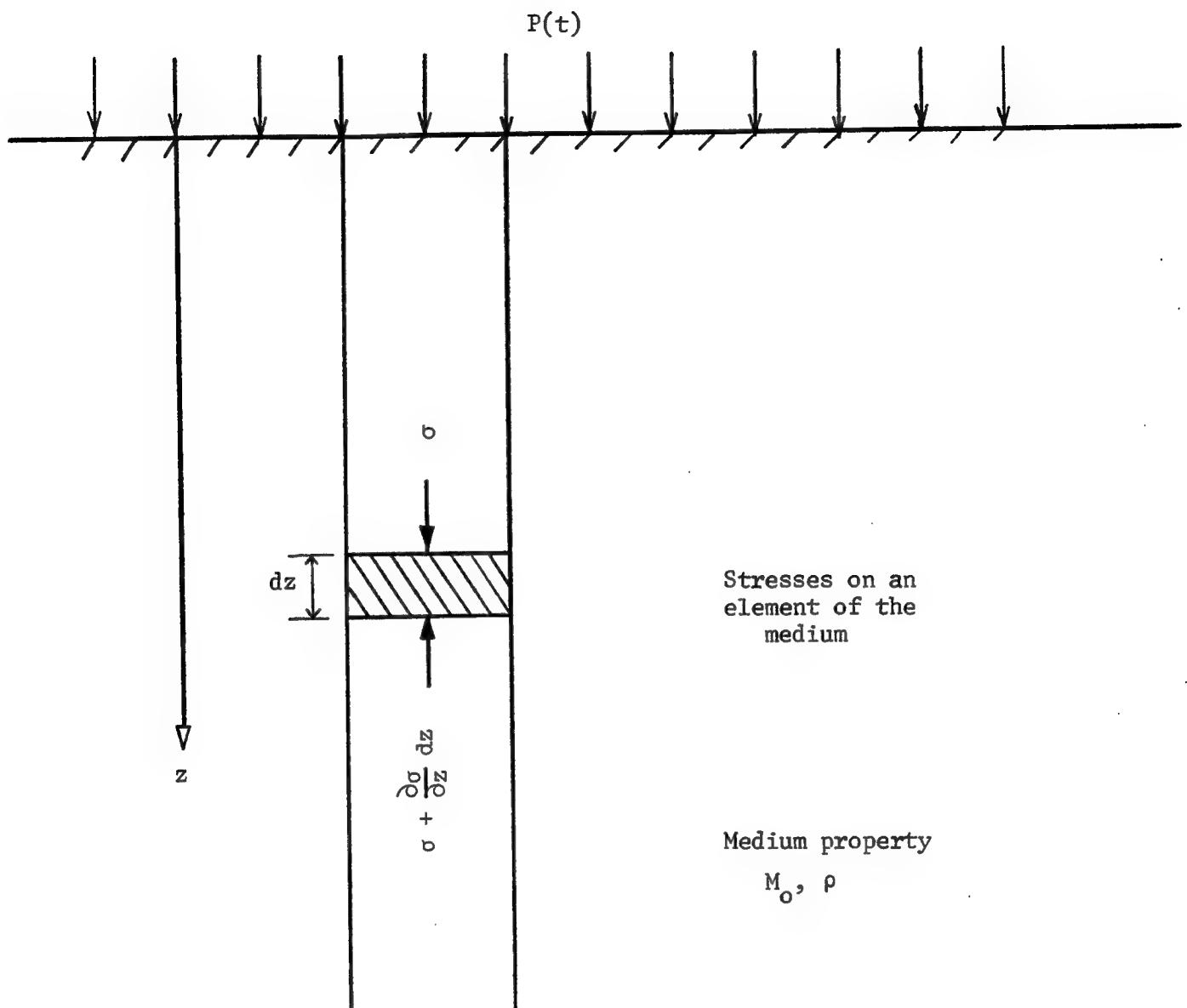
Fig. II-1. One-dimensional wave propagation.

Lame's constants λ and μ or to Young's modulus E and Poisson's ratio ν as follows

$$M_o = \lambda + 2\mu = \frac{E(1 - \nu)}{(1 + \nu)(1 - 2\nu)} \qquad \text{II-5}$$

Substituting equation II-3 in equation II-4 and differentiating with respect to the space variable results in

$$-\frac{\partial \sigma}{\partial z} = M_o \frac{\partial^2 u}{\partial z^2} \qquad \text{II-6}$$

The substitution of equation II-6 into equation II-2 yields the well known equation

$$\frac{\partial^2 u}{\partial t^2} = C_o^2 \frac{\partial^2 u}{\partial z^2} \qquad \text{II-7}$$

where C_o is the propagation velocity of longitudinal waves

$$C_o = \sqrt{\frac{M_o}{\rho}} = \sqrt{\frac{E(1 - \nu)}{\rho(1 + \nu)(1 - 2\nu)}} \qquad \text{II-8}$$

The general solution of equation II-7 is of the form

$$u = f\left(t - \frac{z}{C_o}\right) + g\left(t + \frac{z}{C_o}\right) \qquad \text{II-9}$$

This solution represents the sum of two traveling waves. The first term represents a wave traveling in the positive z direction, and the second term represents a wave traveling in the negative z direction. For a medium of infinite extent where the waves travel only in the positive z direction the solution is given by

$$u = f\left(t - \frac{z}{C_o}\right) \qquad \text{II-10}$$

17

Differentiating both sides of equation II-10 with respect to z and t, respectively, gives

$$\frac{\partial u}{\partial z} = - \frac{1}{C_o} f'\left(t - \frac{z}{C_o}\right) \qquad\qquad \text{II-11}$$

$$\frac{\partial u}{\partial t} = f'\left(t - \frac{z}{C_o}\right) \qquad\qquad \text{II-12}$$

where f' denotes differentiation with respect to the argument $\left(t - \frac{z}{C_o}\right)$, $\frac{\partial u}{\partial t}$ is the particle velocity $\dot{u}$. Combining equations II-11 and II-12 gives

$$\frac{\partial u}{\partial t} = - C_o \frac{\partial u}{\partial z} \qquad\qquad \text{II-13}$$

Using the definition of strain (equation II-3)

$$\dot{u} = C_o \epsilon \qquad\qquad \text{II-14}$$

Substituting for strain from equation II-4

$$\sigma = \frac{M_o}{C_o} \dot{u} = \rho C_o \dot{u} \qquad\qquad \text{II-15}$$

Equation II-14 relates particle velocity and strain; equation II-15 relates particle velocity and stress.

The function $f\left(t - \frac{z}{C_o}\right)$ must be evaluated from the boundary conditions. At $z = 0^-$

$$\sigma(0,t) = P(t) \qquad\qquad \text{II-16}$$

where $P(t)$ is a known arbitrary input pressure. A convenient time parameter, defined by

$$t^* = \left(t - \frac{z}{C_o}\right) \qquad\qquad \text{II-17}$$

18

is usually used to adjust the real time at the surface, by the factor $\frac{z}{C_o}$,
to account for the travel time of the wave to the point of interest.

Substituting equation II-12 for particle velocity into equation II-15
and utilizing equation II-17 gives

$$\sigma = \rho C_o f' \left(t - \frac{z}{C_o} \right) = \rho C_o f'(t*) \qquad \text{II-18}$$

conditions at the boundary, equation II-16, require that

$$\rho C_o f'(t*) = P(t*) \qquad \text{II-19}$$

where $P(t*)$ is the surface overpressure at time $t = t*$. An expression
for $f'\left(t - \frac{z}{C_o} \right)$ can then be derived from equation II-19.

The expressions for stress, strain, and particle velocity, in terms
of the surface overpressure are given by

$$\sigma = P(t*)$$

$$\epsilon = P(t*) / \rho C_o^2 \qquad \text{II-20}$$

and

$$\dot{u} = P(t*) / \rho C_o$$

Equation II-20 demonstrates that there is a linear relation between the
three given wave-form parameters and the surface overpressure $P(t)$,
and that for conditions of one-dimensional wave propagation in an elastic
homogeneous medium an unaltered wave form propagates through the
medium.

The acceleration at a point can be determined from equation II-20 by
differentiating the expression for particle velocity

19

$$\frac{\partial^2 u}{\partial t^2} = \frac{1}{\rho C_o} \frac{d}{dt}\left[P(t*)\right]$$
II-21

Equation II-21 demonstrates that the acceleration depends on the time rate of change of the surface overpressure.

The absolute displacement of a point, at time, t_a , can be obtained by integration of equation II-20 for particle velocity

$$u = \frac{1}{\rho C_o} \int_0^{t_a} P(t*) \, dt$$
II-22

The integral

$$\int_0^{t_a} P(t*) \, dt$$

in equation II-22 is the input impulse (area under the surface overpressure-time curve) between the times $t = \frac{z}{C_o}$ and $t = t_a$.

C. Longitudinal elastic waves in layered elastic media

Consider the semi-infinite body of fig. II-2 made up of two elastic media with different properties separated by a plane interface. The properties in the two layers are subscripted o and 1 . A wave in the first layer incident to the interface is given by equation II-10

$$u = f\left(t - \frac{z}{C_o}\right)$$
II-10

The corresponding incident stress, σ_i , is given by equation II-18

$$\sigma_i = \rho_o C_o f'\left(t - \frac{z}{C_o}\right)$$
II-18

At the interface a reflected wave will form and travel in the negative z

20

Time

t

P(t)

0

σ_i

C_o

1

σ_r

Layer 1

ρ_o, C_o

Layer 2

ρ_1, C_1

C_1

1

σ_t

Depth

z
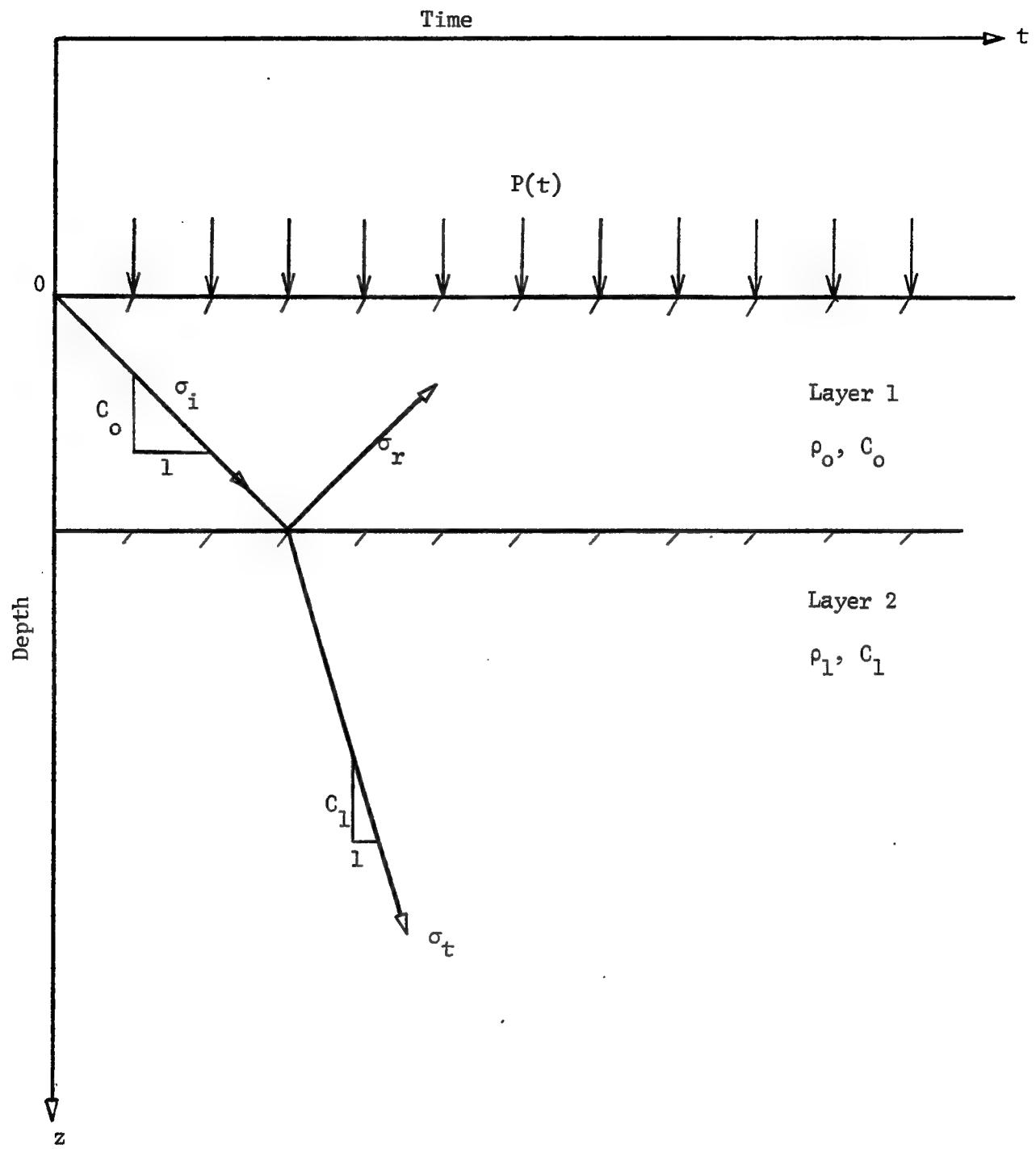
Fig. II-2. Reflection and transmission of a wave at a boundary.

21

direction in layer 1.   The reflected wave is given by the second term of
equation II-9

$$u = g\left(t + \frac{z}{C_o}\right) \qquad\qquad \text{II-9}$$

The reflected stress wave is given as

$$\sigma_r = -\,\rho_o C_o g'\left(t + \frac{z}{C_o}\right) \qquad\qquad \text{II-23}$$

A transmitted wave

$$u = h\left(t - \frac{z}{C_1}\right) \qquad\qquad \text{II-24}$$

will also form at the interface and will travel in the positive z direc-
tion in layer 2.   The transmitted stress wave is given as

$$\sigma_t = \rho_1 C_1 h'\left(t - \frac{z}{C_1}\right) \qquad\qquad \text{II-25}$$

The corresponding particle velocities for the incident, the reflected and
transmitted waves, from equation II-18, are respectively

$$f'\left(t - \frac{z}{C_o}\right) = \frac{\sigma_i}{\rho_o C_o} \qquad\qquad \text{II-26}$$

$$g'\left(t + \frac{z}{C_o}\right) = \frac{-\sigma_r}{\rho_o C_o} \qquad\qquad \text{II-27}$$

$$h'\left(t - \frac{z}{C_1}\right) = \frac{\sigma_t}{\rho_1 C_1} \qquad\qquad \text{II-28}$$

There are two distinct conditions which must be satisfied on both
sides of the interface

(a) For equilibrium

$$\sigma_i + \sigma_r = \sigma_t \qquad\qquad\qquad \text{II-29}$$

(b) For compatibility of particle velocity

$$\frac{\sigma_i}{\rho_o C_o} - \frac{\sigma_r}{\rho_o C_o} = \frac{\sigma_t}{\rho_1 C_1} \qquad\qquad \text{II-30}$$

The negative sign in front of the reflected particle velocity is due to
the fact that its direction is in the negative z direction. Substituting
for $\sigma_r = \sigma_t - \sigma_i$ from equation II-29 in equation II-30 and solving for
σ_t gives

$$\sigma_t = 2\sigma_i \left(\frac{\rho_1 C_1}{\rho_o C_o + \rho_1 C_1} \right) \qquad\qquad \text{II-31}$$

Substituting for σ_t in equation II-31 from equation II-29 and solving
for σ_r gives

$$\sigma_r = \sigma_i \left(\frac{\rho_1 C_1 - \rho_o C_o}{\rho_o C_o + \rho_1 C_1} \right) \qquad\qquad \text{II-32}$$

Interesting conclusions can be drawn from equations II-31 and II-32 re-
garding the nature of the reflected and transmitted waves at the inter-
face. For instance, at a free surface, $\rho_1 C_1 = 0$. From equation II-31,
$\sigma_t = 0$; there is no transmitted wave. From equation II-32, $\sigma_r = -\sigma_i$;
the reflected wave is equal in magnitude to the incident wave, but opposite
in sign. Thus, a compressive wave is reflected as a tensile wave at a free
boundary. At a rigid boundary, $\rho_1 C_1 = \infty$. From equation II-32, the re-
flected wave $\sigma_r = \sigma_i$; the reflected wave is equal in sign and magnitude

to the incident wave. Therefore, at a rigid boundary the stresses are doubled.

In general, from equation II-32, if $\rho_o c_o > \rho_1 c_1$, a compressive wave is reflected as a tensile wave. If, on the other hand, $\rho_o c_o < \rho_1 c_1$, a compressive wave is reflected as a compressive wave.

D. Propagation of plastic waves in strain-rate independent media

The first development of plastic wave propagation was published by Donnell (8) in 1930. Donnell suggested the use of the principle of superposition if the stress-strain curve for a plastic material can be approximated by two straight lines. Consider the plastic stress-strain curve and its approximation in fig. II-3a. If a step pulse of stress σ_o is applied on the surface of a semi-infinite body having such a linearized stress-strain curve, the step pulse will propagate into the body with a velocity

$$C_o = \sqrt{M_o/\rho} \qquad \qquad \text{II-33}$$

as shown in fig. II-3b. If a second step pulse of stress σ_1 is super-imposed on the body it will propagate with a velocity

$$C_1 = \sqrt{M_1/\rho} \qquad \qquad \text{II-34}$$

Thus, at some time, t, the front of the wave $\sigma < \sigma_o$ would have traveled to a position

$$z_1 = C_o t \qquad \qquad \text{II-35}$$

while the remainder of the wave $\sigma > \sigma_o$ would have traveled only to a position

24

$\sigma_o + \sigma_1$

σ_o

Stress

C_1

1

C_o

1

O

Strain

(a)

(b)

Stress

C_1

C_o

z

$C_1 t$

$C_o t$
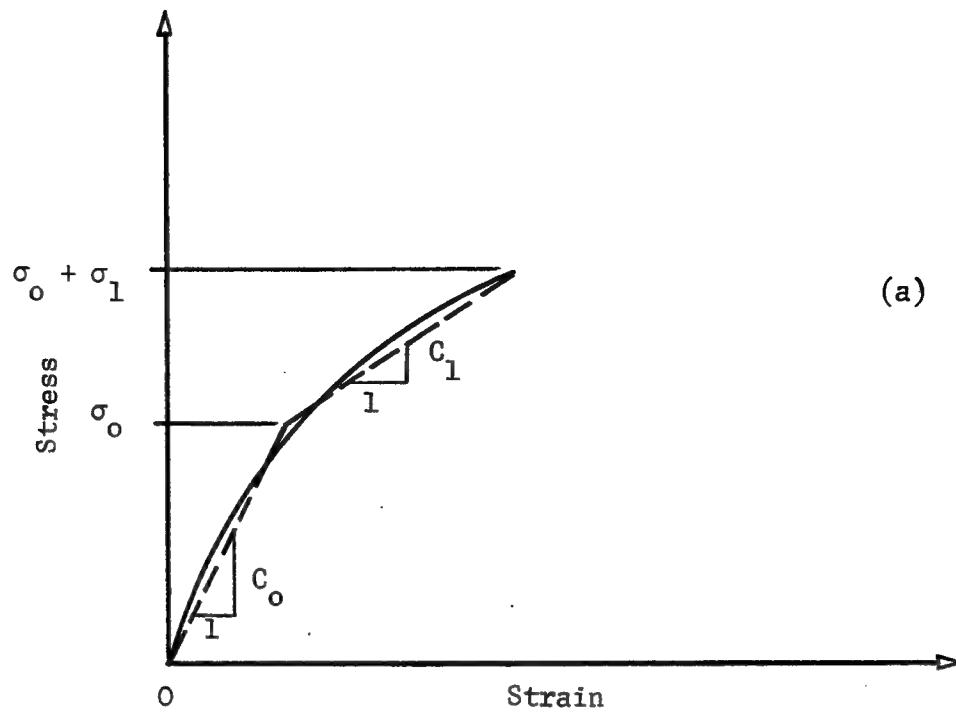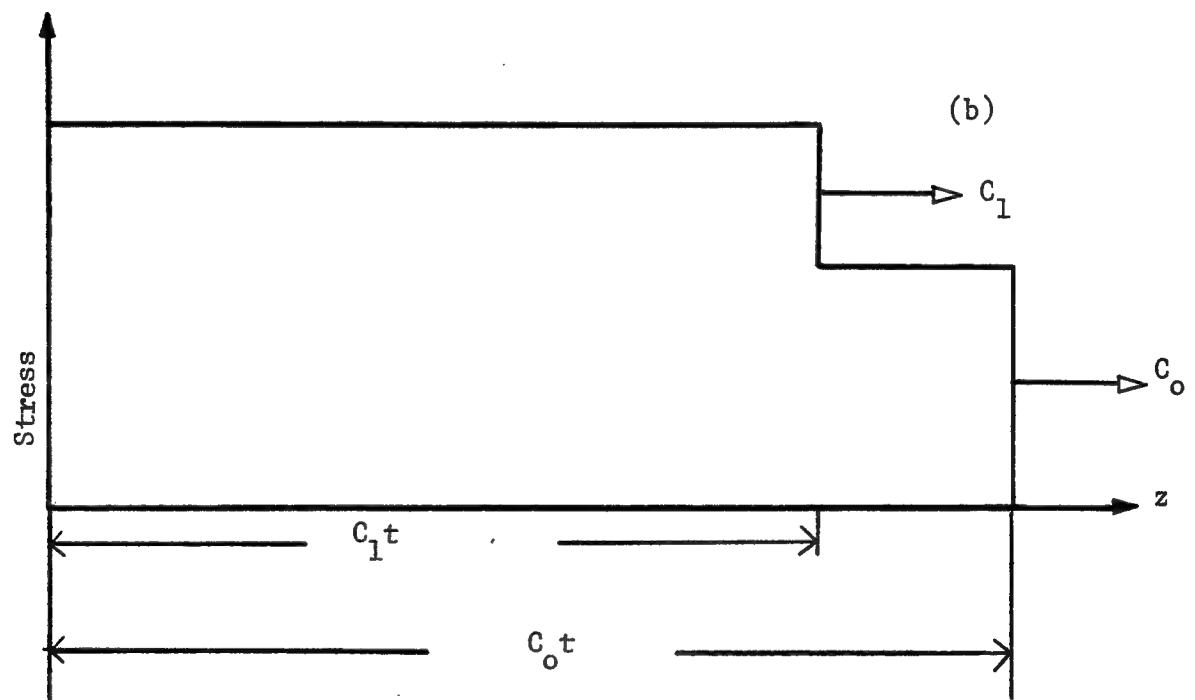
Fig. II-3. Donnell's approximation of plastic wave propagation.

25

$$z_2 = C_1 t$$

as shown in fig. II-3b. Donnell's development simply indicates that if the two stress pulses were applied simultaneously, the action would have been the same and the wave front would have the appearance shown in fig. II-3b. Thus, from Donnell's deductions, one would expect the higher stress levels (for the real plastic stress-strain curve) to travel at lower velocities. The gap $(C_0 t - C_1 t)$ between the two wave fronts, fig. II-3b, would increase with time and the sharp-fronted stress pulse would rapidly become softened. Obviously, stresses greater than the yield stress would not propagate in a plastic medium. From the above reasoning, one would expect that the wave front corresponding to the simultaneous action of two-step waves σ_0 and σ_1 on the surface of a medium having a stress-strain curve such as the one shown in fig. II-4a would have the form shown in fig. II-4b. The mathematical solution of plastic wave propagation obtained by Von Karman and others during the Second World War verifies the correctness of Donnell's superposition approach as will be shown subsequently.

Consider a semi-infinite body extending from $z = 0$ to $z = \infty$, having a unique stress-strain curve which is plastic in character or concave to the strain axis, as shown in fig. II-5. The stress-strain curve can be given as

$$\sigma_P = \sigma_P(\epsilon_P) \qquad \text{II-37}$$

where the subscript P indicates that the curve is concave to the strain axis, or "plastic." The problem being one-dimensional, the equations of motion and continuity from the previous section are given as

26
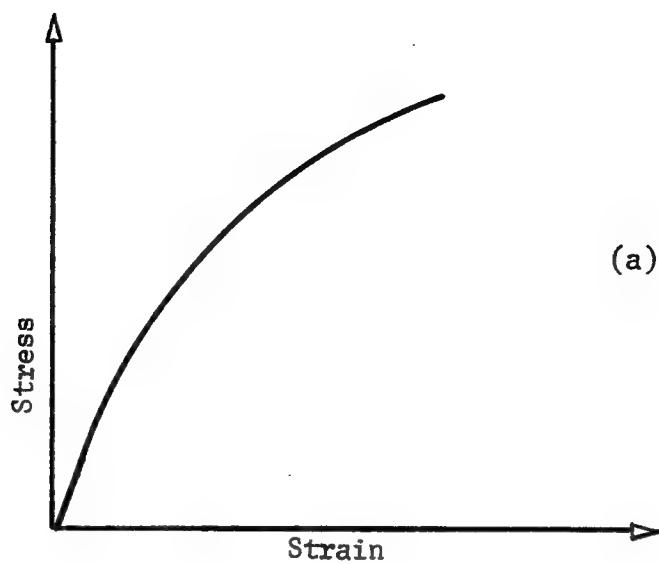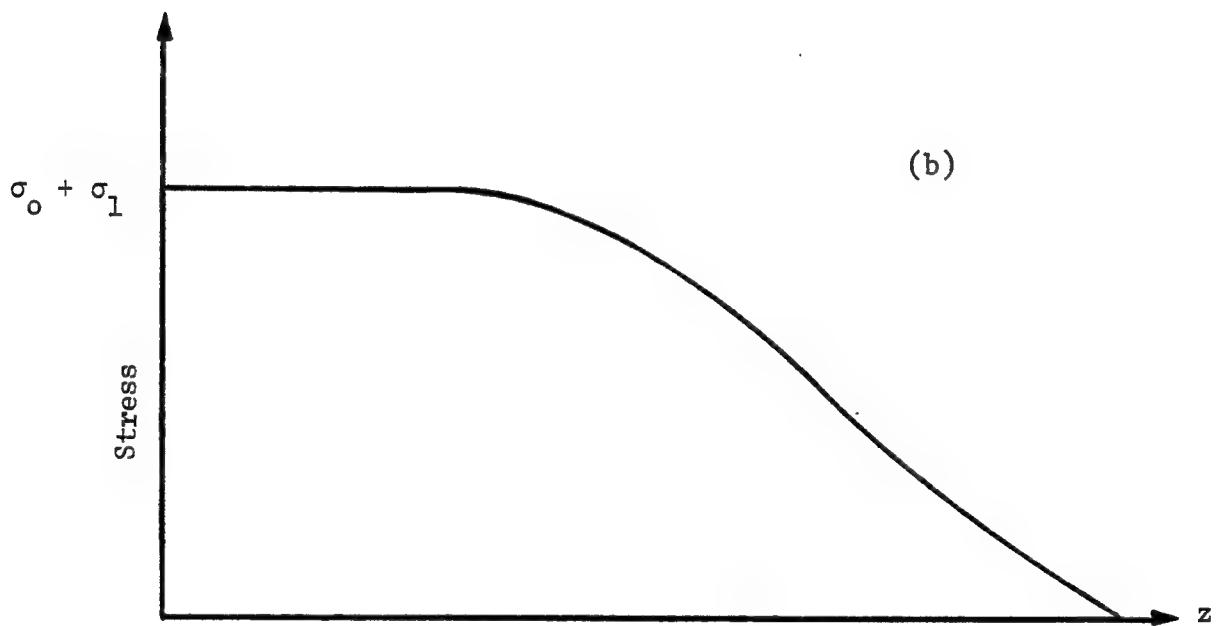
Fig. II-4. Plastic wave propagation as deduced from Donnell's approximation.

27

$$\sigma = -\sigma_1$$

Boundary conditions $\dot{u} = -\dot{u}_1$ at z = 0

$$u = -\dot{u}_1 t$$

Medium property

$$\sigma_P = \sigma_P(\epsilon_P)$$

$$M_P(\epsilon_P) = \frac{\partial \sigma_P}{\partial \epsilon_P}$$

$$C_o = \sqrt{M_o/\rho}$$
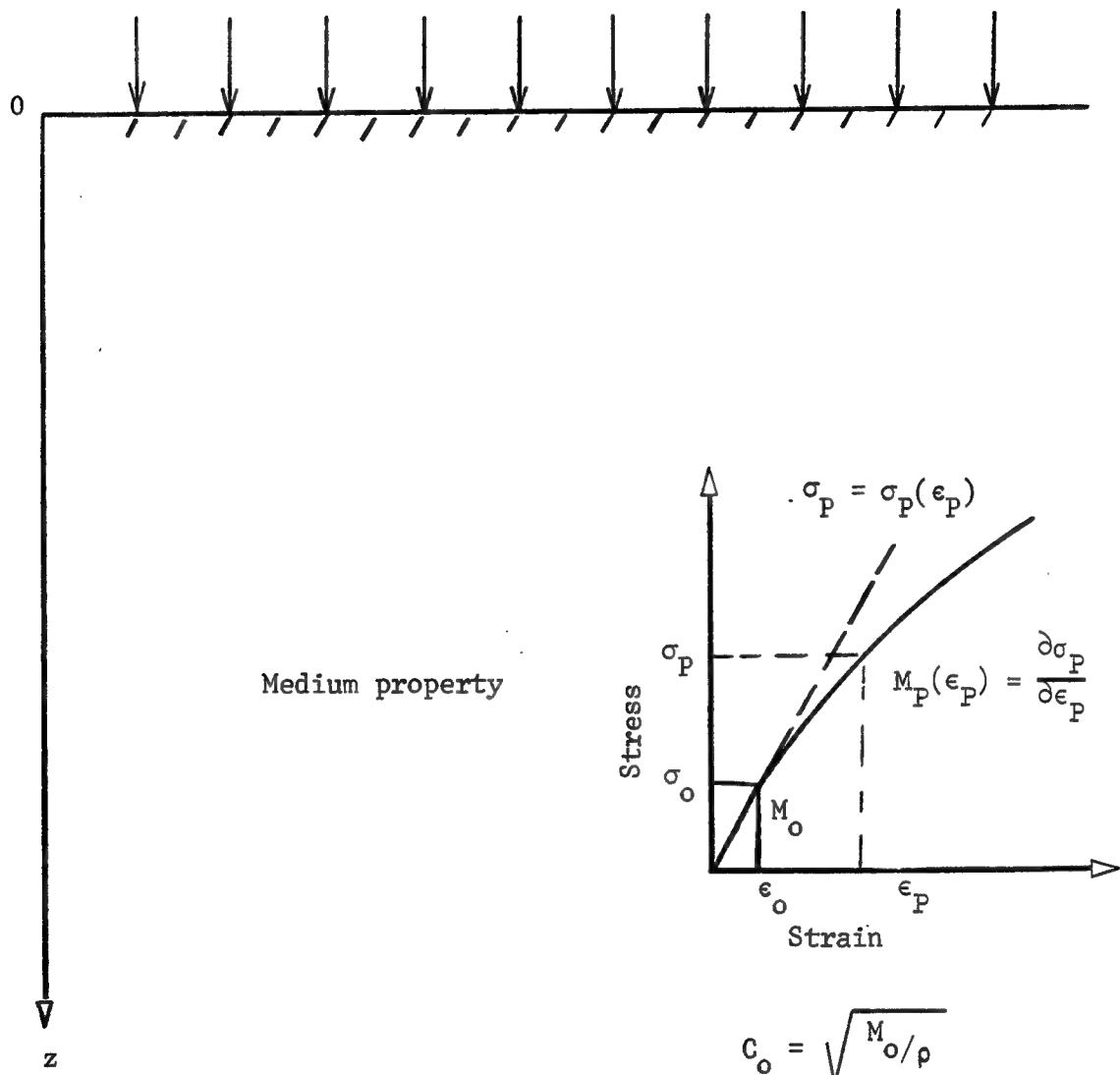
Fig. II-5. Typical plastic stress-strain curve.

$$\rho \, \frac{\partial^2 u}{\partial t^2} = - \frac{\partial \sigma_P}{\partial z} \qquad\qquad \text{II-2}$$

and

$$\epsilon_P = - \frac{\partial u}{\partial z} \qquad\qquad \text{II-3}$$

For any point on the stress-strain curve, the constrained modulus, M_P , is

$$M_P(\epsilon_P) = \frac{\partial \sigma_P}{\partial \epsilon_P} \qquad\qquad \text{II-38}$$

The initial tangent modulus is M_o . From equations II-37, II-3, and II-38

$$\frac{\partial \sigma_P}{\partial z} = \frac{\partial \sigma_P}{\partial \epsilon_P} \frac{\partial \epsilon_P}{\partial z} = - M_P(\epsilon_P) \frac{\partial^2 u}{\partial z^2} \qquad\qquad \text{II-39}$$

Substituting equation II-39 into equation II-2 the equation of motion becomes

$$\rho \, \frac{\partial^2 u}{\partial t^2} = M_P(\epsilon_P) \frac{\partial^2 u}{\partial z^2} \qquad\qquad \text{II-40}$$

For boundary conditions, assume that a constant velocity $- \dot{u}_1$, corresponding to a compressive stress $- \sigma_1$, is suddenly imposed and maintained at the surface of the body ($z = 0$).

Then

$$u = - \dot{u}_1 t \quad \text{at} \quad z = 0$$

and

$$u = 0 \quad \text{at} \quad z = \infty$$

To integrate equation II-40, assume that the compressive strain ϵ_P is a function of $z/t = \psi$, i.e.

$$\epsilon_P = -f(\psi) \qquad\qquad \text{II-41}$$

Then $dz = t \, d\psi$ and $dt = -\dfrac{t^2}{z} \, d\psi$, the displacement u is then determined as

$$u = \int_{\infty}^{z} \frac{\partial u}{\partial z} \, dz = \int_{\infty}^{z} \epsilon_P \, dz = - \int_{\infty}^{z} f(\psi) \, dz$$

$$= - t \int_{\infty}^{\psi} f(\psi) \, d\psi \qquad\qquad \text{II-42}$$

The second space derivative, $\dfrac{\partial^2 u}{\partial z^2}$, becomes

$$\frac{\partial^2 u}{\partial z^2} = \frac{\partial}{\partial z} \epsilon_P = - \frac{\partial}{\partial z} f(\psi) = - \frac{f'(\psi)}{t} \qquad\qquad \text{II-43}$$

and

$$\frac{\partial u}{\partial t} = - \int_{\infty}^{\psi} f(\psi) \, d\psi - t \frac{\partial}{\partial t} \int_{\infty}^{\psi} f(\psi) \, d\psi \qquad\qquad \text{II-44}$$

But

$$t \frac{\partial}{\partial t} = t \frac{\partial}{\partial \psi} \frac{\partial \psi}{\partial t} = - \frac{z}{t} \frac{\partial}{\partial \psi} \qquad\qquad \text{II-45}$$

and

$$- \frac{z}{t} \frac{\partial}{\partial \psi} \int_{\infty}^{\psi} f(\psi) \, d\psi = - \frac{z}{t} f(\psi) = - \psi f(\psi) \qquad\qquad \text{II-46}$$

Substituting equation II-46 into equation II-44

$$\frac{\partial u}{\partial t} = - \int_{\infty}^{\psi} f(\psi) \, d\psi + \psi f(\psi) \qquad\qquad \text{II-47}$$

Therefore

$$\frac{\partial^2 u}{\partial t^2} = \frac{\partial}{\partial t}\left[\psi f(\psi) - \int_\infty^\psi f(\psi)\,d\psi\right]$$

$$= \frac{\partial \psi}{\partial t}\frac{\partial}{\partial \psi}\left[\psi f(\psi) - \int_\infty^\psi f(\psi)\,d\psi\right]$$

$$= -\frac{z}{t^2}\left[f(\psi) + \psi f'(\psi) - f(\psi)\right]$$

$$= -\frac{z}{t^2}\psi f'(\psi) = -\frac{\psi^2}{t} f'(\psi) \qquad\qquad \text{II-48}$$

Substituting equations II-43 and II-48 into equation II-40 the equation of motion becomes

$$\rho \frac{\psi^2}{t} f'(\psi) = M_P(\epsilon_P)\frac{f'(\psi)}{t} \qquad\qquad \text{II-49}$$

or

$$f'(\psi)\left[\rho\psi^2 - M_P(\epsilon_P)\right] = 0 \qquad\qquad \text{II-50}$$

Equation II-50 indicates that either

$$f'(\psi) = 0 \quad \text{or} \quad f(\psi) = \text{constant} \qquad\qquad \text{II-51}$$

or

$$M_P(\epsilon_P) = \rho\psi^2 \qquad\qquad \text{II-52}$$

The first solution given by equation II-51 indicates that there is a strain ϵ_1 which is constant. The displacement, from equation II-42 and the boundary conditions, can be written as

31

$$u = -\dot{u}_1 t - \epsilon_1 z$$

$$= -\dot{u}_1 \left[t + \frac{z}{\left(\dfrac{\dot{u}_1}{\epsilon_1}\right)} \right] \qquad \text{II-53}$$

The second solution given by equation II-52 corresponds to

$$\frac{z}{t} = \sqrt{\frac{M_P(\epsilon_P)}{\rho}} \qquad \text{II-54}$$

The complete solution of the problem can be written as follows

(a) The strain $\epsilon_P = \epsilon_1 = $ constant , from $z = 0$ to $z = C_1 t$ where ϵ_1 is the plastic increment corresponding to stress σ_1 induced by the applied velocity $\dot{u}_1$.

(b) Between $z = C_1 t$ and $z = C_o t$, the relation $\frac{z}{t} = \sqrt{\frac{M_P(\epsilon_P)}{\rho}}$ holds. The strain varies and each strain increment propagates with a velocity $\sqrt{\frac{M_P(\epsilon_P)}{\rho}}$. C_o is the elastic velocity $\sqrt{\frac{M_o}{\rho}}$.

(c) $\epsilon_P = 0$ for $z > C_o t$.

This strain distribution is shown in fig. II-6. The elastic strain front travels with velocity C_o and an amplitude ϵ_o . The peak plastic strain front propagates with a velocity C_1 and a constant amplitude ϵ_1 . Between the two fronts the propagation velocity of any strain increment depends upon the local slope $M_P(\epsilon_P)$ and the strain varies from ϵ_o at the elastic front to ϵ_1 at the peak plastic front. The propagation velocity of the plastic wave peak, C_1 , can be related to ϵ_1 and $\dot{u}_1$ in the following way. From the boundary conditions and equation II-42

$$\dot{u}_1 = \frac{u(0,t)}{t} = - \int_{\infty}^{z=0} f(\psi)\, d\psi \qquad \text{II-55}$$

32
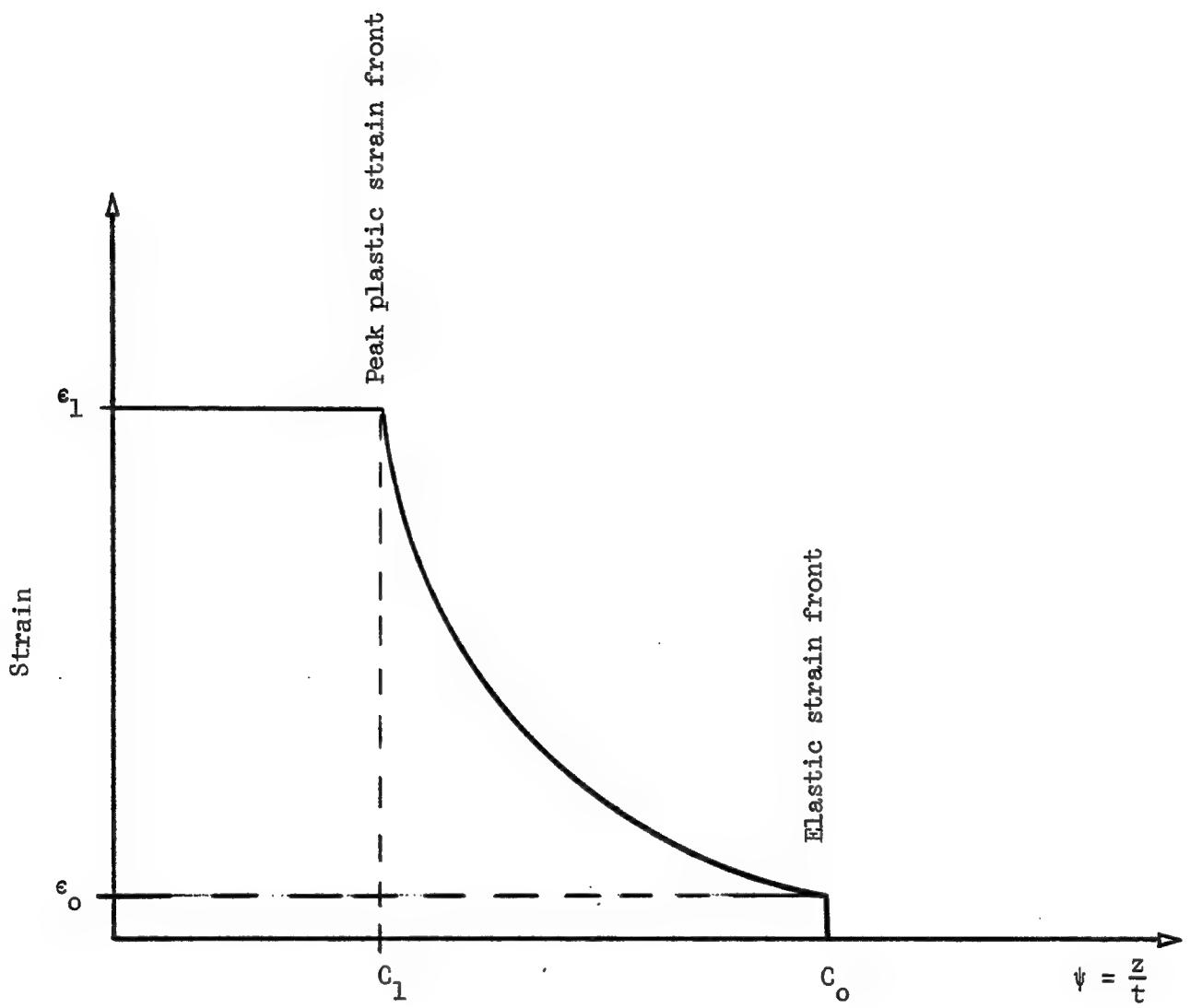
Fig. II-6. Strain distribution for a plastic pulse in a
bar according to the strain-rate independent
theory.

or

$$\dot{u}_1 = \int_0^\infty f(\psi) \, d\psi \qquad\qquad \text{II-56}$$

This integral is the area under the curve in fig. II-6. It may be written
as

$$\dot{u}_1 = \int_0^{\epsilon_1} \psi \, d\epsilon = \int_0^{\epsilon_1} \frac{z}{t} \, d\epsilon \qquad\qquad \text{II-57}$$

Substituting for $\frac{z}{t}$ from equation II-54

$$\dot{u}_1 = \int_0^{\epsilon_1} \sqrt{\frac{M_p(\epsilon_p)}{\rho}} \, d\epsilon \qquad\qquad \text{II-58}$$

The relation $M_p(\epsilon_p)$ is known from the stress-strain curve for the medium.
Equation II-58 gives the relation between ϵ_1 and $\dot{u}_1$. The velocity C_1
is equal to the value of $\sqrt{\frac{M_p(\epsilon_p)}{\rho}}$ at ϵ_1 . The stress distribution is
deduced from the distribution of strain and the stress-strain curve.

E. Propagation of stress waves in linear visco-elastic media

Linear visco-elastic materials are generally defined by linear dif-
ferential equations which relate stresses to strain and strain rate. The
elasticity of the material is presented by linear springs while the
viscosity of the material is presented by viscous elements called dashpots.
The elastic and viscous elements are combined to form the constitutive
equations of the material. The governing differential equations describing
the propagation of one-dimensional stress waves in visco-elastic materials
are obtained from the equilibrium equation of motion, equation II-2,

34

by substituting the appropriate constitutive equation for stress σ

$$\rho \frac{\partial^2 u}{\partial t^2} = -\frac{\partial \sigma}{\partial z} \qquad \text{II-59}$$

Various models of visco-elastic materials can be constructed by suitable combinations of springs and dashpots. The best known models are the two-element Kelvin-Voigt and Maxwell solids and the three-element standard linear solid shown in fig. II-7. The constitutive relation for the Kelvin-Voigt model is, from fig. II-7,

$$\sigma = M\epsilon + \eta \frac{d\epsilon}{dt} \qquad \text{(Kelvin-Voigt)} \qquad \text{II-60}$$

For the Maxwell model

$$\sigma = \eta \frac{d\epsilon_2}{dt} = M\epsilon_1 \qquad \text{II-61}$$

or

$$\sigma = \eta \frac{d(\epsilon - \epsilon_1)}{dt} = \eta \frac{d\epsilon}{dt} - \eta \frac{d\epsilon_1}{dt} \qquad \text{II-62}$$

but

$$\frac{d\epsilon_1}{dt} = \frac{1}{M} \frac{d\sigma}{dt} \qquad \text{II-63}$$

Substituting equation II-63 in equation II-62 results in

$$\sigma = \eta \frac{d\epsilon}{dt} - \frac{\eta}{M} \frac{d\sigma}{dt} \qquad \text{(Maxwell)} \qquad \text{II-64}$$

For the standard linear solid

$$\sigma = M_1 \epsilon_1 + \eta \frac{d\epsilon_1}{dt} = M_o \epsilon_2 \qquad \text{II-65}$$

Since $\epsilon = \epsilon_1 + \epsilon_2$ and

35
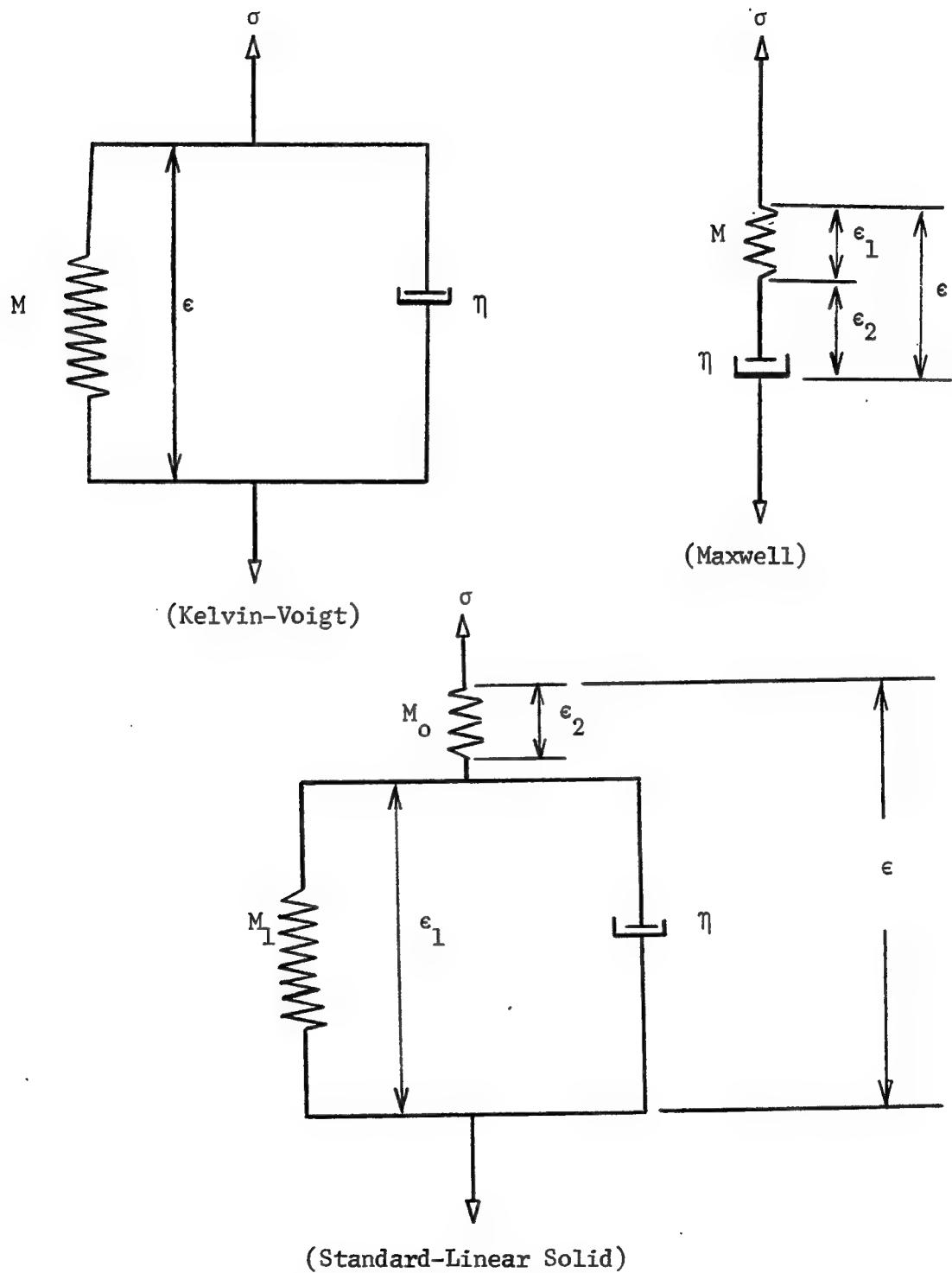
Fig. II-7. Models for linear visco-elastic materials.

$$\frac{d\epsilon_1}{dt} = \frac{d\epsilon}{dt} - \frac{1}{M_o} \frac{d\sigma}{dt} \qquad\qquad \text{II-66}$$

equation II-65 becomes

$$\sigma = \eta \frac{d\epsilon}{dt} - \frac{\eta}{M_o} \frac{d\sigma}{dt} + M_1 \epsilon_1 \qquad\qquad \text{II-67}$$

but

$$\epsilon_1 = \epsilon - \epsilon_2 = \epsilon - \frac{\sigma}{M_o}$$

therefore

$$\sigma = \frac{M_o M_1}{M_o + M_1} \epsilon + \frac{\eta M_o}{M_o + M_1} \frac{d\epsilon}{dt} - \frac{\eta}{M_o + M_1} \frac{d\sigma}{dt} \qquad \text{(Standard Linear Solid)} \qquad \text{II-68}$$

Substitution of equations II-60, II-64, and II-68 for σ, in equation II-59, will result in the following equations of motion for the Kelvin-Voigt, Maxwell, and standard linear solids, respectively (note that strain and displacement are related by equation II-3, that is, $\epsilon = -\frac{\partial u}{\partial z}$):

$$\rho \frac{\partial^2 u}{\partial t^2} = M \frac{\partial^2 u}{\partial z^2} + \eta \frac{\partial^3 u}{\partial z^2 \partial t} \qquad \text{(Kelvin-Voigt)} \qquad \text{II-69}$$

$$\rho \frac{\partial^2 u}{\partial t^2} = \eta \left(\frac{\partial^3 u}{\partial z^2 \partial t} - \frac{\rho}{M} \frac{\partial^3 u}{\partial t^3} \right) \qquad \text{(Maxwell)} \qquad \text{II-70}$$

$$\rho (M_o + M_1) \frac{\partial^2 u}{\partial t^2} = M_1 M_o \frac{\partial^2 u}{\partial z^2} - \rho \eta \frac{\partial^3 u}{\partial t^3} + \eta M_o \frac{\partial^3 u}{\partial z^2 \partial t} \qquad \text{(Standard Linear Solid)} \qquad \text{II-71}$$

Equations II-69, II-70, and II-71 are not in general satisfied by a solution of the type $u = f\left(t \pm \frac{z}{C}\right)$ which satisfies the elastic wave equation (equation II-7). However, solutions for equations II-69, II-70, and II-71

can be obtained from the solution $u = f\left(t \pm \dfrac{z}{C}\right)$ of the elastic wave
equation using the "correspondence principle" (14) provided the boundary
conditions for the two problems are the same. The "correspondence
principle" states that the solution to a visco-elastic problem may be
obtained from the solution for the corresponding problem for an elastic
case by applying the one-sided Fourier transform to the elastic solution,
replacing the elastic constants by the corresponding visco-elastic moduli
or compliances and finally inverting the transform. The complex visco-
elastic compliances for the models in fig. II-7 are given as follows
(see Bland, p. 114-115)

$$J(i\omega) = \frac{M}{M^2 + \omega^2\eta^2} - \frac{i\omega\eta}{M^2 + \omega^2\eta^2} \quad \text{(Kelvin-Voigt)} \quad \text{II-72}$$

$$J(i\omega) = \frac{1}{M} - \frac{i}{\omega\eta} \quad \text{(Maxwell)} \quad \text{II-73}$$

$$J(i\omega) = \frac{1}{M_o} + \frac{M_1}{M_1^2 + \omega^2\eta^2} - \frac{i}{\omega\eta}\left(1 - \frac{M_1^2}{M_1^2 + \omega^2\eta^2}\right) \quad \text{(Standard Linear Solid)} \quad \text{II-74}$$

where $i = \sqrt{-1}$ and ω is the frequency (rad/sec) of the oscillating
force.

   The one-sided Fourier transform of a function such as $f\left(t \pm \dfrac{z}{C}\right)$ is
defined by

$$f(\omega) = \int_0^\infty e^{-i\omega t} f\left(t \pm \frac{z}{C}\right) dt \qquad \text{II-75}$$

The inverse transform is

$$f\left(t \pm \frac{z}{C}\right) = \frac{1}{\pi} R \left[\int_0^\infty e^{i\omega t} f(\omega) \, d\omega\right] \qquad \text{II-76}$$

where R denotes the real part of the expression in brackets. Therefore, the first step in the solution of a linear visco-elastic dynamic problem is to find the solution for the elastic case. As an example consider the solution II-10 given for a semi-infinite elastic medium.

$$u = f\left(t - \frac{z}{C}\right) \qquad \text{(a)}$$

$$\dot{u} = f'\left(t - \frac{z}{C}\right) \qquad \text{(b)}$$

$$\epsilon = \frac{1}{C} f'\left(t - \frac{z}{C}\right) \qquad \text{(c)} \qquad \qquad \text{II-77}$$

$$\sigma = \frac{M}{C} f'\left(t - \frac{z}{C}\right) \qquad \text{(d)}$$

The form of f is determined by the conditions on the boundary $(z = 0)$. If an impulse of magnitude I is applied on the boundary at time $t = 0$, the boundary condition is

$$\sigma(0,t) = I \, \delta(t) \qquad \text{II-78}$$

where $\delta(t)$ is the Dirac delta function. From equation II-77 (d)

$$\frac{M}{C} f'(t) = I \, \dot{\delta}(t) \qquad \text{II-79}$$

Integrating with respect to time

$$u = f\left(t - \frac{z}{C}\right) = \frac{C}{M} \ I \ H\left(t - \frac{z}{C}\right)$$

$$\dot{u} = \frac{C}{M} \ I \ \delta\left(t - \frac{z}{C}\right)$$

<div align="right">II-80</div>

$$\epsilon = \frac{I}{M} \ \delta\left(t - \frac{z}{C}\right)$$

$$\sigma = I \ \delta\left(t - \frac{z}{C}\right)$$

where $H\left(t - \frac{z}{C}\right)$ is the Heaviside step function.

Let us find the stress for a visco-elastic medium under the same boundary load. Applying the "correspondence principle," the one-sided Fourier transform of stress σ is found first

$$\sigma(\omega) = I \int_0^\infty e^{-i\omega t} \ \delta\left(t - \frac{z}{C}\right) dt \qquad \text{II-81}$$

or

$$\sigma(\omega) = Ie^{-i\omega z/C} \qquad \text{II-82}$$

Next the elastic compliance $\frac{1}{M}$ is replaced by the complex compliance $J(i\omega)$ of the visco-elastic medium. Since $C = \sqrt{M/\rho}$ equation II-82 becomes

$$\sigma(\omega) = Ie^{-i\omega z \sqrt{\rho J(i\omega)}} \qquad \text{II-83}$$

The stress itself is found from the inverse of equation II-83

$$\sigma(z,t) = \frac{I}{\pi} R \left[\int_0^\infty e^{i\omega\left(t - \sqrt{\rho J(i\omega)} z\right)} \ d\omega \right] \qquad \text{II-84}$$

For a Maxwell material, $J(i\omega) = \frac{1}{M} - \frac{i}{\omega\eta}$ (equation II-73). After substituting in equation II-84 and integrating

$$\sigma(z,t) = I e^{-\frac{Mt}{2\eta}} \left\{ \delta\left(t - \frac{z}{C}\right) + \right.$$

$$\left. \frac{\sqrt{\rho M} z}{2\eta}\left(t^2 - \frac{z^2}{C^2}\right)^{-1/2}\left[I_1\left(\frac{M}{2\eta}\sqrt{t^2 - \frac{z^2}{C^2}}\right)\right] H\left(t - \frac{z}{C}\right)\right\} \qquad \text{II-85}$$

where I_1 is the first order Bessel function of imaginary argument. The impulse I is propagated with velocity C and attenuation $\sqrt{\rho M/2\eta}$. Similar expressions can be obtained for Kelvin-Voigt and standard linear material by substituting their corresponding compliances, $J(i\omega)$, in equation II-84 and performing the integrations. Thus, the solution to any visco-elastic problem can be found from the solution of the corresponding elastic problem by using the "correspondence principle" as was demonstrated for the case of the impulsive load. In Chapter IV this principle is used for obtaining the solution for a standard linear material from the corresponding solution for the linear hysteretic material.

F. Shock wave propagation

In Section D it was shown that for a nonlinear material each stress level σ_P travels at a velocity which is given by

$$C_P = \sqrt{\frac{M_P}{\rho}} = \sqrt{\frac{1}{\rho}\left(\frac{\partial \sigma_P}{\partial \epsilon_P}\right)} \qquad \text{II-86}$$

If the stress-strain relation for the material is such that increasing stresses are accompanied by increasing values of $\frac{\partial \sigma_P}{\partial \epsilon_P}$ (fig. II-8), then higher stress waves will travel at higher velocities and eventually catch up with the lower stress waves which preceded them (fig. II-8). This is
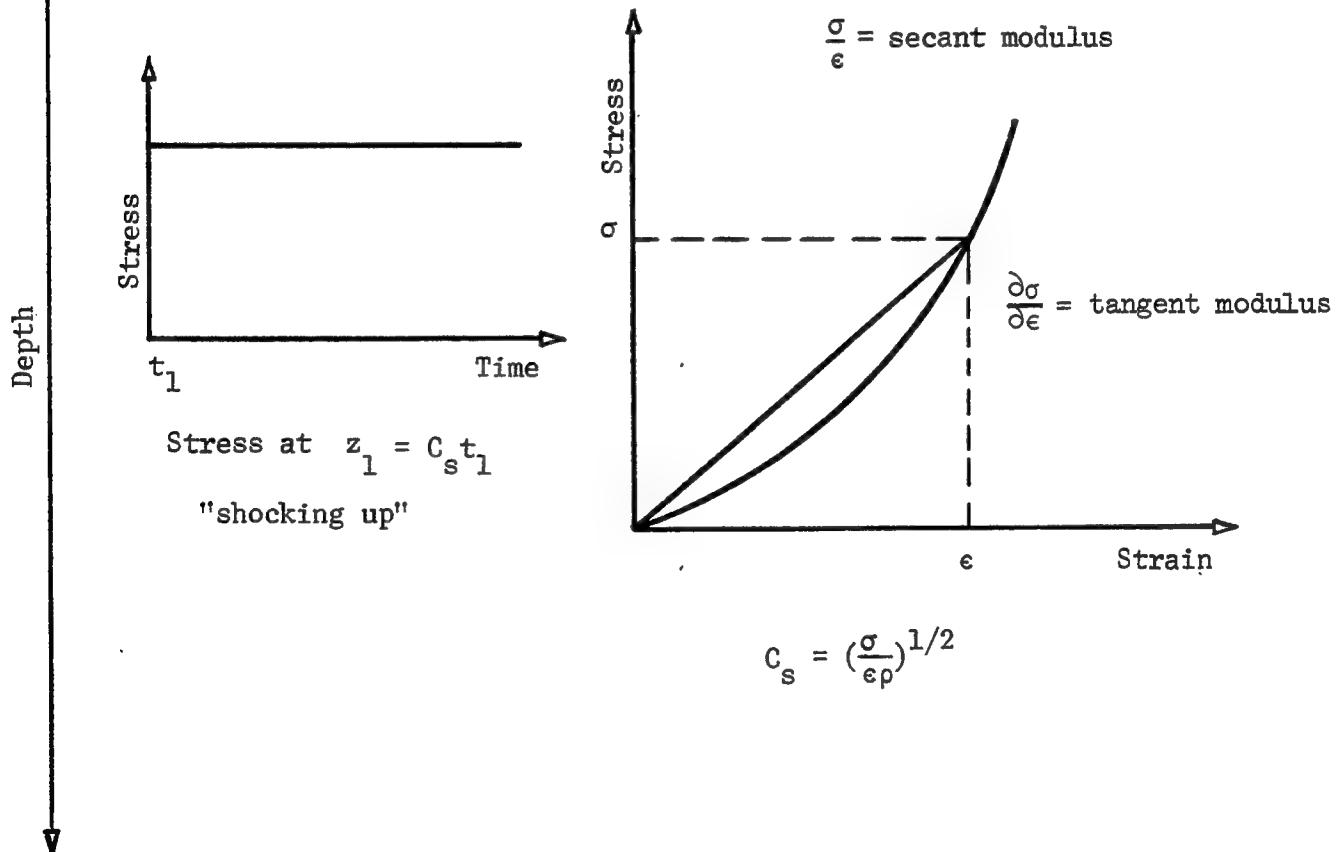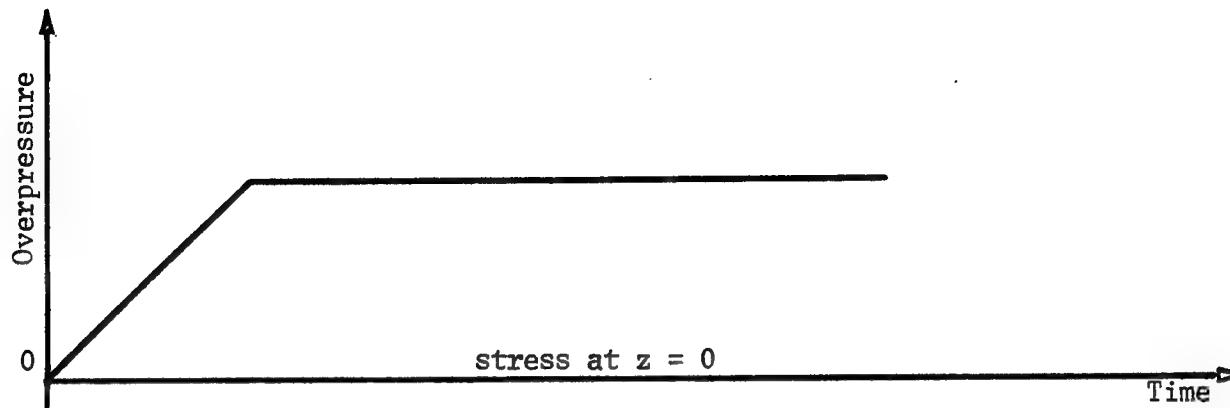
Fig. II-8.   Typical stress-strain curve causing "shocking up"
of the stress wave.

$\dfrac{\sigma}{\epsilon}$ = secant modulus

$\dfrac{\partial \sigma}{\partial \epsilon}$ = tangent modulus

Stress at $z_1 = C_s t_1$

"shocking up"

$$C_s = (\dfrac{\sigma}{\epsilon \rho})^{1/2}$$

stress at z = 0

the process of "shocking up" which is governed by the fundamental shock-wave equations known as the Rankine-Hugoniot equations derived from the equations of conservation of mass and momentum.

Consider a semi-infinite column of material, having a stress-strain curve shown in fig. II-8, subjected to an instantaneous step pressure applied to its surface (fig. II-9). Under the action of the applied pressure P, a shock wave is initiated and propagates down the column with some velocity of propagation C_s. At a time $t = t_a$, the front will reach a position $z = C_s t_a$, as shown in fig. II-9. During an infinitesimal time dt, the shock front will have moved to position $z = C_s(t_a + dt)$. The infinitesimal volume, $AC_s\, dt$, where A is the cross-sectional area of the element, will then obtain a particle velocity $\dot{u}$. From Newton's second law, the relation for impulse-momentum across the shock front is expressed as

$$P\, A\, dt = C_s\, dt\, A\rho_i \dot{u}$$

$$P = C_s \rho_i \dot{u} \qquad\qquad \text{II-87}$$

where ρ_i is the initial density of the material. The strain ϵ in the infinitesimal volume $AC_s\, dt$ is defined as the change in displacement per unit length

$$\epsilon = \frac{\dot{u}\, dt}{C_s\, dt} = \frac{\dot{u}}{C_s} \qquad\qquad \text{II-88}$$

By combining equation II-88 with equation II-87, the shock wave velocity can be expressed as

$$C_s = \sqrt{\frac{P}{\epsilon}\frac{1}{\rho_i}} \qquad\qquad \text{II-89}$$
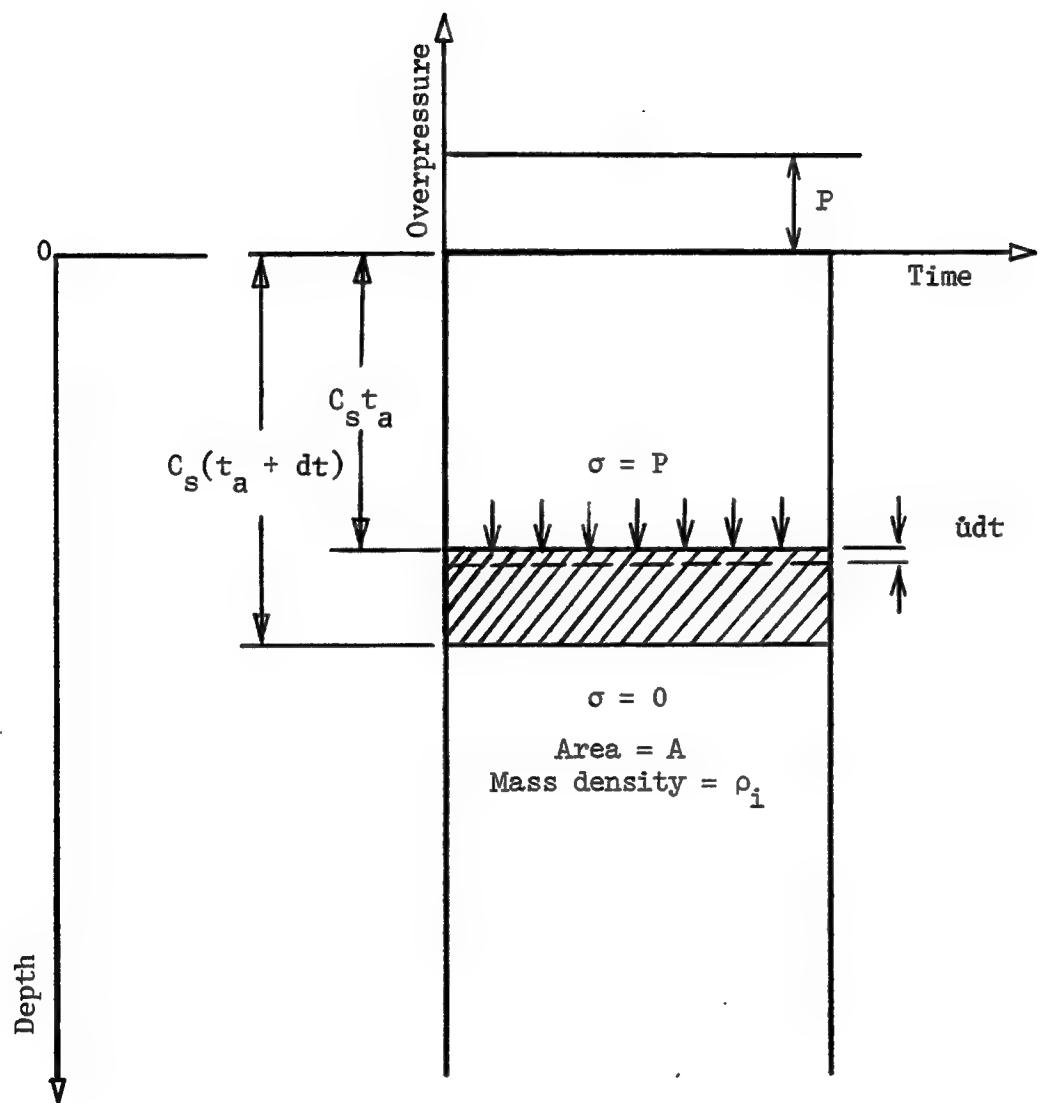
Fig. II-9. Shock-front conditions.

44

From equation II-89, it can be concluded that the shock velocity is a function of the secant modulus $\frac{P}{\epsilon}$ of the material as shown in fig. II-8.

III

Stress Wave Propagation Through
A Laterally Constrained Column of
Linear Hysteretic Material

A. Description of model

The linear hysteretic model was first used by Salvadori, Skalak, and
Weidlinger (16) to approximate the behavior of soils in a uniaxial state of
strain. The model is independent of the rate of load application; hence,
energy dissipation is due only to the compaction (hysteretic) character-
istics of the model.

Consider the stress-strain curve of fig. III-1. The stress-strain
curve is a straight line OA on initial loading to A . The slope of this
line defines an initial modulus M_O defined as the elastic constrained
modulus. M_O is related to Lame's constants λ and μ , or to Young's
modulus E and Poisson's ratio ν , as follows:

$$M_O = \lambda + 2\mu = \frac{E (1 - \nu)}{(1 + \nu)(1 - 2\nu)} \qquad \text{III-1}$$

Upon unloading the stress-strain curve is another straight line AB
which defines a second modulus M_1 (it is assumed herein that Poisson's
ratio is the same for loading and unloading). If the material is reloaded,
it follows line BA to A and then continues along the initial loading
line AC . In the limit when M_1 approaches M_O , the medium will behave
as a linear elastic material.

If the initial peak stress, peak strain and residual strain are re-
spectively denoted as σ_{max} , ϵ_{max} and ϵ_r (fig. III-1), the initial
loading modulus M_O is then given by:

46
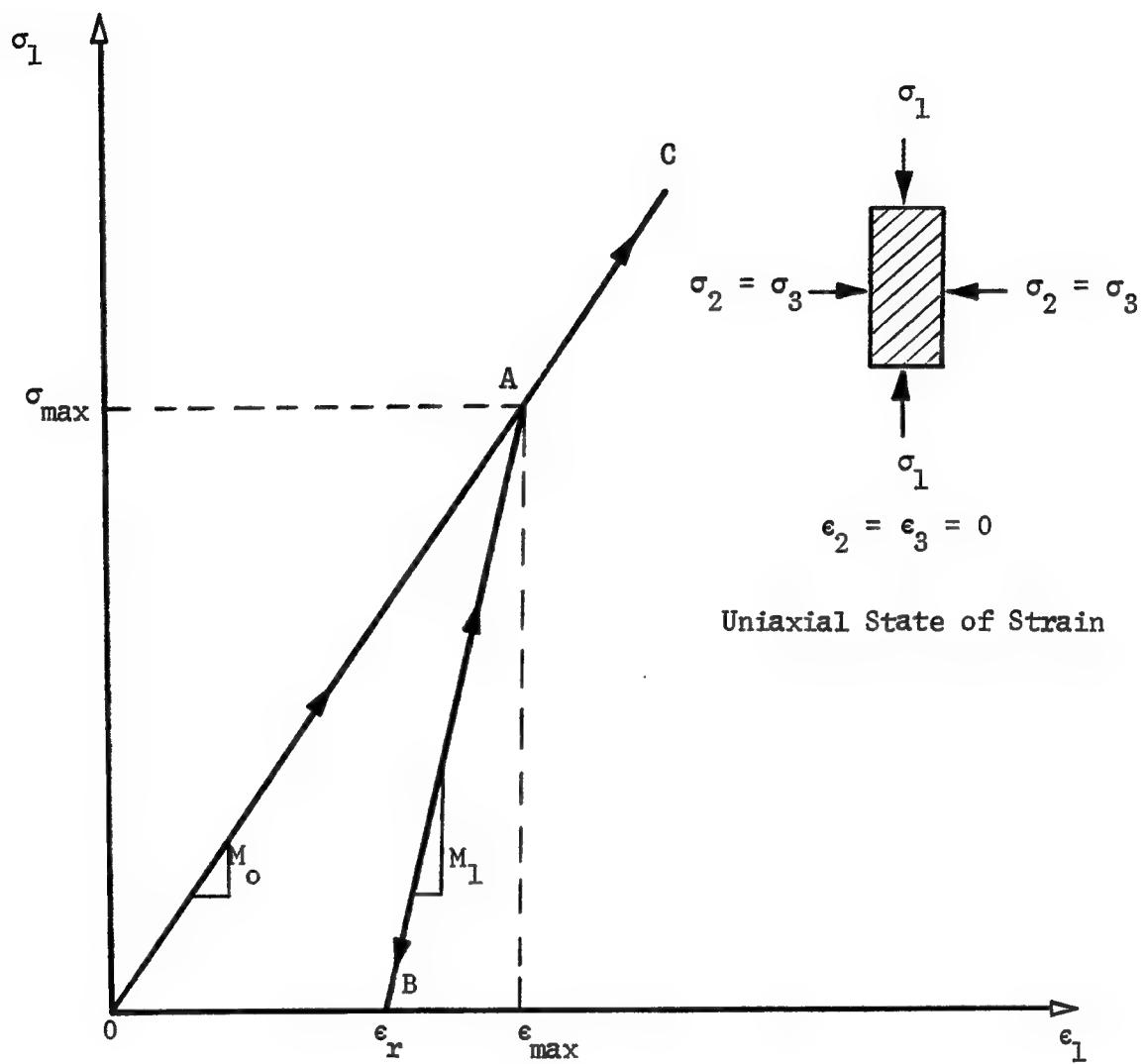
Fig. III-1. Stress-strain curve for linear hysteretic material.

$$M_o = \frac{\sigma_{max}}{\epsilon_{max}} \qquad \text{III-2}$$

The unloading modulus M_1 is given by:

$$M_1 = \frac{\sigma_{max}}{\epsilon_{max} - \epsilon_r} \qquad \text{III-3}$$

The propagation velocity of an initial loading stress wave is given by:

$$C_o = \sqrt{M_o/\rho} \qquad \text{III-4}$$

where ρ is the mass density of the material. The propagation velocity of an unloading or subsequent reloading stress wave is given by:

$$C_1 = \sqrt{M_1/\rho} \qquad \text{III-5}$$

B. Boundary load

The dynamic boundary load used with this model for blast-type problems is a pulse characterized by a peak stress at a shock front and an exponentially decaying behavior thereafter (fig. III-2) given by

$$P(t) = P_o \, e^{-t/\tau} \qquad \text{III-6}$$

where:

P_o = the peak applied pressure

t = time, the independent variable

τ = the exponential time constant $\left(\text{time at which pressure has decayed to 0.368 } P_o\right)$

C. Formulation of the problem

Consider a plane compression wave of general nature (arbitrary rise and decay) propagating into a column of linear hysteretic material extending from $z = 0$ to $z = \infty$. The distribution of pressure along the column length, at a given time t_a, might be as shown in fig. III-3. The

48
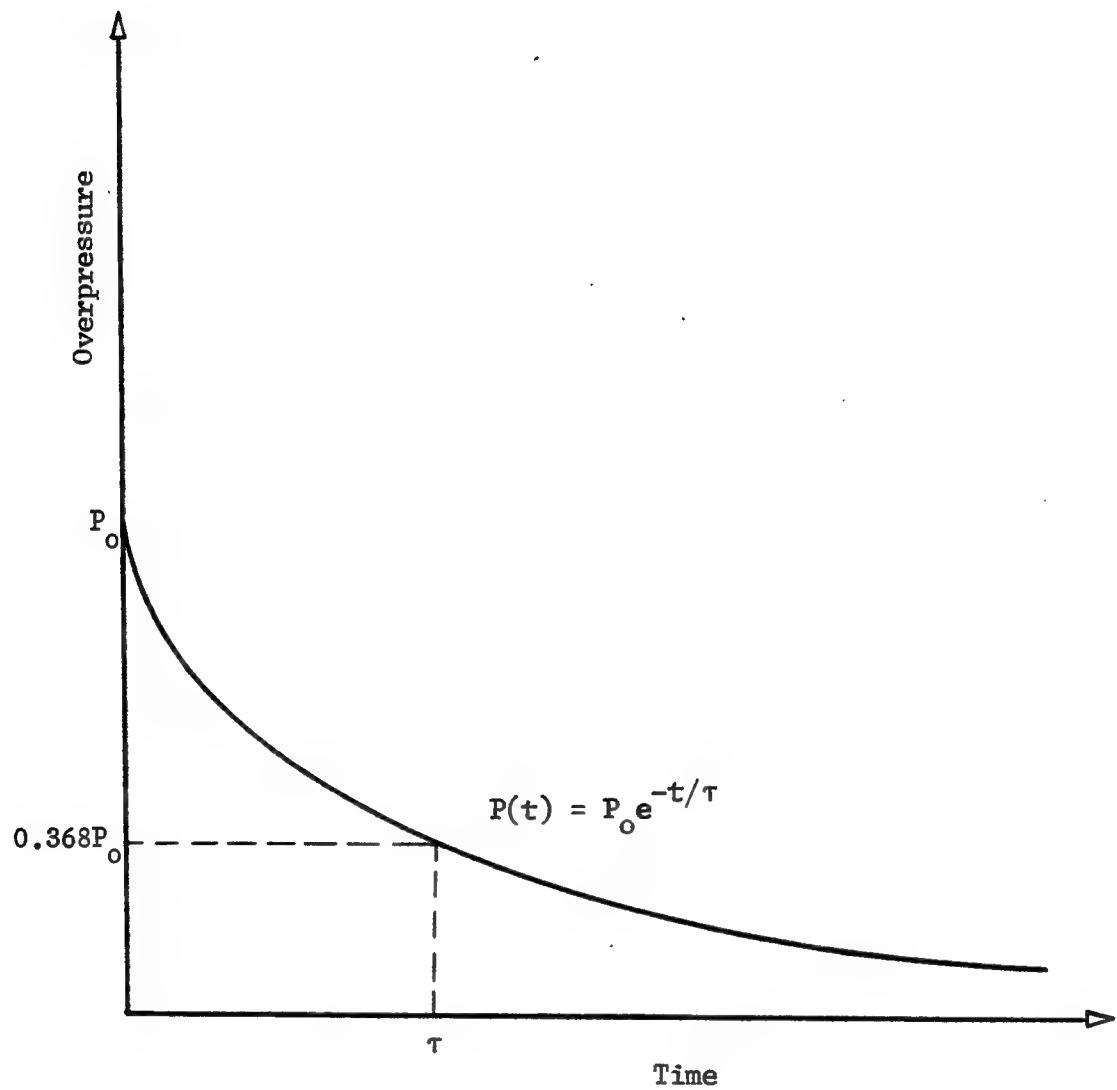
Fig. III-2. Applied pressure pulse on the boundary.
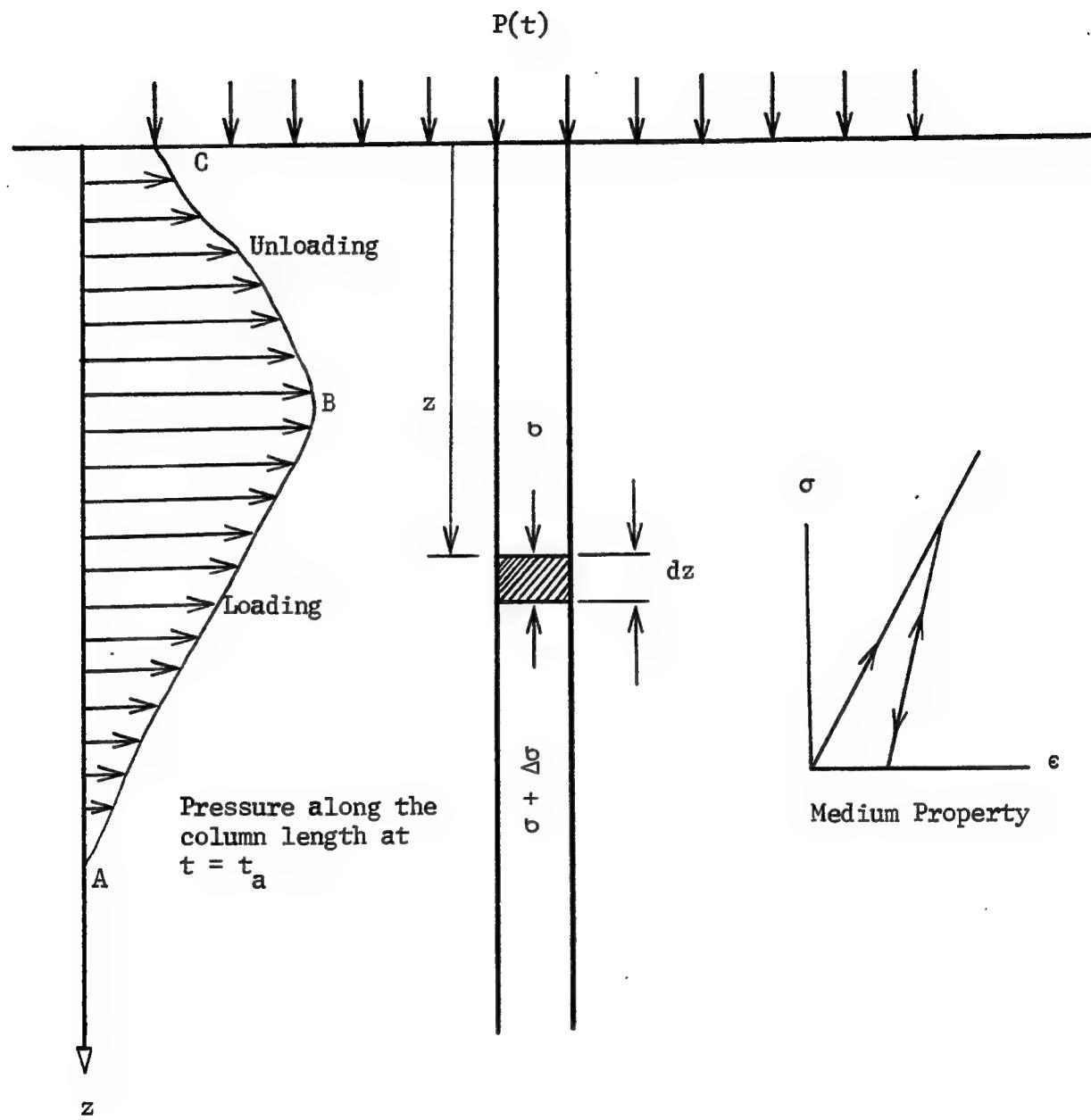
Fig. III-3.   One-dimensional wave conditions.

50

pressure varies from zero at the front of the wave, point A, to a maximum located some distance behind the wave front, point B, to the decayed over-pressure existing at the surface, point C. In the portion of the wave AB the pressure is continuously rising and, hence, this portion of the wave will propagate with velocity C_o corresponding to the loading branch, OA, of the stress-strain curve in fig. III-1. The one-dimensional wave equations governing the motion in zone AB are therefore:

$$\frac{\partial^2 \sigma}{\partial z^2} = \frac{1}{C_o^2} \frac{\partial^2 \sigma}{\partial t^2} \qquad \text{III-7}$$

$$\frac{\partial^2 \dot{u}}{\partial z^2} = \frac{1}{C_o^2} \frac{\partial^2 \dot{u}}{\partial t^2} \qquad \text{III-8}$$

where σ is the stress in the direction of wave propagation, u represents the particle displacement in the direction of wave propagation, and $\dot{u}$ is the particle velocity. In this zone the behavior is the same as that of a linear elastic material; the stress, particle velocity, particle displacement, and strain are related by:

$$\sigma = C_o \rho \dot{u}$$
$$\dot{u} = C_o \epsilon$$
$$u = C_o \int \epsilon dt \qquad \text{III-9}$$

where ϵ is the strain in the direction of wave propagation. In the portion of the wave BC, the stress is less than at B and is continuously decreasing. This portion of the wave will propagate with velocity C_1 corresponding to the unloading branch, AB, of the stress-strain curve in

51

fig. III-1. The governing equations in this zone are:

$$\frac{\partial^2 \sigma}{\partial z^2} = \frac{1}{c_1^2}\frac{\partial^2 \sigma}{\partial t^2} \qquad\qquad \text{III-10}$$

$$\frac{\partial^2 \dot{u}}{\partial z^2} = \frac{1}{c_1^2}\frac{\partial^2 \dot{u}}{\partial t^2} \qquad\qquad \text{III-11}$$

The response of the medium in this zone is not governed by elastic theory because the unloading stress-strain curve is offset from the origin. Since velocity C_1 is greater than C_0, the unloading wave front BC eventually overtakes the loading wave front AB. The resulting interaction, known as internal reflection, will cause a decrease in both peak particle velocity and peak stress. This process continues with time as will be shown in the following section.

D. Response of the medium to a
    discontinuous surface overpressure

A semi-infinite body of linear hysteretic material, such as that in fig. III-3, is loaded uniformly at its surface by a pressure pulse described by $P(t)$. Surface displacement and stress are assumed to be zero before the application of the load. Strains are considered small and, therefore, density is considered constant. The surface pressure pulse is suddenly applied at the time $t = 0$ and it remains constant at a value P_0 until a time $t = t_1$; the pressure then suddenly drops to a value P_1 and remains constant until time $t = \infty$. The more general surface pressure (fig. III-2), $p(t) = P_0 e^{-t/\tau}$, will be analyzed in the next section. At the time $t = 0$ and at $z = 0$ a wave begins to propagate into the body as shown in fig. III-4. For the time $0 < t < t_1$, a step

52

loading wave of pressure P_o propagates into the body with a velocity C_o . The stress in zone 0 of fig. III-4 is determined by the boundary conditions at the surface and is given as

$$\sigma_o = P_o \qquad\qquad \text{III-12}$$

The particle velocity is determined from the elastic theory (equation III-9) and is given by:

$$\dot{u}_o = \frac{P_o}{\rho C_o} \qquad\qquad \text{III-13}$$

At the time $t = t_1$, a step unloading wave of pressure $P_o - P_1$ begins to propagate into the body with a velocity C_1 which is the slope of the line separating zones 0 and 1 in fig. III-4. The stress in zone 1 is determined from the boundary conditions at the surface and is given as:

$$\sigma_1 = P_1 \qquad\qquad \text{III-14}$$

The particle velocity in zone 1, $\dot{u}_1$, is determined from an equation expressing the uniqueness of $\dot{u}_1$

$$\dot{u}_1 = \dot{u}_o - \Delta\dot{u}_{o1} \qquad\qquad \text{III-15}$$

where $\Delta\dot{u}_{o1}$ is the change in particle velocity caused by changing the stress from σ_o to σ_1

$$\Delta\dot{u}_{o1} = \frac{\sigma_o - \sigma_1}{\rho C_1} = \frac{P_o - P_1}{\rho C_1} \qquad\qquad \text{III-16}$$

Substituting equations III-13 and III-16 in equation III-15, one obtains for $\dot{u}_1$

P(t)

Overpressure

P_o

P_1

0

Time

t_1 t_3 t_5

β_o β_1 β_1 β_1 β_1 β_1

z

C_o 0 1 2 3 4

1

z_2

t_2

z_4

σ

t_4

$t_3 = t_1/\alpha$

$t_5 = t_1/\alpha^2$

$\tan \beta_o = C_o$

$\tan \beta_1 = C_1$

ϵ

Medium Property

$(t_5 - \dfrac{z}{C_1})$

$(t_5 + \dfrac{z}{C_1})$

A

Depth
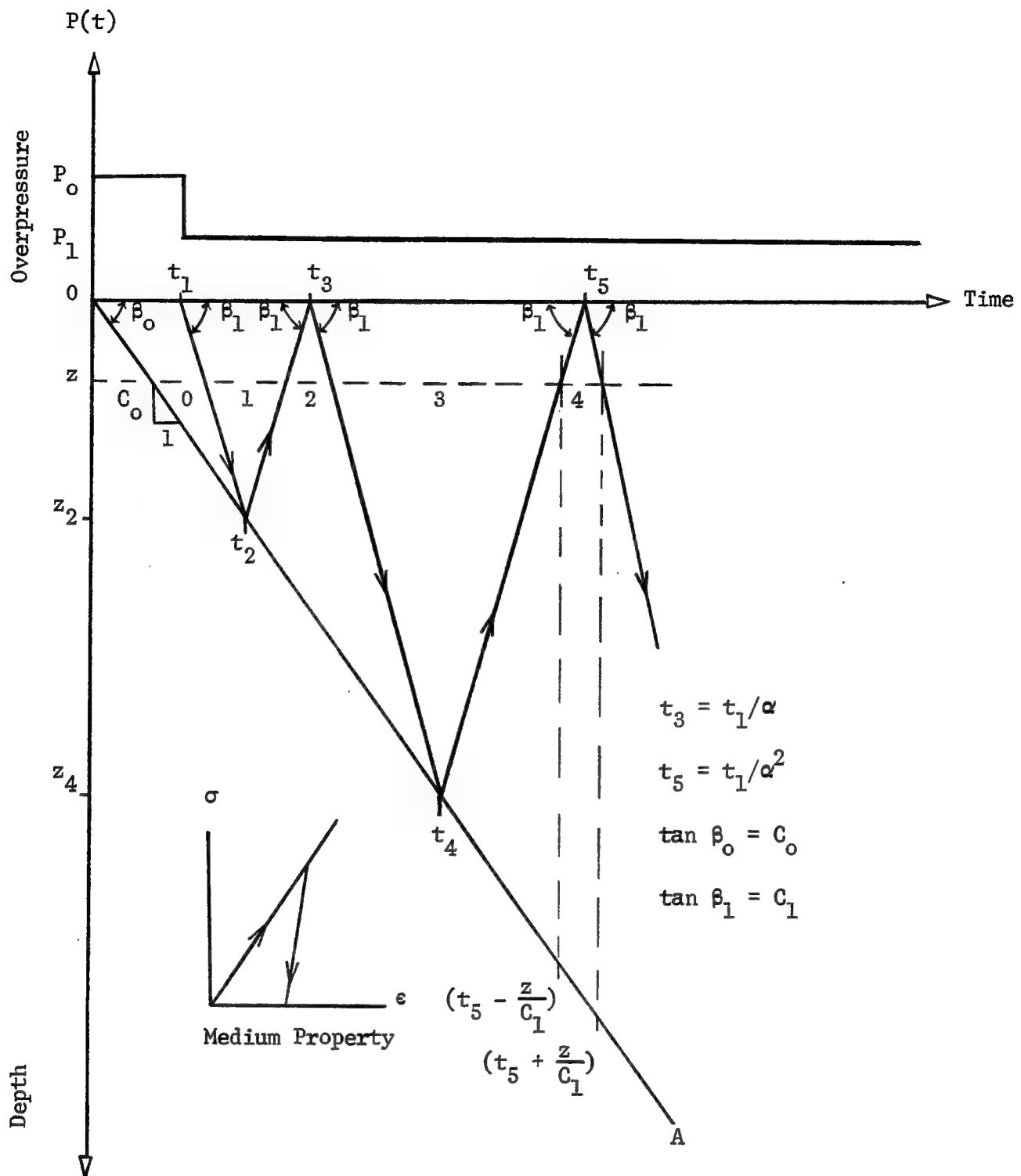
Fig. III-4. Space-time diagram for discontinuous loading in linear
hysteretic material.

$$\dot{u}_1 = \frac{1}{\rho C_o} \left[P_1 + \frac{C_1 - C_o}{C_1} (P_o - P_1) \right] \qquad \text{III-17}$$

The unloading step wave $P_o - P_1$ traveling at velocity C_1 overtakes the loading step wave P_o at the point z_2 at the time t_2. From fig. III-4 it can be seen that:

$$z_2 = C_o t_2 = C_1 (t_2 - t_1)$$

$$C_o t_2 = C_1 t_2 - C_1 t_1 \qquad \text{III-18}$$

$$t_2 = \phi t_1$$

where

$$\phi = \frac{C_1/C_o}{C_1/C_o - 1} \qquad \text{III-19}$$

At time t_2, all the material in zone 1, from $z = 0$ to $z_2 = C_o t_2$, is at a stress of σ_1 and has a particle velocity of $\dot{u}_1$. The material below z_2 is unstressed and at rest. It may be considered that the material in zone 1 is a body of elasticity M_1 striking the lower undisturbed mass of elasticity M_o. The resulting elastic interaction is governed by the equations of continuity of stress and particle velocity across the boundary. The transmitted wave travels downward with velocity C_o, and the reflected wave, which divides zones 1 and 2, travels upward with velocity C_1. The particle velocity in zone 2, for the transmitted wave is

$$\dot{u}_2 = \frac{\sigma_2}{\rho C_o} \qquad \text{III-20}$$

where σ_2 is the stress in zone 2. The particle velocity for the reflected wave is

$$\dot{u}_2 = \dot{u}_1 - \frac{\sigma_R}{\rho C_1} \qquad \text{III-21}$$

where σ_R is the reflected stress. From continuity of stress across the boundary:

$$\sigma_1 + \sigma_R = \sigma_2 \qquad \text{III-22}$$

Substituting equation III-22 in equation III-21 obtains

$$\dot{u}_2 = \dot{u}_1 - \frac{\sigma_2 - \sigma_1}{\rho C_1} \qquad \text{III-22}$$

From equations III-17, III-20, and III-23 it is found that:

$$\sigma_2 = P_1 + \alpha(P_0 - P_1) \qquad \text{III-24}$$

where:

$$\alpha = \frac{C_1/C_0 - 1}{C_1/C_0 + 1} = \frac{1}{2\emptyset - 1} \qquad \text{III-25}$$

Since $\alpha > 0$ for all cases, the upward traveling wave is a reloading wave. Substituting equation III-24 in equation III-20 yields the particle velocity in zone 2

$$\dot{u}_2 = \frac{1}{\rho C_0}\left[P_1 + \alpha(P_0 - P_1)\right] \qquad \text{III-26}$$

The reflected wave reaches the surface ($z = 0$) at time t_3 which is determined from fig. III-4 as

$$t_3 = t_2 + (t_3 - t_1)/2$$
$$= 2t_2 - t_1 \qquad \text{III-27}$$
$$= \frac{C_1 + C_0}{C_1 - C_0}\, t_1 = \frac{t_1}{\alpha}$$

56

Conditions at time t_3 are similar to those at time t_1. The stress is defined from the boundary condition at t_3

$$\sigma_3 = P_1 \qquad \text{III-28}$$

The particle velocity may be written down by analogy to $\dot{u}_1$, replacing $\dot{u}_o$ by $\dot{u}_2$ and σ_o by σ_2, respectively, in equations III-15 and III-16 obtains

$$\dot{u}_3 = \dot{u}_2 - \Delta\dot{u}_{23}$$

$$= \dot{u}_2 - \frac{\sigma_2 - \sigma_3}{\rho C_1} \qquad \text{III-29}$$

Substituting equations III-24, III-26, and III-28 in equation III-29, one obtains for $\dot{u}_3$

$$\dot{u}_3 = \frac{1}{\rho C_o} \left[P_1 + \frac{2\alpha^2}{1 + \alpha} (P_o - P_1) \right] \qquad \text{III-30}$$

The reflection from the moving wave front at t_4, fig. III-4, may be analyzed in the same way as the reflection at t_2. The unloading wave traveling at velocity C_1 overtakes the loading wave at the point z_4 at the time t_4. From fig. III-4 it can be seen that

$$z_4 = C_o t_4 = C_1(t_4 - t_3)$$

$$t_4 = \frac{C_1}{C_1 - C_o} \quad t_3 = \frac{C_1}{C_1 - C_o} \frac{t_1}{\alpha} = \frac{\emptyset}{\alpha} t_1 \qquad \text{III-31}$$

The particle velocity for the transmitted wave in zone 4 is

$$\dot{u}_4 = \frac{\sigma_4}{\rho C_o} \qquad \text{III-32}$$

57

where σ_4 is the stress in zone 4. The particle velocity for the reflected wave is

$$\dot{u}_4 = \dot{u}_3 - \frac{\sigma_4 - \sigma_3}{\rho C_1} \qquad \text{III-33}$$

From equations III-28, III-30, III-32, and III-33 it is found that

$$\sigma_4 = P_1 + \alpha^2(P_0 - P_1) \qquad \text{III-34}$$

Substituting equation III-34 in equation III-32 for particle velocity in zone 4,

$$\dot{u}_4 = \frac{1}{\rho C_0} \left[P_1 + \alpha^2(P_0 - P_1) \right] \qquad \text{III-35}$$

The above process can be continued indefinitely by finding the stress at the surface from the boundary condition, computing the new velocity, taking into account the change of stress, and then analyzing the interaction from the unloading wave overtaking the initial loading wave. From equations III-18, III-31, III-24, III-34, III-26, and III-35, one can deduce the following general expressions for arrival time t_n, stress σ_n and particle velocity $\dot{u}_n$ in any even numbered zone, that is, $n = 2, 4, 6, \ldots$.

$$t_n = \phi \alpha^{1-n/2} t_1 \qquad \text{III-36}$$

$$\sigma_n = \left[P_1 + \alpha^{n/2}(P_0 - P_1) \right] \qquad \text{III-37}$$

$$\dot{u}_n = \frac{1}{\rho C_0} \sigma_n \qquad \text{III-38}$$

Similar expressions can be deduced for any odd numbered zone, that is,

58

$n = 1, 3, 5, \ldots$, from equations III-27, III-14, III-28, III-17, and III-30

$$t_n = \alpha^{(1-n)/2} \, t_1 \qquad\qquad \text{III-39}$$

$$\sigma_n = P_1 \qquad\qquad \text{III-40}$$

$$\dot{u}_n = \frac{1}{\rho C_o} \left[P_1 + \frac{2\alpha^{(n+1)/2}}{1 + \alpha} \, (P_o - P_1) \right] \qquad\qquad \text{III-41}$$

It is apparent from equations III-40 and III-37 that the stress oscillates from P_1 for n odd to the value given by equation III-37 for n even, and approaches P_1 for large values of t since $\alpha < 1$ because $C_1/C_o > 1$ and

$$\underset{n \to \infty}{\text{Limit}} \; \alpha^{n/2} = 0 \qquad\qquad \text{III-42}$$

Therefore, for large values of t, equation III-37 yields the same results as equation III-40.

$$\sigma \, (z \, , \, \infty) = P_1 \qquad\qquad \text{III-43}$$

The limiting particle velocity from both equations III-38 and III-41 is

$$\dot{u} \, (z \, , \, \infty) = \frac{P_1}{\rho C_o} \qquad\qquad \text{III-44}$$

It is now desirable to write expressions for stress and particle velocity, as functions of time, which are valid in the zone $0 < z < C_o t$. Examination of equations III-37 and III-40, for stress in even and odd numbered zones, reveals the fact that the stress in each new zone is made up of values from the previous zone plus a contribution due to the wave

59

traveling upwards or downwards at velocity C_1 . The upwards traveling

wave is a reloading wave, it has a positive contribution on stress. The

downwards traveling wave is an unloading wave and it has a negative con-

tribution on stress. For instance, the stress in zone 3, from equation

III-40, is $\sigma_3 = P_1$. The stress in zone 2, from equation III-37, is

$\sigma_2 = P_1 + \alpha(P_0 - P_1)$. Thus, the contributing wave is an unloading wave

of magnitude $\alpha(P_0 - P_1)$ separating zones 2 and 3. The stress in zone 4,

from equation III-37, is $\sigma_4 = P_1 + \alpha^2(P_0 - P_1)$ indicating a contribution

of $\alpha^2(P_0 - P_1)$ from the reloading wave which separates zone 3 from 4.

In general, stress in zone $n \neq 0$ is equal to stress in zone $n - 1$ plus a

contribution due to the unloading or reloading wave which separates zones

n and $n - 1$. Stress in zone $n - 1$ is also made up of stress in zone $n - 2$

plus a contribution from the unloading or reloading wave separating zones

$n - 2$ and $n - 1$. Therefore, stress in any zone n is made up of the sum of

all waves traveling downwards and upwards plus a contribution $\sigma_0 = P_0$ from

zone 0. The sum of all waves traveling upwards, from fig. III-4 and equa-

tions III-37 and III-40 is

$$G\left(t + \frac{z}{C_1}\right) = \alpha(P_0 - P_1) + \alpha^2(P_0 - P_1) + \alpha^3(P_0 - P_1)$$

$$+ \alpha^4(P_0 - P_1) + \ldots + \alpha^n(P_0 - P_1) \qquad \text{III-45}$$

where $\dfrac{z}{C_1}$ is the travel time of the reloading wave from point z to the

surface. Equation III-45 can be written in the following form,

$$G\left(t + \frac{z}{C_1}\right) = \sum_{n=1}^{\infty} f_n\left(t + \frac{z}{C_1}\right) \qquad \text{III-46}$$

60

where

$$f_n(t) = \begin{cases} 0 \, , & t < t_1/\alpha^n \\ \alpha^n(P_0 - P_1) \, , & t > t_1/\alpha^n \end{cases} \qquad \text{III-47}$$

The sum of all waves traveling downwards (unloading waves), from fig. III-4 and equations III-37 and III-40 is

$$F\left(t - \frac{z}{C_1}\right) = - (P_0 - P_1) - \alpha(P_0 - P_1)$$

$$- \alpha^2(P_0 - P_1) - \ldots - \alpha^n(P_0 - P_1) \qquad \text{III-48}$$

or using equation III-47

$$F\left(t - \frac{z}{C_1}\right) = - (P_0 - P_1) - \sum_{n=1}^{\infty} f_n\left(t - \frac{z}{C_1}\right)$$

$$= - (P_0 - P_1) - G\left(t - \frac{z}{C_1}\right) \qquad \text{III-49}$$

Therefore, stress in any zone $n \neq 0$, fig. III-4, can be expressed as

$$\sigma(z,t_n) = G\left(t + \frac{z}{C_1}\right) - F\left(t - \frac{z}{C_1}\right) + P_0$$

$$= G\left(t + \frac{z}{C_1}\right) - G\left(t - \frac{z}{C_1}\right) - (P_0 - P_1) + P_0 \qquad \text{III-50}$$

$$= P_1 + G\left(t + \frac{z}{C_1}\right) - G\left(t - \frac{z}{C_1}\right)$$

To include zone 0 and thus write an expression for stress which is valid in the zone $0 < z < C_0 t$, one must replace P_1 with a function $P(t)$ so that

61

$$P(t) = \begin{cases} P_o \,, t < t_1 \\[2mm] P_1 \,, t > t_1 \end{cases} \qquad \text{III-51}$$

This function is the original input wave $P(t)$ corrected by the travel

time $\frac{z}{C_1}$, that is, $P\left(t - \frac{z}{C_1}\right)$. Therefore

$$\sigma(z,t) = P\left(t - \frac{z}{C_1}\right) + G\left(t + \frac{z}{C_1}\right) - G\left(t - \frac{z}{C_1}\right) \qquad \text{III-52}$$

As an example we will compute the stress at some arbitrary point z,

fig. III-4, at a time $t = t_5$.

$$\sigma(z,t_5) = P\left(t_5 - \frac{z}{C_1}\right) + G\left(t_5 + \frac{z}{C_1}\right) - G\left(t_5 - \frac{z}{C_1}\right) \qquad \text{III-53}$$

$P\left(t_5 - \frac{z}{C_1}\right)$ is the value of the input wave at $\left(t_5 - \frac{z}{C_1}\right)$, from fig. III-4

this value is P_1 . $G\left(t_5 + \frac{z}{C_1}\right)$ is the sum of all the reloading waves

from $t = 0$ to $\left(t_5 + \frac{z}{C_1}\right)$, from equation III-46

$$G\left(t_5 + \frac{z}{C_1}\right) = \sum_{n=1}^{\infty} f_n\left(t_5 + \frac{z}{C_1}\right) \qquad \text{III-54}$$

To evaluate equation III-54, one must use equation III-47 in the following

way

$$\text{for} \quad n = 1 \,, \quad t_5 + \frac{z}{C_1} > \frac{t_1}{\alpha} = t_3 \,, \quad f_1\left(t_5 + \frac{z}{C_1}\right) = \alpha(P_o - P_1)$$

$$\text{for} \quad n = 2 \,, \quad t_5 + \frac{z}{C_1} > \frac{t_1}{\alpha^2} = t_5 \,, \quad f_2\left(t_5 + \frac{z}{C_1}\right) = \alpha^2(P_o - P_1)$$

$$\text{for} \quad n \geq 3 \,, \quad t_5 + \frac{z}{C_1} < \frac{t_1}{\alpha^3} = t_7 \,, \quad f_3\left(t_5 + \frac{z}{C_1}\right) = f_n = 0$$

62

therefore

$$G\left(t_5 + \frac{z}{C_1}\right) = \alpha(P_o - P_1) + \alpha^2(P_o - P_1) \qquad \text{III-55}$$

The last term in equation III-53, which is the sum of all the unloading waves from $t = 0$ to $\left(t_5 - \frac{z}{C_1}\right)$, can be evaluated in the same manner

$$G\left(t_5 - \frac{z}{C_1}\right) = \sum_{n=1}^{\infty} f_n\left(t_5 - \frac{z}{C_1}\right) \qquad \text{III-56}$$

from equation III-47

for $n = 1$, $t_5 - \frac{z}{C_1} > \frac{t_1}{\alpha} = t_3$, $f_1\left(t_5 - \frac{z}{C_1}\right) = \alpha(P_o - P_1)$

for $n \geq 2$, $t_5 - \frac{z}{C_1} < \frac{t_1}{\alpha^2} = t_5$, $f_2\left(t_5 - \frac{z}{C_1}\right) = f_n = 0$

therefore

$$G\left(t - \frac{z}{C_1}\right) = \alpha(P_o - P_1) \qquad \text{III-57}$$

Substituting equations III-55, III-57, and the value of $P\left(t_5 - \frac{z}{C_1}\right) = P_1$ in equation III-53, one obtains for $\sigma(z,t_5)$

$$\sigma(z,t_5) = P_1 + \alpha^2(P_o - P_1) \qquad \text{III-58}$$

which is the stress in zone 4 obtained from equation III-37.

The particle velocity time history can be derived in the same manner by considering the particle velocity in each new zone of fig. III-4 to be made up of values from the previous zone plus a contribution f_n (equation III-47) due to the wave traveling upwards or downwards. Since $C_1 > C_o$, from the

63

interaction equations the reflected (reloading) particle velocity will have the same sign as the incident (unloading) particle velocity. Therefore, the contributions of all the reloading waves on particle velocity are

$$\frac{-G\left(t + \frac{z}{C_1}\right)}{\rho C_1}$$ III-59

and the contributions of all the unloading waves are

$$\frac{-G\left(t - \frac{z}{C_1}\right)}{\rho C_1} - \frac{P_o - P_1}{\rho C_1}$$ III-60

The contributions of the original input wave should be written in a form that the following conditions will be satisfied

$$\text{Particle velocity due to original input wave} = \begin{cases} \dfrac{P_o}{\rho C_o} & \text{when } t \leq t_1 \\[3mm] \dfrac{P_o}{\rho C_o} - \dfrac{P_o - P_1}{\rho C_1} & \text{when } t > t_1 \end{cases}$$ III-61

These conditions are satisfied if the contributions of the original input wave on particle velocity are expressed as

$$\frac{P\left(t - \frac{z}{C_1}\right)}{\rho C_1} + P_o\left(\frac{1}{\rho C_o} - \frac{1}{\rho C_1}\right)$$ III-62

as can be checked by direct substitution. The velocity time history, from equations III-59, III-60, and III-62, becomes

$$\dot{u}(z,t) = \frac{1}{\rho C_1}\left[P\left(t - \frac{z}{C_1}\right) - G\left(t + \frac{z}{C_1}\right) - G\left(t - \frac{z}{C_1}\right)\right] + P_o\left(\frac{1}{\rho C_o} - \frac{1}{\rho C_1}\right)$$ III-63

E. Response of the medium to a con-
    tinuously variable surface pressure

Consider the decreasing surface pressure as shown in fig. III-2. The

64

pressure $P(t)$ rises from zero to P_o at $t = 0$. For $t > 0$, the pressure decays continuously to zero. This surface pressure may be regarded as a step wave of amplitude P_o plus a series of infinitesimal, negative steps, dP. Each pressure change dP may be treated in the manner of the single pressure change from P_o to P_1 of the previous section. When the surface pressure shown in fig. III-2 is applied to the boundary of a semi-infinite body of linear hysteretic material, there will result a term like $P(t - z/C_1)$ (equation III-51) where in this case

$$P\left(t - \frac{z}{C_1}\right) = P_o\, e^{\dfrac{-\left(t - \dfrac{z}{C_1}\right)}{\tau}} \qquad \text{III-64}$$

There will also be a series of contributions like $G(t \pm z/C_1)$ in equation III-52. In the case of the continuously decreasing surface pressure each term of the series in equations III-46 and III-49 will itself be a series. For a time t, the sum of contributions of the first term $f_1(t)$, from equation III-47, will be

$$f_1(t) = \begin{cases} 0 \,, \ t = 0 \\[2mm] \alpha \displaystyle\sum_{t=0}^{t=dt} - dP \,, \ t > 0 \end{cases} \qquad \text{III-65}$$

Integrating equation III-65 over all times for which contributions of the form $f_1(t)$ are different from zero, one obtains

$$f_1(t) = \alpha \int_0^{\alpha t} - \frac{dP}{dt}\, dt = \alpha P_o - \alpha P(\alpha t) \qquad \text{III-66}$$

In the same manner contributions of the form $f_n(t)$ may be written as

$$f_n(t) = \alpha^n P_o - \alpha^n P(\alpha^n t) \qquad\qquad \text{III-67}$$

where

$$P(\alpha^n t) = P_o e^{\dfrac{-\alpha^n t}{\tau}} \qquad\qquad \text{III-68}$$

From equations III-46, III-67, and III-68 the contributions of all the reloading and unloading waves, $G(t \pm z/C_1)$, become

$$G\left(t \pm \frac{z}{C_1}\right) = \sum_{n=1}^{\infty} \alpha^n \left[P_o - P_o\, e^{\dfrac{-\alpha\left(t \pm \frac{z}{C_1}\right)}{\tau}} \right] \qquad \text{III-69}$$

Substituting equations III-64 and III-69 in equations III-52 and III-63 one obtains the following expressions for stress and particle velocity for the continuously variable surface pressure.

$$\sigma(z,t) = P_o\, e^{\dfrac{-\left(t - \frac{z}{C_1}\right)}{\tau}} + P_o \sum_{n=1}^{\infty} \alpha^n \left[e^{\dfrac{-\alpha^n\left(t - \frac{z}{C_1}\right)}{\tau}} - e^{\dfrac{-\alpha^n\left(t + \frac{z}{C_1}\right)}{\tau}} \right] \quad \text{III-70}$$

$$\dot{u}(z,t) = P_o\left(\frac{1}{\rho C_o} - \frac{1}{\rho C_1}\right) + \frac{P_o}{\rho C_1}\, e^{\dfrac{-\left(t - \frac{z}{C_1}\right)}{\tau}} -$$

$$\frac{P_o}{\rho C_1} \left[\sum_{n=1}^{\infty} 2\alpha^n - e^{\dfrac{-\alpha^n\left(t - \frac{z}{C_1}\right)}{\tau}} - e^{\dfrac{-\alpha^n\left(t + \frac{z}{C_1}\right)}{\tau}} \right] \quad \text{III-71}$$

F. Computer program

A computer code is available for the numerical evaluation of equations III-70 and III-71. The results of the code computations are valid for any

66

positive τ and for any α in the range

$$0 \leq \alpha < 1.0 \qquad\qquad \text{III-67}$$

The computations are made for successive times at selected depths so that stress-time and particle velocity-time wave forms can be constructed. Code output is provided in two forms:

Form 1   Attenuation of peak vertical stress and particle velocity
        with depth

        DEPTH (ft)   SIGMAX (psi)   VMAX (fps)

Form 2   Stress and velocity time histories at specified depth

        TIME (sec)   SIGZZ (psi)   VELOCITY (fps)

where

    SIGMAX = Maximum vertical stress at a given depth

      VMAX = Maximum particle velocity at a given depth

     SIGZZ = Vertical stress

  VELOCITY = Particle velocity

The input variables for the code consist of the following:

Variable	Description	Format
EL	Loading modulus (psf) - M_o (fig. III-1)	E 10.2
EU	Unloading modulus (psf) - M_1 (fig. III-1)	E 10.2
POP	Peak applied overpressure (psi) - P_o (fig. III-2)	E 10.2
DM	Mass density (slugs/cu ft) - ρ	E 10.2
TO	Exponential time constant (sec) - τ (fig. III-2)	E 10.2
IZ	Maximum number of depth increments + 1	E 10.2

(Continued)

Variable	Description	Format
DZ	Length of each depth increment (ft)	E 10.2
DT	Time increment	E 10.2
TEND	Time after arrival of the front at each depth at which the program ends (sec)	E 10.2

The first five input variables need no explanation. The selection of ΔZ and IZ specifies the uniform spacing and total number of evenly spaced depths at which output is required. TEND provides a fixed amount of total time-history to be computed at each output depth; since it is referenced to the time of arrival of the front at each depth, computed durations at each depth will be the same. DT regulates the number of history points to be computed between the time of arrival and TEND at each output depth.

The program is written in FORTRAN II card language. Computer time on a GE 225 for a typical problem is approximately three minutes. A complete listing of the program and an example of typical resulting output is presented in Appendix-III.

Figure III-5 shows computed stress-time histories at three different depths for an example problem. This figure shows the principal features of the linear hysteretic model, that is, attenuation of peak stress and the lengthening of the duration of the stress pulse with depth. The attenuation of peak particle velocity is equal to that of stress.
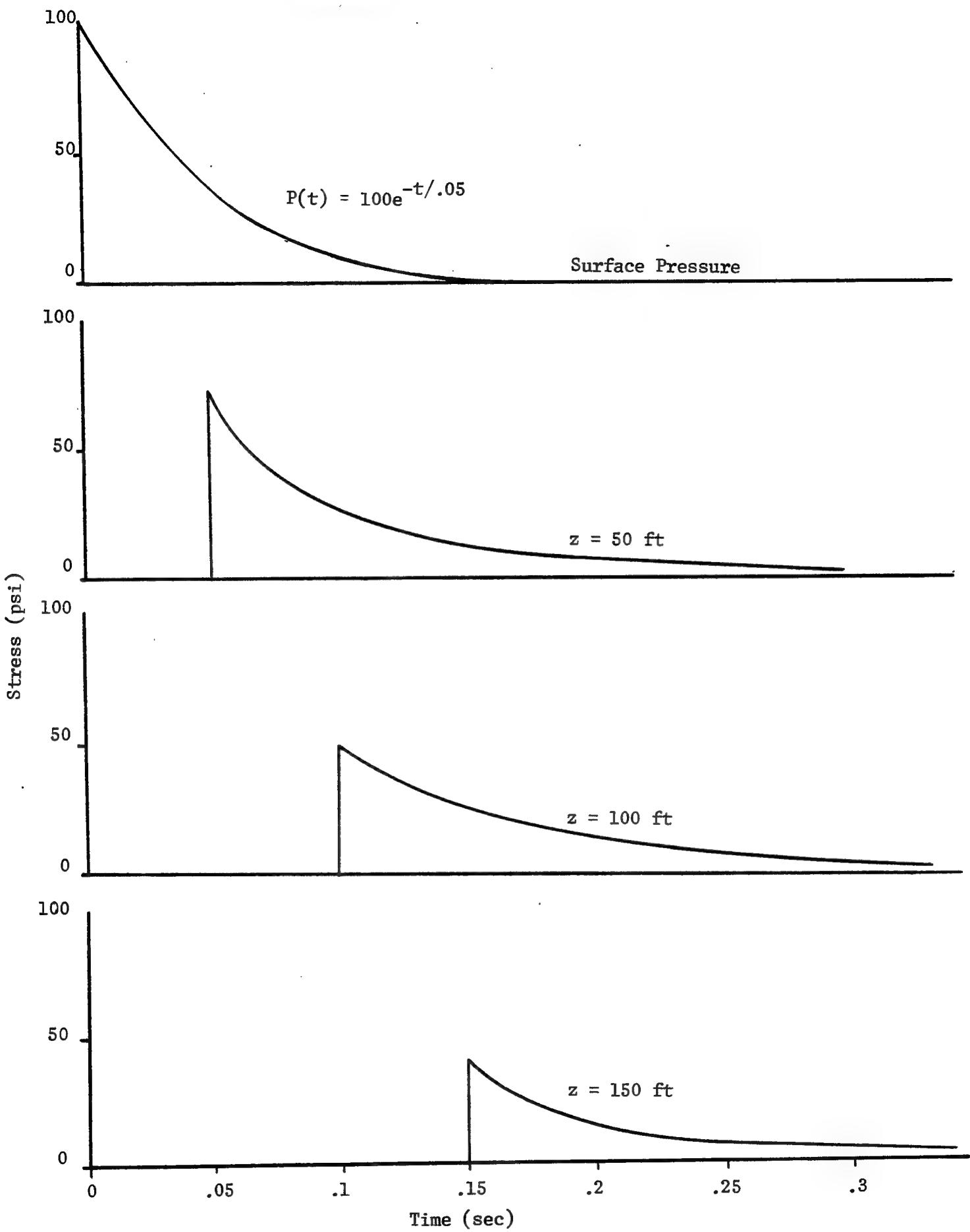
Fig. III-5. Typical stress-time histories for several depths; linear hysteretic model.

69

APPENDIX III

LINEAR HYSTERETIC MODEL

.

```
C       PROGRAM TITLE                                                       01
C       STRESS WAVE PROPAGATION THROUGH A LATERALLY CONSTRAINED COLUMN OF   02
C       LINEAR HYSTERETIC MATERIAL                                          03
C       PROGRAM NO.    41-Z5-093                                            04
C       PROGRAMMER     ROHANI,B                                             05
C       SHORT TITLE 1D LINEAR  HYSTERETIC  MODEL                            06
C                                                                           07
C                               *                    .                      08
C           ASSUMED       S *                      .                        09
C           STRESS        T *                    .                          10
C           STRAIN        R * LOADING  ..                                   11
C           RELATION      E *            .                                  12
C                         S *              . .                              13
C                         S *            .                                  14
C                           *           .    .                              15
C                         P *        .                                      16
C                         S *      .     .  UNLOADING                       17
C                         I *    .                                          18
C                           *  .        .                                   19
C                           * .                                             20
C                          *.        .                                      21
C                         ************************                          22
C                                                                           23
C                                          STRAIN                           24
C       OUTPUT                                                              25
C       PEAK STRESS AND PARTICLE VELOCITY AT DIFFERENT DEPTHS(ATTENUATION   26
C       OF PEAK STRESS AND VELOCITY)                                        261
C       STRESS-TIME AND VELOCITY-TIME HISTORY AT DIFFERENT DEPTH            262
C       REQUIRED INPUT DATA                                                 27
C           EL=LOADING MODULUS(PSF)                                         28
C           EU=UNLOADING MODULUS(PSF)                                       29
C           POP=PEAK OVER PRESSURE(PSI)                                     30
C           DM=MASS DENSITY(SLUGS/CU.FT.)                                   31
C           TO=EXPONENTIAL TIME CONSTANT(SEC)                               32
C           IZ=TOTAL NO. OF DEPTH INCREMENTS+1                              321
C           DZ=DEPTH INCREMENT(FT.)                                         322
C           DT=TIME INCREMENT(SEC)                                          323
C           TEND=TIME AFTER ARRIVAL OF THE FRONT(SEC)                       324
C       GLOSSARY                                                            33
C           ALPHA=THE PARAMETER WHICH CAUSES THE PEAK STRESS TO ATTENUATE   34
C           CU=UNLOADING WAVE VELOCITY(FPS)                                 35
C           CL=LOADING WAVE VELOCITY(FPS)                                   36
C           SIGMAX=PEAK STRESS(PSI)                                         37
C           Z=VARIABLE DEPTH(FT.)                                           38
C       SIGZZ=STRESS(PSI)                                                   381
C       VELOCITY(FPS)                                                       382
C       VMAX=MAX VELOCITY(FPS)                                              383
C           TP=NONDIMENSIONAL ARRIVAL TIME,                                 39
C           TA=TP*TO=ARRIVAL TIME OF THE FRONT(SEC)                         391
C           TFINAL=TEND+TA                                                  392
C       END OF GLOSSARY                                                     40
      9 READ 10,EL,EU,POP,DM,TO,IZ,DZ,DT,TEND                              41
     10 FORMAT(7E10.2)                                                     42
        CL=SQRTF(EL/DM)                                                    43
        CU=SQRTF(EU/DM)                                                    44
```

```
      ALPHA=[1.-[CL/CU]]/[1.+[CL/CU]]                                      45
      PRINT 12,EL,EU,DM,CL,CU,ALPHA                                        451
   12 FORMAT[1H1,21X,5HEL = F10.1,4H PSF,3X,5HEU = F10.1,4H PSF,3X,5HDM    452
     1= F3.1,16H SLGS.PER CU.FT.,//,21X,5HCL = F10.3,4H FPS,3X,5HCU = F1   453
     20.3,4H FPS,3X,8HALPHA = F6.2,//,21X,68HATTENUATION OF PEAK VERTICA   454
     3L STRESS AND PARTICLE VELOCITY WITH DEPTH,//,28X,10HDEPTH[FT.],10X   455
     4,11HSIGMAX[PSI],10X,10HVMAX[FPS] ,//]                               456
      Z=0.                                                                 46
      DO 600 I=1,IZ                                                        47
      TP=Z/[CL*TO]                                                         48
      SIGMAX=POP                                                           49
C                                                                          50
      J=0                                                                  501
  100 K=J+1                                                                502
      TERMSE=-POP*[1.-ALPHA]*[ALPHA**J]*[1.-EXPF[[-2.*TP*ALPHA**K]/[1.+A   51
     1LPHA]]]                                                              52
      IF[ABSF[TERMSE]-0.0005*POP] 120,110,110                              53
  110 CONTINUE                                                             54
      SIGMAX=SIGMAX+TERMSE                                                 55
      J=J+1                                                                56
      GO TO 100                                                            57
  120 SIGMAX=SIGMAX+TERMSE                                                 58
      VMAX=[SIGMAX*144]/[DM*CL]                                            581
      PRINT 11,Z,SIGMAX,VMAX                                               59
      Z=Z+DZ                                                               60
   11 FORMAT[1H ,28X,F5.1,15X,F7.2,15X,F7.2]                               601
  600 CONTINUE                                                             61
C                                                                          62
C                                                                          63
C                                                                          64
C                                                                          65
      Z=0.                                                                 66
      DO 601 N=1,IZ                                                        67
      TA=Z/CL                                                              68
      TFINAL=TEND+TA                                                       69
      PRINT 13,Z,TA                                                        691
  130 FORMAT[1H1,21X,33HSTRESS AND VELOCITY TIME HISTORY.,//,22X,          692
     14HZ = F7.2,3HFT.,5X,5HTA = F7.4,4H SEC,//,22X,9HTIME[SEC],9X,10HSI   693
     2GZZ[PSI],9X,13HVELOCITY[FPS],//]                                     694
      T=TA                                                                 70
   19 SIGZZ=POP*EXPF[-[T-Z/CU]/TO]                                         71
      VV=[POP*EXPF[-[T-Z/CU]/TO]]/[DM*CU]+[POP]/[DM*CL]-[POP]/[DM*CU]      713
      VV=VV*144.                                                           72
      M=1                                                                  73
   20 TERM=POP*2.*[ALPHA**M]*EXPF[-[ALPHA**M]*T/TO]*[EXPF[[ALPHA**M]*Z/[   74
     1TO*CU]]-EXPF[-[ALPHA**M]*Z/[TO*CU]]]/2.                              75
      XX=[[-2.*POP]/[DM*CU]]*[[ALPHA**M]-.5*[ALPHA**M]*[EXPF[-[ALPHA**M]   751
     1*T/TO]]*[EXPF[[ALPHA**M]*Z/[TO*CU]]+EXPF[-[ALPHA**M]*Z/[TO*CU]]]]    752
      XX=XX*144.                                                           753
      IF[ABSF[TERM]-0.0005*POP] 220,210,210                               76
  210 CONTINUE                                                             77
      SIGZZ=SIGZZ+TERM                                                     78
      VV=VV+XX                                                             781
      M=M+1                                                                79
      GO TO 20                                                             80
  220 SIGZZ=SIGZZ+TERM                                                     81
      VV=VV+XX                                                             811
      PRINT 14,T,SIGZZ,VV                                                  82
   14 FORMAT[1H ,21X,F6.4,12X,F7.2,12X,F7.2]                               83
      T=T+DT                                                               831
```

```
          IF(T-TFINAL) 19,19,21                                              84
       21 Z=7+DZ                                                             85
      601 CONTINUE                                                           86
          GO TO 9                                                            87
          END                                                                88
       11437, 17766
```

```
,KP    0000000
/00009 0000007
/00010 0000065
EL     0000004
EU     0000014
POP    0000016
DM     000002C
TO     0000022
IZ     0000024
DZ     0000026
DT     0000030
TEND   0000032
CL     0000034
SQRTF  0140036   EXT PROG
CU     0000040
ALPHA  0000042
1.     0000104
/00012 0000173
Z      0000114
0.     0000116
I      0000120
+00001 0000121
TP     0000122
SIGMAX 0000124
J      0000126
+00000 0000127
/00100 0000356
K      0000130
TERMSE 0000362
,IM    0100364   EXT PROG
EXPF   0140366   EXT PROG
2.     0000370
ABSF   0140404   EXT PROG
0.0005 0000406
/00120 0000503
/00110 0000474
VMAX   0000410
+00144 0000507
/00011 0000571
/00600 0000604
N      0000510
TA     0000512
TFINAL 0000514
/00013 0000635
T      0000516
/00019 0000722
SIGZZ  0000520
VV     0000522
144.   0001022
M      0001024
/00020 0001057
TERM   0001026
XX     0001044
```

```
.5    0001046
/00220 0001360
/00210 0 01346
/00014 0 01400
/00021 0 01423
/00601 0 01426
```

EL   EU   POP   DM   TO   IZ   DZ

DT   TEND

Typical input for the linear hysteretic model

EL = 3110000.0 PSF   EU = 12440000.0 PSF   DM = 3.1 SLGS.PER CU.FT.

CL = 1000.000 FPS   CU = 2000.000 FPS   ALPHA = 0.33

ATTENUATION OF PEAK VERTICAL STRESS AND PARTICLE VELOCITY WITH DEPTH

DEPTH(FT.)	SIGMAX(PSI)	VMAX(FPS)
0.0	100.00	4.63
50.0	69.91	3.24
100.0	50.68	2.35
150.0	38.18	1.77
200.0	29.87	1.38
250.0	24.20	1.12
300.0	20.22	0.94
350.0	17.32	0.80
400.0	15.15	0.70

TYPICAL CODE OUTPUT, LINEAR HYSTERETIC MODEL

STRESS AND VELOCITY TIME HISTORY.

Z =   0.00FT.   TA = 0.0000 SEC

TIME[SEC]	SIGZZ[PSI]	VELOCITY[FPS]
0.0000	100.00	4.63
0.0100	81.87	4.11
0.0200	67.03	3.67
0.0300	54.88	3.31
0.0400	44.93	2.99
0.0500	36.79	2.73
0.0600	30.12	2.50
0.0700	24.66	2.31
0.0800	20.19	2.14
0.0900	16.53	2.00
0.1000	13.53	1.88
0.1100	11.08	1.77
0.1200	9.07	1.68
0.1300	7.43	1.59
0.1400	6.08	1.52
0.1500	4.98	1.45
0.1600	4.08	1.40
0.1700	3.34	1.35
0.1800	2.73	1.30
0.1900	2.24	1.26
0.2000	1.83	1.22
0.2100	1.50	1.19
0.2200	1.23	1.16
0.2300	1.01	1.13
0.2400	0.82	1.10
0.2500	0.67	1.08
0.2600	0.55	1.06
0.2700	0.45	1.04
0.2800	0.37	1.02
0.2900	0.30	1.00
0.3000	0.25	0.99
0.3100	0.20	0.97
0.3200	0.17	0.96
0.3300	0.14	0.95
0.3400	0.11	0.93
0.3500	0.09	0.92
0.3600	0.07	0.91
0.3700	0.06	0.90
0.3800	0.05	0.90
0.3900	0.04	0.89
0.4000	0.03	0.88

TYPICAL CODE OUTPUT, LINEAR HYSTERETIC MODEL

STRESS AND VELOCITY TIME HISTORY.

Z =   50.00FT.   TA =   0.0500 SEC

TIME(SEC)	SIGZZ(PSI)	VELOCITY(FPS)
0.0500	69.90	3.24
0.0600	58.37	2.90
0.0700	48.86	2.61
0.0800	41.01	2.37
0.0900	34.53	2.16
0.1000	29.18	1.98
0.1100	24.74	1.82
0.1200	21.06	1.69
0.1300	18.00	1.57
0.1400	15.46	1.46
0.1500	13.34	1.37
0.1600	11.56	1.29
0.1700	10.08	1.22
0.1800	8.83	1.15
0.1900	7.78	1.10
0.2000	6.89	1.04
0.2100	6.13	1.00
0.2200	5.49	0.95
0.2300	4.94	0.91
0.2400	4.46	0.88
0.2500	4.06	0.84
0.2600	3.70	0.81
0.2700	3.39	0.78
0.2800	3.12	0.75
0.2900	2.89	0.73
0.3000	2.68	0.70
0.3100	2.49	0.68
0.3200	2.32	0.66
0.3300	2.18	0.64
0.3400	2.04	0.62
0.3500	1.92	0.61
0.3600	1.81	0.59
0.3700	1.71	0.57
0.3800	1.62	0.56
0.3900	1.53	0.54
0.4000	1.45	0.53
0.4100	1.38	0.52
0.4200	1.32	0.50
0.4300	1.25	0.49
0.4400	1.20	0.48
0.4500	1.14	0.47

TYPICAL CODE OUTPUT, LINEAR HYSTERETIC MODEL

STRESS AND VELOCITY TIME HISTORY.

Z =   100.00FT.   TA =   0.1000 SEC

TIME(SEC)	SIGZZ(PSI)	VELOCITY(FPS)
0.1000	50.68	2.35
0.1100	43.21	2.13
0.1200	37.01	1.94
0.1300	31.84	1.78
0.1400	27.52	1.64
0.1500	23.91	1.52
0.1600	20.88	1.42
0.1700	18.33	1.32
0.1800	16.17	1.24
0.1900	14.35	1.17
0.2000	12.80	1.11
0.2100	11.47	1.05
0.2200	10.34	1.00
0.2300	9.36	0.95
0.2400	8.52	0.91
0.2500	7.78	0.87
0.2600	7.14	0.84
0.2700	6.58	0.80
0.2800	6.09	0.77
0.2900	5.65	0.75
0.3000	5.26	0.72
0.3100	4.91	0.70
0.3200	4.59	0.67
0.3300	4.31	0.65
0.3400	4.05	0.63
0.3500	3.82	0.62
0.3600	3.61	0.60
0.3700	3.41	0.58
0.3800	3.23	0.57
0.3900	3.07	0.55
0.4000	2.91	0.54
0.4100	2.77	0.52
0.4200	2.64	0.51
0.4300	2.52	0.50
0.4400	2.40	0.49
0.4500	2.29	0.48
0.4600	2.19	0.46
0.4700	2.10	0.45
0.4800	2.01	0.44
0.4900	1.93	0.44
0.5000	1.85	0.43

TYPICAL CODE OUTPUT, LINEAR HYSTERETIC MODEL

STRESS AND VELOCITY TIME HISTORY.

Z =   150.00FT.   TA =   0.1500 SEC

TIME(SEC)	SIGZZ(PSI)	VELOCITY(FPS)
0.1500	38.17	1.77
0.1600	33.24	1.62
0.1700	29.10	1.50
0.1800	25.61	1.39
0.1900	22.66	1.30
0.2000	20.15	1.21
0.2100	18.02	1.14
0.2200	16.19	1.08
0.2300	14.62	1.02
0.2400	13.27	0.97
0.2500	12.10	0.92
0.2600	11.08	0.88
0.2700	10.19	0.84
0.2800	9.40	0.81
0.2900	8.71	0.78
0.3000	8.09	0.75
0.3100	7.55	0.72
0.3200	7.05	0.70
0.3300	6.61	0.67
0.3400	6.21	0.65
0.3500	5.85	0.63
0.3600	5.52	0.61
0.3700	5.21	0.59
0.3800	4.93	0.58
0.3900	4.68	0.56
0.4000	4.44	0.55
0.4100	4.22	0.53
0.4200	4.02	0.52
0.4300	3.83	0.51
0.4400	3.65	0.49
0.4500	3.49	0.48
0.4600	3.34	0.47
0.4700	3.19	0.46
0.4800	3.06	0.45
0.4900	2.93	0.44
0.5000	2.81	0.43
0.5100	2.70	0.42
0.5200	2.59	0.41
0.5300	2.49	0.41
0.5400	2.40	0.40
0.5500	2.31	0.39

TYPICAL CODE OUTPUT, LINEAR HYSTERETIC MODEL

STRESS AND VELOCITY TIME HISTORY.

Z = 200.00FT.   TA = 0.2000 SEC

TIME[SEC]	SIGZZ[PSI]	VELOCITY[FPS]
0.2000	29.87	1.38
0.2100	26.53	1.29
0.2200	23.69	1.20
0.2300	21.26	1.13
0.2400	19.18	1.06
0.2500	17.39	1.00
0.2600	15.83	0.95
0.2700	14.49	0.90
0.2800	13.31	0.86
0.2900	12.27	0.82
0.3000	11.36	0.79
0.3100	10.55	0.76
0.3200	9.83	0.73
0.3300	9.19	0.70
0.3400	8.61	0.68
0.3500	8.08	0.66
0.3600	7.61	0.63
0.3700	7.18	0.61
0.3800	6.78	0.60
0.3900	6.42	0.58
0.4000	6.09	0.56
0.4100	5.78	0.55
0.4200	5.50	0.53
0.4300	5.23	0.52
0.4400	4.99	0.51
0.4500	4.76	0.49
0.4600	4.54	0.48
0.4700	4.34	0.47
0.4800	4.16	0.46
0.4900	3.98	0.45
0.5000	3.82	0.44
0.5100	3.66	0.43
0.5200	3.52	0.42
0.5300	3.38	0.41
0.5400	3.25	0.40
0.5500	3.13	0.40
0.5600	3.01	0.39
0.5700	2.90	0.38
0.5800	2.80	0.37
0.5900	2.70	0.37
0.6000	2.60	0.36

TYPICAL CODE OUTPUT, LINEAR HYSTERETIC MODEL

STRESS AND VELOCITY TIME HISTORY.

Z = 250.00FT.   TA = 0.2500 SEC

TIME(SEC)	SIGZZ(PSI)	VELOCITY(FPS)
0.2500	24.20	1.12
0.2600	21.87	1.05
0.2700	19.86	0.99
0.2800	18.12	0.94
0.2900	16.60	0.89
0.3000	15.28	0.85
0.3100	14.11	0.81
0.3200	13.08	0.78
0.3300	12.17	0.74
0.3400	11.36	0.72
0.3500	10.62	0.69
0.3600	9.97	0.66
0.3700	9.37	0.64
0.3800	8.83	0.62
0.3900	8.34	0.60
0.4000	7.89	0.58
0.4100	7.48	0.57
0.4200	7.10	0.55
0.4300	6.74	0.54
0.4400	6.42	0.52
0.4500	6.12	0.51
0.4600	5.84	0.49
0.4700	5.57	0.48
0.4800	5.33	0.47
0.4900	5.10	0.46
0.5000	4.88	0.45
0.5100	4.68	0.44
0.5200	4.49	0.43
0.5300	4.31	0.42
0.5400	4.14	0.41
0.5500	3.98	0.40
0.5600	3.83	0.40
0.5700	3.69	0.39
0.5800	3.56	0.38
0.5900	3.43	0.37
0.6000	3.31	0.37
0.6100	3.19	0.36
0.6200	3.09	0.35
0.6300	2.98	0.35
0.6400	2.88	0.34
0.6500	2.79	0.34

TYPICAL CODE OUTPUT, LINEAR HYSTERETIC MODEL

STRESS AND VELOCITY TIME HISTORY.

Z = 3?0.00FT.   TA = 0.3000 SEC

TIME(SEC)	SIGZZ(PSI)	VELOCITY(FPS)
0.3000	20.21	0.94
0.3100	18.53	0.89
0.3200	17.07	0.84
0.3300	15.78	0.80
0.3400	14.64	0.77
0.3500	13.63	0.74
0.3600	12.72	0.71
0.3700	11.91	0.68
0.3800	11.18	0.66
0.3900	10.52	0.63
0.4000	9.93	0.61
0.4100	9.38	0.59
0.4200	8.88	0.57
0.4300	8.42	0.56
0.4400	8.00	0.54
0.4500	7.61	0.53
0.4600	7.24	0.51
0.4700	6.91	0.50
0.4800	6.60	0.49
0.4900	6.30	0.47
0.5000	6.03	0.46
0.5100	5.77	0.45
0.5200	5.53	0.44
0.5300	5.31	0.43
0.5400	5.10	0.42
0.5500	4.90	0.41
0.5600	4.71	0.41
0.5700	4.53	0.40
0.5800	4.36	0.39
0.5900	4.20	0.38
0.6000	4.05	0.37
0.6100	3.91	0.37
0.6200	3.78	0.36
0.6300	3.65	0.35
0.6400	3.53	0.35
0.6500	3.41	0.34
0.6600	3.30	0.34
0.6700	3.19	0.33
0.6800	3.09	0.33
0.6900	3.00	0.32
0.7000	2.91	0.32

TYPICAL CODE OUTPUT, LINEAR HYSTERETIC MODEL

STRESS AND VELOCITY TIME HISTORY.

Z = 350.00FT.   .   TA = 0.3500 SEC

TIME(SEC)	SIGZ7(PSI)	VELOCITY(FPS)
0.3500	17.32	0.80
0.3600	16.07	0.77
0.3700	14.96	0.73
0.3800	13.98	0.70
0.3900	13.09	0.68
0.4000	12.29	0.65
0.4100	11.57	0.63
0.4200	10.92	0.61
0.4300	10.32	0.59
0.4400	9.78	0.57
0.4500	9.28	0.55
0.4600	8.82	0.54
0.4700	8.39	0.52
0.4800	8.00	0.51
0.4900	7.63	0.49
0.5000	7.29	0.48
0.5100	6.97	0.47
0.5200	6.67	0.46
0.5300	6.39	0.45
0.5400	6.13	0.44
0.5500	5.88	0.43
0.5600	5.65	0.42
0.5700	5.43	0.41
0.5800	5.23	0.40
0.5900	5.03	0.39
0.6000	4.85	0.38
0.6100	4.67	0.38
0.6200	4.51	0.37
0.6300	4.35	0.36
0.6400	4.20	0.36
0.6500	4.06	0.35
0.6600	3.93	0.34
0.6700	3.80	0.34
0.6800	3.68	0.33
0.6900	3.57	0.33
0.7000	3.46	0.32
0.7100	3.35	0.32
0.7200	3.25	0.31
0.7300	3.16	0.31
0.7400	3.07	0.30
0.7500	2.98	0.30

TYPICAL CODE OUTPUT, LINEAR HYSTERETIC MODEL

STRESS AND VELOCITY TIME HISTORY.

Z = 400.00FT.   TA = 0.4000 SEC

TIME[SEC]	SIGZZ[PSI]	VELOCITY[FPS]
0.4000	15.15	0.70
0.4100	14.19	0.67
0.4200	13.33	0.65
0.4300	12.55	0.62
0.4400	11.84	0.60
0.4500	11.20	0.58
0.4600	10.61	0.56
0.4700	10.07	0.55
0.4800	9.57	0.53
0.4900	9.11	0.52
0.5000	8.69	0.50
0.5100	8.29	0.49
0.5200	7.92	0.48
0.5300	7.58	0.46
0.5400	7.26	0.45
0.5500	6.96	0.44
0.5600	6.68	0.43
0.5700	6.41	0.42
0.5800	6.16	0.41
0.5900	5.92	0.40
0.6000	5.70	0.40
0.6100	5.49	0.39
0.6200	5.30	0.38
0.6300	5.11	0.37
0.6400	4.93	0.37
0.6500	4.76	0.36
0.6600	4.60	0.35
0.6700	4.45	0.35
0.6800	4.30	0.34
0.6900	4.17	0.33
0.7000	4.04	0.33
0.7100	3.91	0.32
0.7200	3.79	0.32
0.7300	3.68	0.31
0.7400	3.57	0.31
0.7500	3.47	0.30
0.7600	3.37	0.30
0.7700	3.27	0.29
0.7800	3.18	0.29
0.7900	3.10	0.29
0.8000	3.02	0.28

TYPICAL CODE OUTPUT, LINEAR HYSTERETIC MODEL

Stress Wave Propagation Through a Laterally Confined
Column of Visco-Elastic Hysteretic Material

A. Introduction

Dynamic compression and wave propagation tests have indicated that
some soils, like clay, exhibit both strain-rate and hysteretic effects.
Increase in modulus with strain-rate and lag of maximum strain behind
maximum stress, an indication of viscous behavior, have been observed by
many investigators (17,24) during dynamic compression tests of some soils.
Smoothing of the stress pulse during one-dimensional wave propagation
tests also supports the viscous behavior of such materials. In order to
predict wave propagation phenomena in such soils a mathematical model
should be constructed to account for both the hysteretic energy loss
and the viscous behavior of soils. The viscous behavior of materials is
frequently represented in terms of rheological models consisting of linear
springs and dashpots. Three types of such models were discussed in
Chapter II and the stress-strain-time relationships for each model were
derived in terms of the spring constants and the viscosities of the dashpots
(equations II-60, II-64, II-68). It is a difficult task to decide
which of these models would best describe the viscous behavior of soils.
In fact, no single model can describe viscous phenomena in all
soils. The limited research performed in this area (19) has indicated
that the three element standard linear visco-elastic model (fig. II-7) may
be used to describe the viscous behavior of some clays and sands within cer-
tain ranges of boundary and loading conditions. Further experimental work
is required in this area if rational rheological models are to be constructed

which will describe the viscous phenomena of soils more accurately and over a broader range of boundary and loading conditions. For the present analysis however, the standard linear visco-elastic model will be used to describe strain-rate effects. The "correspondence principle," described in Chapter II, will be utilized to obtain visco-elastic solutions from equations III-70 and III-71 for stress and particle velocity in a linear hysteretic halfspace subjected to a uniform time-dependent pressure wave at its surface. The solution for any other linear rheological model may be obtained by the same procedure. The linear hysteretic model is used here to account for the hysteretic energy loss of the soil.

B. Formulation and solution of the problem

The linear hysteretic model was analyzed in Chapter III. The following expressions were obtained for particle velocity and stress within the medium (subjected to an exponentially decaying input shock) as functions of time:

$$\dot{u}(z,t) = P_o\left(\frac{1}{\rho C_o} - \frac{1}{\rho C_1}\right) + \frac{P_o}{\rho C_1} e^{-(t - z/C_1)/\tau}$$

$$- \frac{P_o}{\rho C_1}\left[\sum_{n=1}^{\infty} 2\alpha^n - e^{-\alpha^n(t - z/C_1)/\tau} - e^{-\alpha^n(t + z/C_1)/\tau}\right] \qquad \text{IV-1}$$

$$\sigma(z,t) = P_o e^{-(t - z/C_1)/\tau} + P_o \sum_{n=1}^{\infty} \alpha^n\left[e^{-\alpha^n(t - z/C_1)/\tau}\right.$$

$$\left. - e^{-\alpha^n(t - z/C_1)/\tau}\right] \qquad \text{IV-2}$$

where

$\dot{u}(z,t)$ = particle velocity at depth z and time t

$\sigma(z,t)$ = stress at depth z and time t

where

$$e = 2.7183...$$

P_o = peak applied stress

C_1 = unloading reloading wave velocity

C_o = loading wave velocity

$$\alpha = \frac{C_1/C_o - 1}{C_1/C_o + 1}$$

τ = exponential decay constant of the input stress pulse

ρ = mass density of the medium

The front of the wave propagates with the loading wave velocity C_o and reaches the point z at the time $t = z/C_o$. The medium at z is undisturbed for times $t < z/C_o$ therefore, the one-sided Fourier transforms (equation II-75) of equations IV-1 and IV-2 are non-zero when

$$z/C_o \leqslant t \leqslant \infty \qquad\qquad \text{IV-3}$$

The first step in the "correspondence principle" is to evaluate the one-sided Fourier transforms of equations IV-1 and IV-2 within the limits given by equation IV-3

$$\dot{u}(\omega) = \int_{z/C_o}^{\infty} e^{-i\omega t} \, \dot{u}(z,t) \, dt \qquad\qquad \text{IV-4}$$

$$\sigma(\omega) = \int_{z/C_o}^{\infty} e^{-i\omega t} \, \sigma(z,t) \, dt \qquad\qquad \text{IV-5}$$

where $\dot{u}(\omega)$ and $\sigma(\omega)$ are the one-sided Fourier transforms of particle velocity and stress respectively. Substituting for $\dot{u}(z,t)$ and $\sigma(z,t)$ from equations IV-1 and IV-2 and integrating one obtains
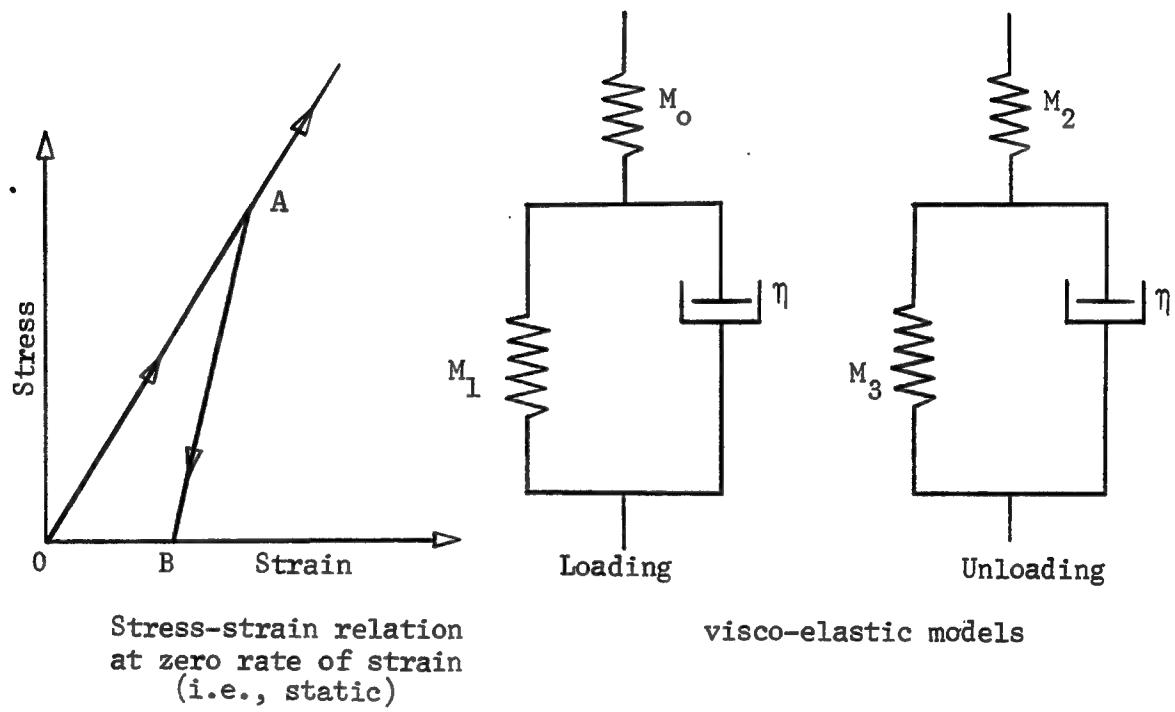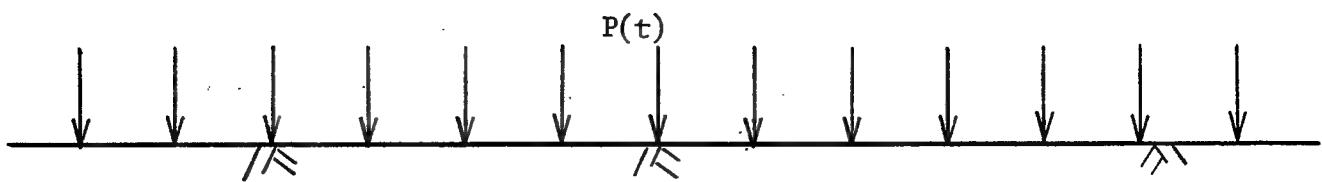
Fig. IV-1. Rate-dependent model for the linear-hysteretic medium.

89

$$\dot{u}(\omega) = S_o \sum_{n=o}^{\infty} \frac{1}{\dfrac{\alpha^n}{\tau} + i\omega} \lambda_1$$

$$+ S_o \left[\sum_{n=1}^{\infty} \frac{1}{\dfrac{\alpha^n}{\tau} + i\omega} \lambda_2 - \frac{2\alpha^n \lambda_o}{i\omega} \right] + \frac{S_1 \lambda_o}{i\omega} \qquad \text{IV-6}$$

and

$$\sigma(\omega) = P_o \sum_{n=o}^{\infty} \frac{\alpha^n}{\dfrac{\alpha^n}{\tau} + i\omega} \lambda_1 - P_o \sum_{n=1}^{\infty} \frac{\alpha^n}{\dfrac{\alpha^n}{\tau} + i\omega} \lambda_2 \qquad \text{IV-7}$$

where

$$S_o = \frac{P_o}{\rho C_1}$$

$$S_1 = P_o \left(\frac{1}{\rho C_o} - \frac{1}{\rho C_1} \right)$$

$$\lambda_o = e^{-\,i\omega z/C_o} \qquad\qquad \text{IV-8}$$

$$\lambda_1 = e^{-\left[i\omega z + \alpha^n z/\tau \left(1 - \dfrac{C_o}{C_1} \right) \right] /C_o}$$

$$\lambda_2 = e^{-\left[i\omega z + \alpha^n z/\tau \left(1 + \dfrac{C_o}{C_1} \right) \right] /C_o}$$

The second step is replace the elastic constants C_o and C_1 in equations
IV-6 and IV-7 by $\left[\rho J_o(i\omega) \right]^{-1/2}$ and $\left[\rho J_1(i\omega) \right]^{-1/2}$ respectively, where
$J_o(i\omega)$ and $J_1(i\omega)$ are the visco-elastic complex compliances of the segments
OA and AB of the hysteretic stress-strain curve shown in fig. IV-1. An
assumption will be made here to reduce the number of parameters and simplify
the analysis, that is

$$\frac{J_o(i\omega)}{J_1(i\omega)} = \left(\frac{C_1}{C_o}\right)^2 \qquad\qquad \text{IV-11}$$

The complex compliance of the standard linear model was given in Chapter II by

$$J_o(i\omega) = \frac{1}{M_o} + \frac{M_1}{M_1^2 + \omega^2\eta^2} - \frac{i}{\omega\eta}\left(1 - \frac{M_1^2}{M_1^2 + \omega^2\eta^2}\right) \qquad \text{IV-12}$$

If one introduces the notation

$$\phi = \frac{M_1}{M_o}$$

$$\mu = \eta/M_o \qquad\qquad \text{IV-13}$$

$$\beta = C_o/C_1$$

then

$$\sqrt{\rho J_o(i\omega)} = \sqrt{\rho/M_o}\sqrt{1 + \frac{\phi}{\phi^2 + \omega^2\mu^2} - \frac{i\omega\mu}{\phi^2 + \omega^2\mu^2}} \qquad \text{IV-14}$$

Equation IV-14 can be written in terms of its real and imaginary parts as follows

$$\sqrt{\rho J_o(i\omega)} = k_1(\omega) - ik_2(\omega) \qquad\qquad \text{IV-15}$$

where $k_1(\omega)$ and $k_2(\omega)$ are the real and imaginary parts of $\sqrt{\rho J_o(i\omega)}$. From equations IV-11 and IV-15, the elastic constants C_o and C_1 should then be replaced by

$$\left[\rho J_o(i\omega)\right]^{-1/2} = \frac{1}{k_1(\omega) - ik_2(\omega)} \qquad\qquad \text{IV-16}$$

and

$$\left[\rho J_1(i\omega)\right]^{-1/2} = \frac{1}{\beta}\frac{1}{k_1(\omega) - ik_2(\omega)} \qquad\qquad \text{IV-17}$$

respectively. Therefore the parameters λ_o , λ_1 , λ_3 , S_o and S_1 in equation IV-8 become

$$\lambda_o = e^{-i\omega\left[zk_1(\omega)-izk_2(\omega)\right]}$$

$$\lambda_1 = e^{-\left[\omega zk_2(\omega)+k_1(\omega)\frac{\alpha^n z}{\tau}(1-\beta)\right]+i\omega\left[-zk_1(\omega)+k_2(\omega)\frac{\alpha^n z}{\tau\omega}(1-\beta)\right]}$$

$$\lambda_2 = e^{-\left[\omega zk_2(\omega)+k_1(\omega)\frac{\alpha^n z}{\tau}(1+\beta)\right]+i\omega\left[-zk_1(\omega)+k_2(\omega)\frac{\alpha^n z}{\tau\omega}(1+\beta)\right]} \qquad \text{IV-18}$$

$$S_o = \frac{P_o}{\rho}\beta\left[k_1(\omega) - ik_2(\omega)\right]$$

$$S_1 = \frac{P_o}{\rho}(1-\beta)\left[k_1(\omega) - ik_2(\omega)\right]$$

The third and the final step in obtaining the visco-elastic solution is to take the inverse transforms of equations IV-6 and IV-7 (see equation II-76) with parameters S_o , S_1 , λ_o , λ_1 , and λ_2 given by equation IV-18 and then choose the real parts of the transforms, that is

$$\dot{u}(z,t) = \frac{1}{\pi}R\left[\int_o^\infty e^{i\omega t}\ \dot{u}(\omega)\ d\omega\right] \qquad\qquad \text{IV-19}$$

$$\sigma(z,t) = \frac{1}{\pi}R\left[\int_o^\infty e^{i\omega t}\ \sigma(\omega)\ d\omega\right] \qquad\qquad \text{IV-20}$$

where R denotes the real part of the expression in brackets. From the

theory of integration of a complex-valued function (15) equations IV-19
and IV-20 can be written in the following forms.

$$\dot{u}(z,t) = \frac{1}{\pi} \int_{0}^{\infty} R\left[e^{i\omega t} \, \dot{u}(\omega)\right] d\omega \qquad\qquad \text{IV-21}$$

$$\sigma(z,t) = \frac{1}{\pi} \int_{0}^{\infty} R\left[e^{i\omega t} \, \sigma(\omega)\right] d\omega \qquad\qquad \text{IV-22}$$

The functions $R\left[e^{i\omega t} \, \dot{u}(\omega)\right]$ and $R\left[e^{i\omega t} \, \sigma(\omega)\right]$ are determined from equations IV-6, IV-7, and IV-18 by using Euler's formula, $e^{i\theta} = \cos\theta + i\sin\theta$, and selecting the real part of each expression. The process is lengthy but straight forward; as an example, the real part of the first term in equation IV-6 will be calculated here

$$R_1 = R\left[e^{i\omega t} \, S_o \, \frac{1}{\frac{\alpha^n}{\tau} + i\omega} \, \lambda_1\right] = R\left[\frac{1}{\frac{\alpha^{2n}}{\tau^2} + \omega^2} \, S_o \lambda_1 e^{i\omega t} \left(\frac{\alpha^n}{\tau} - \omega\right)\right] \qquad \text{IV-23}$$

Substituting for S_o and λ_1 from equation IV-18 and simplifying, one obtains

$$R_1 = R\left\{\frac{\frac{P_o}{\rho} \beta\left[k_1(\omega) - ik_2(\omega)\right]\left[\frac{\alpha^n}{\tau} - i\omega\right] e^{-A} \, e^{i\omega B}}{\frac{\alpha^{2n}}{\tau^2} + \omega^2}\right\} \qquad \text{IV-24}$$

where

$$A = \omega z k_2(\omega) + k_1(\omega) \frac{\alpha^n z}{\tau} (1 - \beta) \qquad\qquad \text{IV-25}$$

$$B = t - z k_1(\omega) + k_2(\omega) \frac{\alpha^n z}{\omega \tau} (1 - \beta) \qquad\qquad \text{IV-26}$$

Substituting Euler's formula

$$e^{i\omega B} = \cos \omega B + i \sin \omega B \qquad \text{IV-27}$$

into equation IV-24 and simplifying, obtains

$$R_1 = R\left(\frac{\frac{P_o}{\rho}\beta e^{-A}\left\{\left[k_1(\omega)\frac{\alpha^n}{\tau} - \omega k_2(\omega)\right]\cos\omega B + \left[k_2(\omega)\frac{\alpha^n}{\tau} + \omega k_1(\omega)\right]\sin\omega B\right\}}{\frac{\alpha^{2n}}{\tau^2} + \omega^2}\right.$$

$$+ \left.\frac{i\frac{P_o\beta}{\rho}e^{-A}\left\{\left[-k_2(\omega)\frac{\alpha^n}{\tau} - \omega k_1(\omega)\right]\cos\omega B + \left[k_1(\omega)\frac{\alpha^n}{\tau} - \omega k_2(\omega)\right]\sin\omega B\right\}}{\frac{\alpha^{2n}}{\tau^2} + \omega^2}\right) \qquad \text{IV-28}$$

or

$$R_1 = \frac{\frac{P_o}{\rho}\beta e^{-A}\left\{\left[k_1(\omega)\frac{\alpha^n}{\tau} - \omega k_2(\omega)\right]\cos\omega B + \left[k_2(\omega)\frac{\alpha^n}{\tau} + \omega k_1(\omega)\right]\sin\omega B\right\}}{\frac{\alpha^{2n}}{\tau^2} + \omega^2} \qquad \text{IV-29}$$

Following the same procedure and substituting the values of $R\left[e^{i\omega t}\,\dot{u}(\omega)\right]$
and $R\left[e^{i\omega t}\,\sigma(\omega)\right]$ in equations IV-21 and IV-22, one obtains the following general expressions for the particle velocity and stress in the viscoelastic hysteretic medium shown in fig. IV-1.

94

$$\dot{u}(z,t) = \frac{P_o \beta}{\rho \pi} \sum_{n=o}^{\infty} \int_o^{\infty} \frac{e^{-A}\left\{\left[k_1(\omega)\frac{\alpha^n}{\tau} - \omega k_2(\omega)\right] \cos \omega B + \left[k_2(\omega)\frac{\alpha^n}{\tau} + \omega k_1(\omega)\right] \sin \omega B\right\}}{\frac{\alpha^{2n}}{\tau^2} + \omega^2} \, d\omega$$

$$+ \frac{P_o \beta}{\rho \pi} \sum_{n=1}^{\infty} \int_o^{\infty} \frac{e^{-A_1}\left\{\left[k_1(\omega)\frac{\alpha^n}{\tau} - \omega k_2(\omega)\right] \cos \omega B_1 + \left[k_2(\omega)\frac{\alpha^n}{\tau} + \omega k_1(\omega)\right] \sin \omega B_1\right\}}{\frac{\alpha^{2n}}{\tau^2} + \omega^2} \, d\omega$$

$$+ \frac{P_o \beta}{\rho \pi} \sum_{n=1}^{\infty} 2\alpha^n \int_o^{\infty} \frac{e^{-\omega z k_2(\omega)}}{\omega} \left\{ k_2(\omega) \cos \omega \left[t - z k_1(\omega)\right] - k_1(\omega) \sin \omega \left[t - z k_1(\omega)\right] \right\} \, d\omega$$

$$- \frac{P_o(1 - \beta)}{\pi \rho} \int_o^{\infty} \frac{e^{-\omega z k_2(\omega)}}{\omega} \left\{ k_2(\omega) \cos\omega\left[t - z k_1(\omega)\right] - k_1(\omega) \sin \omega \left[t - z k_1(\omega)\right] \right\} \, d\omega \qquad \text{IV-30}$$

and

$$\sigma(z,t) = \frac{P_o}{\pi} \sum_{n=0}^{\infty} n \int_o^{\infty} \frac{e^{-A_1}\left(\frac{\alpha^n}{\tau}\cos \omega B + \omega \sin \omega B\right)}{\frac{\alpha^{2n}}{\tau^2} + \omega^2}\, d\omega$$

$$- \frac{P_o}{\pi} \sum_{n=1}^{\infty} \alpha^n \int_o^{\infty} \frac{e^{-A_1}\left(\frac{\alpha^n}{\tau}\cos \omega B_1 + \omega \sin \omega B_1\right)}{\frac{\alpha^{2n}}{\tau^2} + \omega^2}\, d\omega \qquad \text{IV-31}$$

where

$$A_1 = \omega z k_2(\omega) + k(\omega) \frac{\alpha^n z}{\tau}(1+\beta) \qquad \text{IV-32}$$

$$B_1 = t - z k_1(\omega) + k_2(\omega) \frac{\alpha^n z}{\tau}(1+\beta) \qquad \text{IV-33}$$

and A and B are given by equations IV-25 and IV-26 respectively.

C. Evaluation of $k_1(\omega)$ and $k_2(\omega)$

To evaluate equations IV-30 and IV-31, one must know $k_1(\omega)$ and $k_2(\omega)$, the real and imaginary parts of $\sqrt{\rho J_o(i\omega)}$ (equation IV-14). This can be accomplished if equation IV-14 is written in the polar form of a complex number. The polar form of a complex number, $z = x \pm iy$, is given as $z = r(\cos\theta \pm i \sin\theta)$ where $r = \sqrt{x^2 + y^2}$ and $\theta = \tan^{-1}\frac{y}{x}$. Therefore,

$$\rho J_o(i\omega) = \frac{\rho}{M_o}\left(1 + \frac{\phi}{\phi^2 + \omega^2 \mu^2} - \frac{i\omega\mu}{\phi^2 + \omega^2 \mu^2}\right)$$

$$= \frac{\rho}{M_o} r(\cos\theta - i\sin\theta) \qquad \text{IV-34}$$

where

$$r = \left[\left(1 + \frac{\phi}{\phi^2 + \omega^2 \mu^2}\right)^2 + \left(\frac{\omega u}{\phi^2 + \omega^2 \mu^2}\right)^2\right]^{1/2} \qquad \text{IV-35}$$

96

$$\theta = \tan^{-1}\left(\frac{\omega\mu}{\phi^2 + \omega^2\mu^2 + \phi}\right) \qquad \text{IV-36}$$

or

$$\sqrt{\rho J_o(i\omega)} = \sqrt{\rho/M_o} \ \sqrt{r}\ (\cos\theta - i\sin\theta)^{1/2} \qquad \text{IV-37}$$

Since $(\cos\theta - i\sin\theta)^{1/2} = e^{-i\theta/2} = \cos\frac{\theta}{2} - i\sin\frac{\theta}{2}$, equation IV-37

becomes

$$\sqrt{\rho J_o(i\omega)} = \sqrt{\rho/M_o}\ \sqrt{r}\ \left(\cos\frac{\theta}{2} - i\sin\frac{\theta}{2}\right) \qquad \text{IV-38}$$

The real and imaginary parts of $\sqrt{\rho J_o(i\ )}$ are therefore

$$k_1(\omega) = \sqrt{\rho/M_o}\ \sqrt{r}\ \ \cos\frac{\theta}{2} \qquad \text{IV-39}$$

and

$$k_2(\omega) = \sqrt{\rho/M_o}\ \sqrt{r}\ \sin\frac{\theta}{2} \qquad \text{IV-40}$$

respectively.

D. <u>Determination of visco-elastic parameters for application to</u>

   <u>soil problems.</u>

There are five material constants for the linear hysteretic visco-
elastic model under consideration which have to be determined experi-
mentally, they are

$$\phi = \frac{M_1}{M_o}$$

$$\mu = \eta/M_o$$

$$\beta = \frac{C_o}{C_1} \qquad \text{IV-41}$$

$$\alpha = \frac{C_1/C_o - 1}{C_1/C_o + 1}$$

$$\text{wave velocity} = \sqrt{M_o/\rho}$$

97

The visco-elastic parameters ϕ and μ can be determined from a dynamic uniaxial strain test in which a step loading is applied and the resultant strain-time history is measured (fig. IV-2). The strain response of the three-element visco-elastic material to a step pulse $\Delta\sigma_s$, from equation II-68, is given as

$$\Delta\sigma_s = \frac{M_1 M_o}{M_1 + M_o} \epsilon + \frac{\eta M_o}{M_1 + M_o} \frac{d\epsilon}{dt} \qquad \text{IV-42}$$

The solution of this differential equation yields the following expression for strain-time history.

$$\Delta\epsilon(t) = \frac{\Delta\sigma_s}{M_o} \left[1 + \frac{M_o}{M_1} \left(1 - e^{-\frac{M_1}{\eta}t} \right) \right] \qquad \text{IV-43}$$

Substituting for M_o/M_1 and M_1/η from equation IV-41 and simplifying one obtains

$$\frac{\Delta\epsilon(t)}{\Delta\sigma_s} M_o = 1 + \frac{1}{\phi} \left(1 - e^{-\frac{\phi}{\mu}t} \right) \qquad \text{IV-44}$$

At the time $t = 0$, $\dfrac{\Delta\epsilon(0)}{\Delta\sigma_s} M_o = 1$, or

$$M_o = \frac{\Delta\sigma_s}{\Delta\epsilon} \bigg|_{t=0} \qquad \text{IV-45}$$

Therefore M_o is the secant modulus at the stress level $\Delta\sigma_s$ at $t = 0$ (fig. IV-2). The slope of equation IV-44 at $t = 0$ is given as

$$\frac{d}{dt} \left(\frac{\Delta\epsilon(t)}{\Delta\sigma_s} M_o \right) \bigg|_{t=0} = \frac{1}{\mu} \qquad \text{IV-46}$$

For large values of time, equation IV-44 reduces to
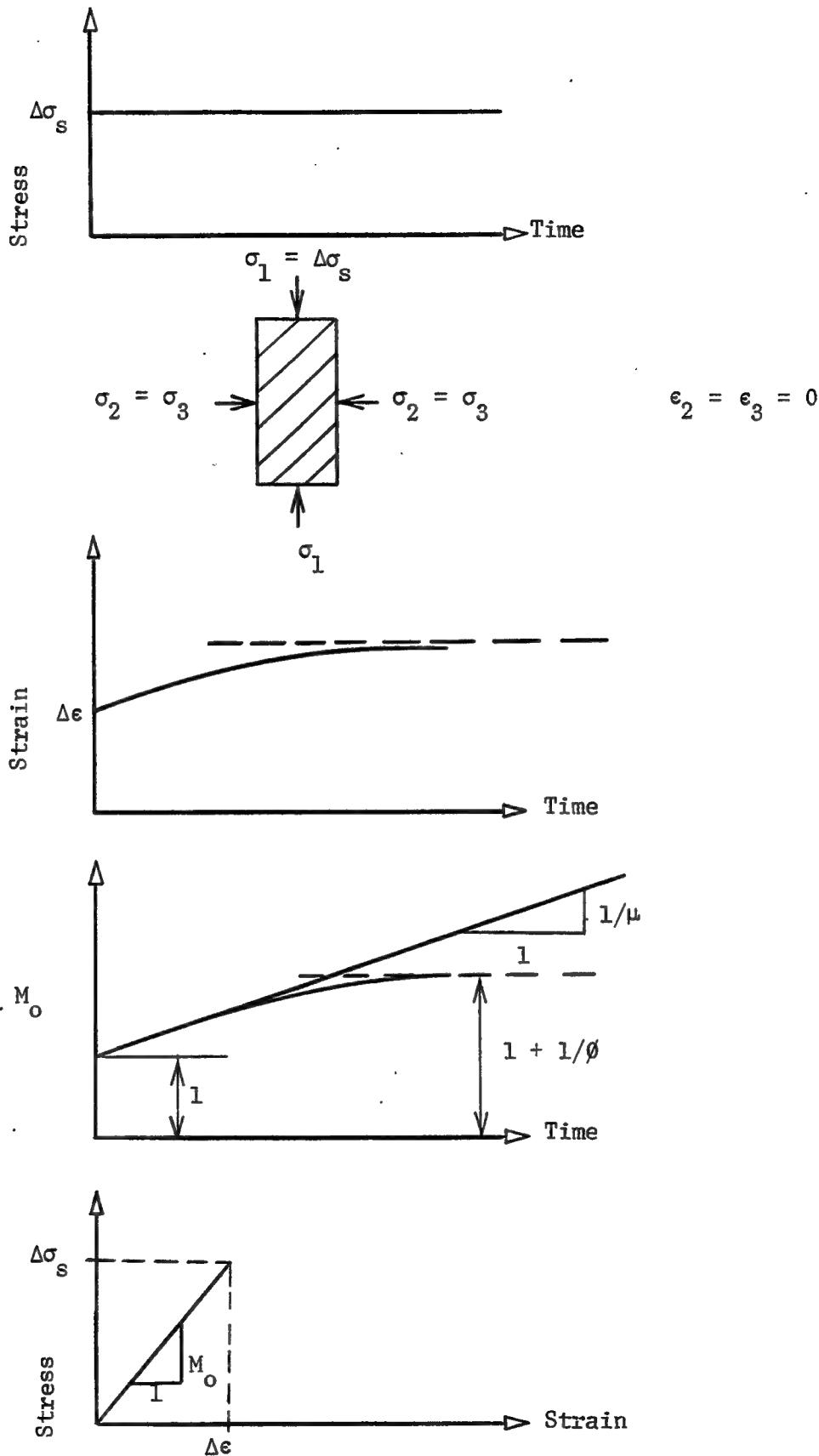
Fig. IV-2. Response of visco-elastic model to step load.

$$\frac{\Delta\varepsilon(t)}{\Delta\sigma_s} M_o = 1 + \frac{1}{\phi} \qquad\qquad \text{IV-47}$$

Therefore, the visco-elastic constants M_o, μ, and ϕ can be obtained from the measured strain-time history using equations IV-45, IV-46, and IV-47 (see fig. IV-2). However, due to the fact that an instantaneous step load cannot be applied in a uniaxial strain device, approximations (20) to laboratory data (measured strain-time history) are needed for the measurement of the visco-elastic constants.

The parameter β in equation IV-41 can be expressed in terms of α as

$$\beta = \frac{1 - \alpha}{1 + \alpha} \qquad\qquad \text{IV-48}$$

The compacting dissipative parameter α, is given by the ratio of the slopes at zero strain-rate, that is, by the ratio of the moduli M_o and M_2 (fig. IV-1).

$$\alpha = \frac{1 - \sqrt{M_o/M_2}}{1 + \sqrt{M_o/M_2}} \qquad\qquad \text{IV-49}$$

If there were no viscous effects, the moduli M_o and M_2 would be proportional to the loading and unloading slopes of the static stress-strain curve. The rate-dependent character of the material however, will modify the proportionality to some extent and will alter the definition of α (see equation III-25). Seaman (17) has developed an iterative procedure for the approximate measurement of α from the dynamic uniaxial test data. Typical values of α obtained by Seaman (17) are 0.12 for dry

sand (110 pcf dry density) and 0.02 for kaolinite (102 pcf dry density

and 33 percent water content) under 100 psi dynamic stress.

V

Stress Wave Attenuation Through a One-Dimensional Column of Nonlinear Locking Material

A. Description of locking media

The dynamic behavior of certain soils and rocks under uniaxial strain conditions may be approximated by the stress-strain curve of fig. V-1. This type of material response is referred to as locking behavior. The loading branch of the stress-strain curve is defined by the relation

$$\frac{d^2\sigma}{d\epsilon^2} > 0 \qquad\qquad \text{V-1}$$

During unloading the stress-strain curve is defined by

$$\epsilon = \epsilon_{max} \qquad\qquad \text{V-2}$$

If the material is reloaded, it will follow the vertical branch of equation V-2 to the previous peak stress level, σ_{max} (corresponding to ϵ_{max}), and from there on the curve of equation V-1.

Experimentally obtained loading stress-strain curves are often reasonably fitted by a parabolic relation (21) of the form

$$\sigma = \left(\frac{\epsilon}{k}\right)^n \qquad\qquad \text{V-3}$$

in which k and n are constant characteristics of the medium. Because of the condition $\frac{d^2\sigma}{d\epsilon^2} > 0$, it is required that $k > 0$ and $n > 1$. The following treats only the relation given by equation V-3; other analytical fits may be dealt with in a similar manner.

B. Boundary load

The dynamic boundary load considered is the pulse characterized by a
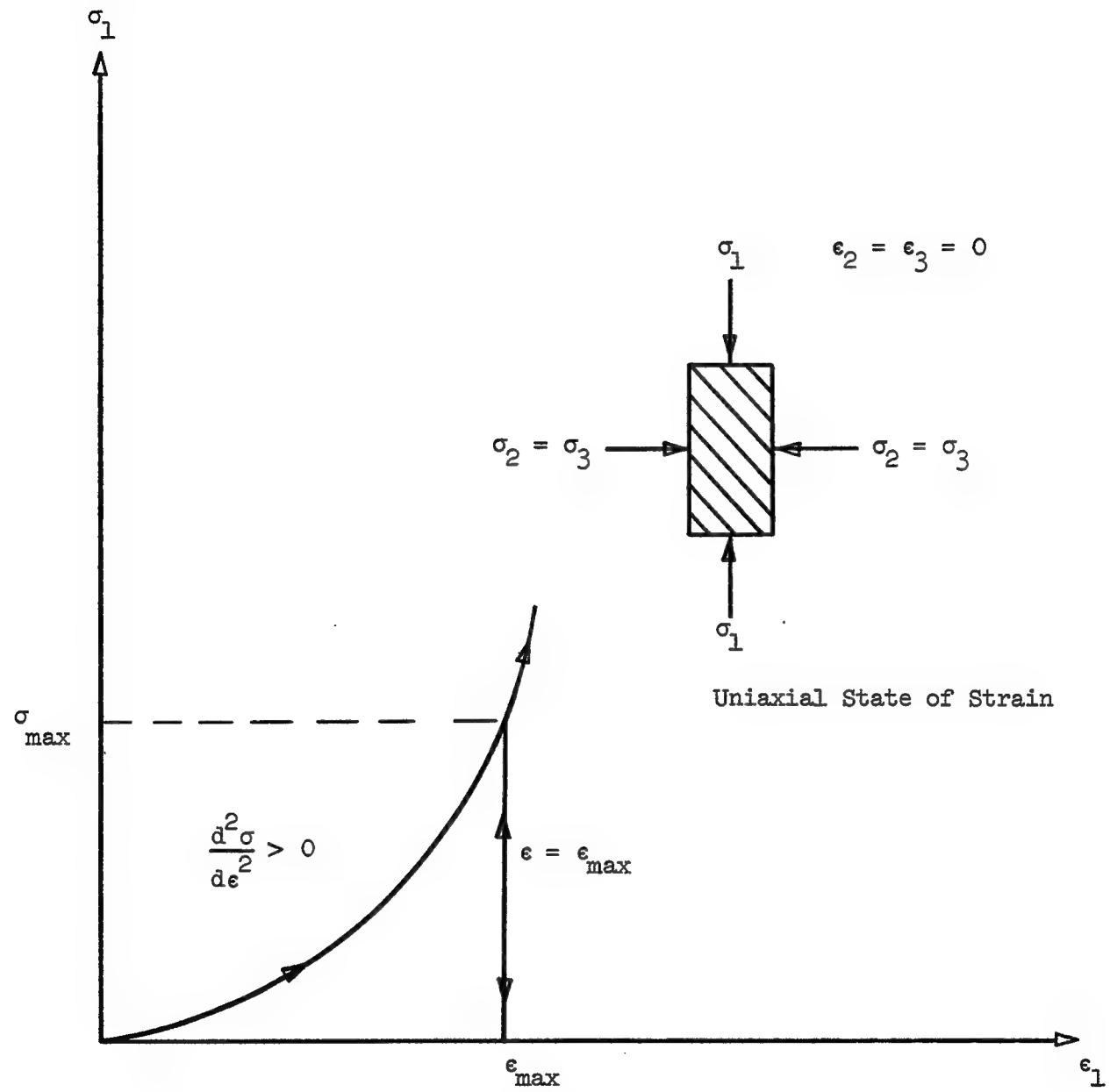
Fig. V-1. Typical load-unload stress-strain curve
for nonlinear locking medium

103

peak stress at a shock front and an exponentially decaying behavior there-
after (fig. III-2) given by

$$P(t) = P_o e^{-t/\tau} \qquad\qquad \text{V-4}$$

where

   P_o = the peak applied pressure

   t = the independent variable time

   τ = the exponential time constant, time at which pressure has
   decayed to $0.368 \; P_o$

C. Formulation of the problem

Consider a semi-infinite locking medium (fig. V-2) that is subjected
to a suddenly applied pressure pulse given by equation V-4 on its entire
free boundary. As a result of the pulse, a shock is propagated into the
medium, compacting it to a density, ρ (note that ρ will vary with depth).
Due to the nature of the stress-strain relation (fig. V-1), the density
change will be permanent. When the shock front has progressed to a depth,
z , at a time, t , the mass mobilized (involved) in the momentum transfer
(assuming unit area) is

$$m = \rho_i z \qquad\qquad \text{V-5}$$

where ρ_i is the initial mass density of the medium. Because of the
monotonically decaying character of the input pulse, the material behind
the shock front is continually unloaded along the vertical branch
$\epsilon = \epsilon_{max}$ of the stress-strain curve (no strain recovery). Consequently,
the mobilized mass, $\rho_i z$, acts as a rigid body causing all the material
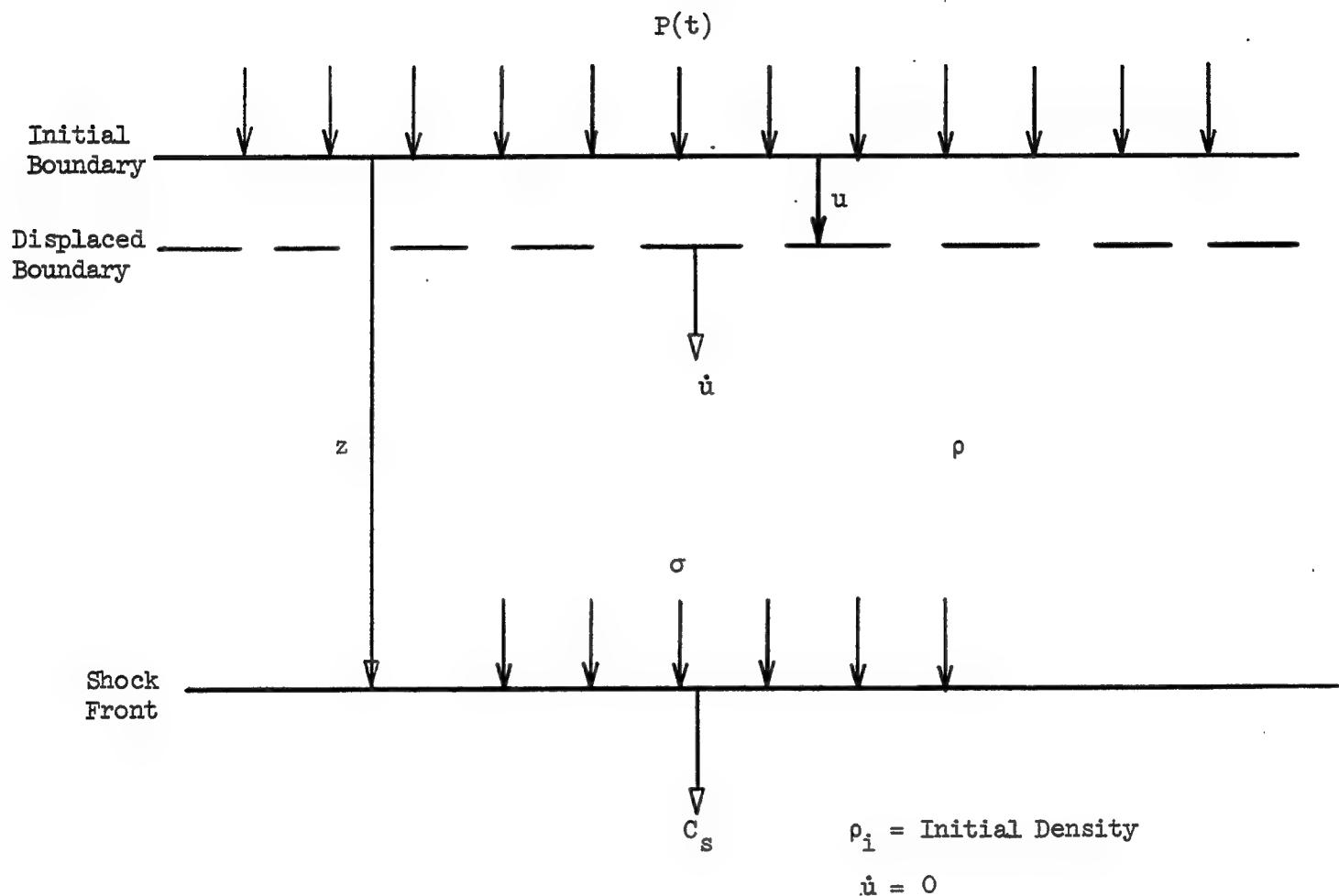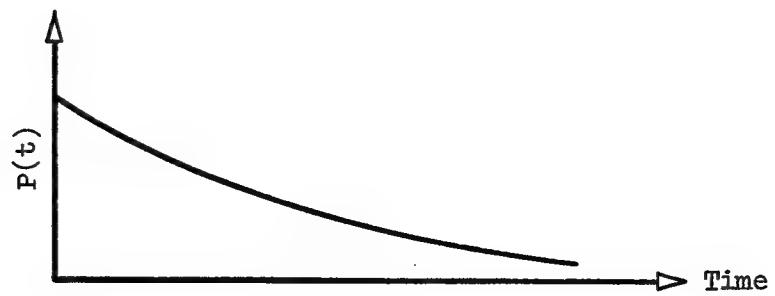
Fig. V-2. Shock-wave propagation conditions in locking media

behind the shock front to move with an identical velocity $\dot{u}(t)$, while the free boundary is displaced by the amount $u(t)$. In accordance with the Newton's law, the integrated impulse, I

$$I = \int_0^t P_o e^{-t/\tau} \, dt \qquad\qquad \text{V-6}$$

applied in the same period of time equates to the sum of the product of elements of the mobilized mass and their individual particle velocities, that is

$$\rho_i z \dot{u} = \int_0^t P_o e^{-t/\tau} \, dt \qquad\qquad \text{V-7}$$

The stress, σ , at the shock front is given by (see equation II-86)

$$\sigma = \rho_i \dot{u} C_s \qquad\qquad \text{V-8}$$

where C_s is the shock-front velocity given by (see equation II-88)

$$C_s = \frac{dz}{dt} = \left(\frac{\sigma}{\rho_i \epsilon} \right)^{1/2} \qquad\qquad \text{V-9}$$

and, ϵ , is the strain corresponding to σ at the shock front which is related to the particle velocity, $\dot{u}$, by (see equation II-14)

$$\epsilon = \frac{\dot{u}}{C_s} \qquad\qquad \text{V-10}$$

Substituting equation V-10 into equation V-7, using equation V-9 and rearranging, yields

$$z \frac{dz}{dt} = \frac{1}{\rho_i \epsilon} \int_0^t P_o e^{-t/\tau} \, dt \qquad\qquad \text{V-11}$$

or

$$z \frac{dz}{dt} = \frac{\tau P_o}{\rho_i \epsilon} (1 - e^{-t/\tau})$$ V-12

Substituting equation V-9 and its first integral into equation V-12

results in the following nonlinear differential equation

$$(\sigma \epsilon)^{1/2} \int_0^t \left(\frac{\sigma}{\epsilon}\right)^{1/2} dt = P_o \tau (1 - e^{-t/\tau})$$ V-13

Differentiating both sides of equation V-13 with respect to time yields

$$\frac{1}{2}\left[(\sigma \epsilon)^{-1/2} \left(\sigma \frac{d\epsilon}{dt} + \epsilon \frac{d\sigma}{dt}\right)\right] \int_0^t \left(\frac{\sigma}{\epsilon}\right)^{1/2} dt + \sigma = P_o e^{-t/\tau}$$ V-14

Since

$$\frac{d\epsilon}{dt} = \frac{d\epsilon}{d\sigma}\frac{d\sigma}{dt} = \frac{d\sigma/dt}{d\sigma/d\epsilon}$$ V-15

Equation V-14 becomes

$$\frac{1}{2}(\sigma \epsilon)^{1/2} \frac{1}{\sigma} \frac{d\sigma}{dt}\left[1 + \frac{\sigma/\epsilon}{d\sigma/d\epsilon}\right] \int_0^t \left(\frac{\sigma}{\epsilon}\right)^{1/2} dt + \sigma = P_o e^{-t/\tau}$$ V-16

Using the results of equation V-13, equation V-16 becomes

$$\frac{1}{2} \frac{P_o \tau}{\sigma} \frac{d\sigma}{dt}\left[1 + \frac{\sigma/\epsilon}{d\sigma/d\epsilon}\right](1 - e^{-t/\tau}) + \sigma = P_o e^{-t/\tau}$$ V-17

The variable coefficient in the brackets depends on the stress-strain

curve. The ratio

$$\frac{\sigma}{\varepsilon} = M_s \qquad\qquad \text{V-18}$$

is the secant modulus and

$$\frac{d\sigma}{d\varepsilon} = M_t \qquad\qquad \text{V-19}$$

is the tangent modulus. The case

$$M_t = M_s \qquad\qquad \text{V-20}$$

corresponds to a linear locking material (fig. V-3).

From equation V-3, the stress-strain relation, one obtains

$$\left[1 + \frac{\sigma/\varepsilon}{d\sigma/d\varepsilon} \right] = 1 + \frac{1}{n} \qquad\qquad \text{V-21}$$

Substituting equation V-21 into equation V-17, it reduces to Bernoulli equation (22).

$$\frac{1}{2} \frac{P_o \tau}{\sigma} \frac{d\sigma}{dt} \left(1 + \frac{1}{n} \right)(1 - e^{-t/\tau}) + \sigma = P_o e^{-t/\tau} \qquad\qquad \text{V-22}$$

With the initial condition

$$\sigma(0) = P(0) = P_o \qquad\qquad \text{V-23}$$

the solution to equation V-22 is

$$\sigma = \frac{\tau P_o [1 - e^{-t/\tau}]^{\frac{2n}{n+1}}}{\frac{2n}{n+1} \int_0^t [1 - e^{-t/\tau}]^{\frac{n-1}{n+1}} \, dt} \qquad\qquad \text{V-24}$$
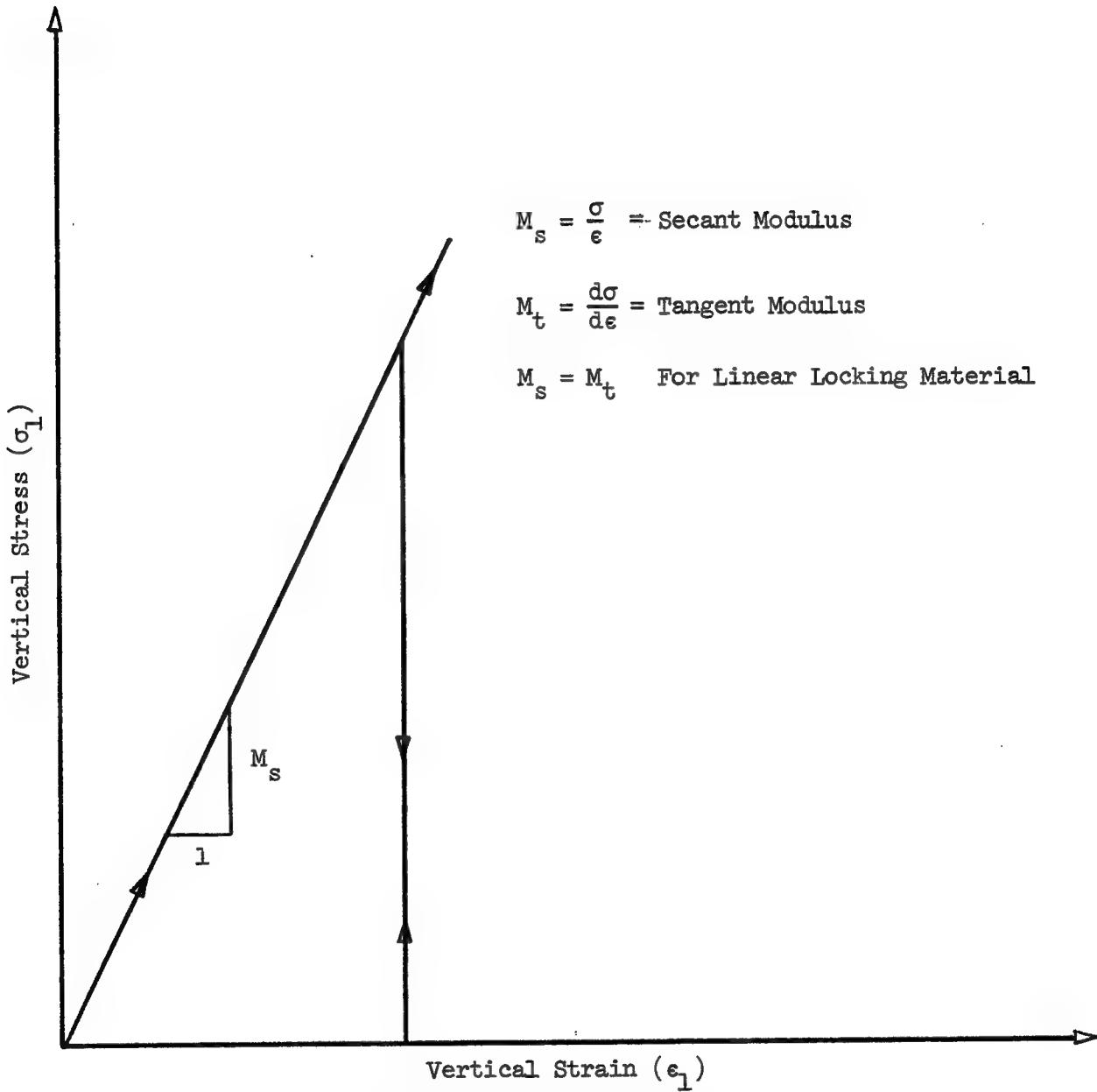
Fig. V-3. Stress-strain curve for linear locking material

Equation V-24 relates the stress, σ , at the shock front with the corresponding arrival time. The shock-front velocity, from equations V-3 and V-9, is

$$C_s = \frac{\sigma^{\frac{n-1}{2n}}}{(k\rho_i)^{1/2}} \qquad \text{V-25}$$

The shock-front location, z , from equation V-12, is given by

$$z = \frac{\tau P_o}{\rho_i \epsilon} \frac{1}{C_s} (1 - e^{-t/\tau}) \qquad \text{V-26}$$

Utilizing equations V-3, V-24, and V-25, the shock-front location time relation becomes

$$z = \frac{\left(\frac{2n}{n+1}\right)^{\frac{n+1}{2n}} (\tau P_o)^{\frac{n-1}{2n}}}{(\rho_i k)^{1/2}} \left[\int_0^t (1 - e^{-t/\tau})^{\frac{n-1}{n+1}} dt \right]^{\frac{n+1}{2n}} \qquad \text{V-27}$$

Equations V-24 and V-27 relate the peak stress, σ , at the shock front, to the shock-front location, z , from which one obtains the attenuation of peak stress with depth. The corresponding peak particle velocity-depth relation, from equations V-8 and V-25, is given by

$$\dot{u} = \sigma^{\frac{n+1}{2n}} \left(\frac{k}{\rho_i}\right)^{1/2} \qquad \text{V-28}$$

D. Numerical calculation

A numerical procedure, based on the conservation laws of mass and momentum and described by Zaccor (23), has been adopted for the calculation of peak stress and particle velocity attenuation in the nonlinear locking

110

medium. This procedure treats soil models composed of all nonlinear loading branch forms for which stress-strain behavior is described by the relation

$$\frac{d^2\sigma}{d\epsilon^2} \geq 0 \qquad\qquad \text{V-29}$$

and a vertical unloading branch given by equation V-2. Hence, the material defined by equation V-3 is included as a special case. The applied boundary load can be any pulse characterized by a peak stress at a shock front and a constant or steadily decaying behavior thereafter.

The procedure has been validated (23) by comparison with the closed-form solutions presented in section C of this chapter for a parabolic loading stress-strain curve and an exponentially decaying input pulse.

E. Computational procedure

The computational procedure described by Zaccor involves the impulse-momentum law given by equation V-7 and the concept of the mobilized mass acting as a rigid body behind the shock front. Material properties (loading branch of the stress-strain curve and the initial mass density) and boundary conditions determine the velocity, C_s , of the shock front and, hence, its location, z , at any time. The shock-front location at any time identifies the mass, m , mobilized in the momentum transfer up to that time. The integrated impulse, I , applied in the same period equates to the total momentum transferred, from which one obtains the peak particle velocity and stress at the shock front, that is

$$m\dot{u} = I$$
$$\dot{u} = \frac{I}{m} \qquad\qquad \text{V-30}$$
$$\sigma = \rho_i C_s \dot{u}$$

111

The step-by-step procedure used in the program is given below to illustrate some of the concepts involved in the theory.

1. Compute the shock-front velocity, C_s , at a discrete number of stress levels (the program will accept 50 values of C_s), from the loading branch of the stress-strain curve (for $0 \leq \sigma \leq P_o$) using the relation

$$C_s = \left(\frac{\sigma}{\rho_i \epsilon}\right)^{1/2} \qquad \text{V-31}$$

and store the information in tabular form.

2. Take a small time increment Δt .

3. Compute the impulse, $I(1)$, at the time, $t = \Delta t$, as the product of the time increment Δt , and the average value of the overpressure pulse in that time increment

$$I(1) = \Delta t [P_o + P(\Delta t)]/2 \qquad \text{V-32}$$

where $P(\Delta t)$ is the value of overpressure pulse at $t = \Delta t$.

4. From the shock-front velocity versus stress table of step 1 determine the average shock-front velocity

$$\bar{C}_s = \frac{C_s(P_o) + C_s(\Delta t)}{2} \qquad \text{V-33}$$

in the interval Δt as if the stress in the medium at the time $t = \Delta t$ were the same as the surface overpressure at the time $t = \Delta t$. $C_s(P_o)$ is the shock-front velocity corresponding to $\sigma = P_o$ and $C_s(\Delta_t)$ is the shock-front velocity corresponding to $\sigma = P(\Delta t)$.

5. Compute the shock-front location z_1 , at the end of the time increment Δt

$$z_1 = \bar{C}_s \, \Delta t \qquad\qquad\qquad \text{V-34}$$

6. From $I(1)$ obtained in step 3 compute a value for the particle velocity $\dot{u}_1$ at the end of the time increment Δt (see equation V-30)

$$\dot{u}_1 = \frac{I(1)}{\rho_i z_1} \qquad\qquad\qquad \text{V-35}$$

where $\rho_i z_1$ is the mobilized mass at the time $t = \Delta t$.

7. From $\dot{u}_1$ obtained in step 6 and $C_s(\Delta t)$ from step 4, compute the stress σ_1 at the shock front at the time $t = \Delta t$ and depth z_1 (see equation V-30)

$$\sigma_1 = \rho_1 C_s(\Delta t) \dot{u}_1 \qquad\qquad\qquad \text{V-36}$$

This value of stress is now a more accurate representation of the true stress in the medium at z_1 than the assumption made in step 4, that is, $\sigma_1 = P(\Delta t)$.

8. Compute a new value of $\bar{C}_s$ using

$$\bar{C}_s = \frac{C_s(P_o) + C_s(\sigma_1)}{2} \qquad\qquad\qquad \text{V-37}$$

where $C_s(\sigma_1)$ is the shock-front velocity corresponding to the current stress σ_1 found in step 7. $C_s(\sigma_1)$ may be determined by interpolation in the table computed for step 1.

9. Start again at step 5 and continue to repeat this iterative procedure until all values agree (within a specified convergence criterion) with those on the previous iteration and store the values obtained on the final iteration, that is, z_1 , $\dot{u}_1$, σ_1 . Note that $\dot{u}_1$ and σ_1 are the peak particle velocity and stress at depth z_1 .

10. Take the next time increment. The total elapsed time is now

$t = 2\Delta t$.

11. Compute the impulse for the second time increment as

$$I(2) = \Delta t[P(\Delta t) + P(2\Delta t)]/2 \qquad\qquad \text{V-38}$$

where $P(2\Delta t)$ is the value of overpressure pulse at $t = 2\Delta t$.

12. Compute the total impulse $I(2\Delta t)$, to the time $t = 2\Delta t$ as

$$I(2\Delta t) = I(1) + I(2) \qquad\qquad \text{V-39}$$

13. Assume an average shock-front velocity

$$\overline{C}_s = C_s(\sigma_1) \qquad\qquad \text{V-40}$$

where $C_s(\sigma_1)$ is the shock-front velocity corresponding to the final value
of σ_1 as found in step 9, and compute the shock-front location z_2 at
the end of the total elapsed time $t = 2\Delta t$

$$z_2 = z_1 + \overline{C}_s\Delta t \qquad\qquad \text{V-41}$$

14. From $I(2\Delta t)$ obtained in step 12 and z_2 obtained in step 13,
compute a value for the particle velocity $\dot{u}_2$ at the time $t = 2\Delta t$ and
location z_2

$$\dot{u}_2 = \frac{I(2\Delta t)}{\rho_i z_2} \qquad\qquad \text{V-42}$$

15. Repeat the outlined analogous procedures starting at step 7
until values of z_2 , $\dot{u}_2$, σ_2 are obtained which satisfy the convergence
criterion in step 9, and then index to the next time increment starting in
step 10.

114

F. Computer program

The above procedure is programmed in FORTRAN II language for a GE 225 computer with 8K memory.

The input variables for the computer code (program) consist of the following:

Variable	Description	Comments
ROE	Initial mass density (slugs/cu ft) - ρ_i	Singular parameter
DT	Time increment (sec) - Δt	Singular parameter
SIG(I)	Stress (psi) - σ	Discrete stress values from stress-strain curve
EPS(I)	Strain (in./in.) - ϵ	Discrete strain values from stress-strain curve
T	Time (sec) - t	Discrete values; $t = 0$ at $P = P_o$
P	Overpressure (psi) - $P(t)$	Discrete values; $P = P_o$ at $t = 0$

The input sequence and formats are as follows:

Input Card	Format
(A) (ROE, DT)	(F7.2, 4X, F7.5)
(B) [SIG(I), EPS(I), I = 1, 50]	(F7.2, 5X, F8.6)
(C) (T,P)	(F8.6, 5X, F7.2)

Card form (B) is repeated 50 times (for the 50 discrete points on the stress-strain curve). Card form (C) is repeated (pulse duration/DT + 1) times, i.e., discrete values of the input pressure pulse are read in and stored in tabular form. The code conveniently accepts these values at

115

times which are continuous multiples of the time increment DT . Note that

SIG(1) = EPS(1) = 0.0 (see fig. V-1); SIG(50) = P_o , the peak overpressure; and T = 0.0 when P = P_o .

The output variables are given in two groups as follows:

Group 1 Shock-front velocity calculation

STRESS (psi)	STRAIN (in./in.)	SHK-VEL (fps)
Format (F7.2)	Format (F8.6)	Format (F7.2)

Group 2 Attenuation of peak particle velocity and stress with depth

Z (ft)	V(fps)	STRESS (psi)
Format (F6.2)	Format (F8.3)	Format (F9.3)

G. Additional program information

The program contains a function subprogram, VELOC, that interpolates linearly in the shock-front velocity versus stress table calculated in step 1. The following error indications are given by subprogram VELOC:

a. STRESS TABLE OVERFLOW

This message is printed out if the maximum value of the overpressure pulse exceeds the peak stress input, i.e., P_o > SIG(50) .

b. STRESS DATA OUT OF ORDER

This message is printed out if the stress-strain input are not in an ascending order, i.e., SIG(I)-SIG(I-1) $\leq$ 0 .

H. Run time information

Computer time for a typical problem is about 15 minutes. A complete

116

FORTRAN II listing of the program and typical input and the resulting

output for an example problem is presented in Appendix V.

APPENDIX V

LOCKING MODEL

```
C          PROGRAM TITLE                                                          1
C          ONE-DIMENSIONAL STRESS WAVE PROPAGATION IN LOCKING AND DISSIPATIVE     2
C          MEDIA                                                                  3
C          PROGRAM NO.   41-Z5-111      DATE   AUGUST 1967                        4
C          PROGRAMMER  ROHANI,B    ILS                                            5
C                                                                                 6
C                                                                                 7
C                ASSUMED          *                                              8
C                STRESS-          *                       . .                    9
C                STRAIN           *                      .                       10
C                RELATION    S    *                     .    .      UNIAXIAL      11
C                            T    *                   .    .         STRAIN       12
C                            R    *                  .    .          DATA         13
C                            E    *                 .    .                        14
C                            S    *               .    .                          15
C                            S    *              .    .                           16
C                                 *            .    .                             17
C                                 *           .    .                              18
C                                 *          .    .                               19
C                                 *        .    .                                 20
C                                 *      .          .                             21
C                                 *    .          .                               22
C                                 *******************************                 23
C                                         STRAIN                                  24
C                                                                                 25
C          GLOSSARY                                                               26
C            ROE=MASS DENSITY OF SOIL[SLUGS/CU.FT]                                28
C            SIG[I]=STRESS AT POINT I ON STRESS-STRAIN CURVE[PSI]                 29
C            EPS[I]=STRAIN AT POINT I ON STRESS-STRAIN CURVE[IN/IN]               30
C            U[I]=SHOCK FRONT VELOCITY AT STRESS LEVEL SIG[I][FPS]                31
C            DT=TIME INCREMENT          [SEC]                                     32
C            P=OVERPRESSURE[PSI]                                                  33
C            T=TIME A VARIABLE[SEC]                                               34
C            PULS=IMPULS[SEC-PSI]                                                 35
C            Z=DEPTH A VARIABLE[FT.]                                              36
C            UBAR=AVE. SHOCK-FRONT VELOCITY[FPS]                                  37
C            V=PARTICLE VELOCITY[FPS]  [MAX]                                      38
C            STRESS=STRESS[MAX] [PSI]                                             39
C            VELOC=DUMMY                                                          40
C                                                                                 41
C          INPUT                                                                  42
C            ROE,DT,SIG[I],EPS[I],T,P                                             43
C          OUTPUT                                                                 44
C            MAX. STRESS,VELOCITY  AS A FUNCTION OF DEPTH [ATTENUATION]           45
C                                                                                 46
C                                                                                 47
C                                                                                 48
           COMMON SIG[50],EPS[50],U[50]                                           50
C                                                                                 51
C                                                                                 52
C                                                                                 53
C                                                                                 54
C                                                                                 55
       1 READ 100,ROE,DT                                                          56
     100 FORMAT[F7.2,4X,F7.5]                                                     57
         PRINT 99,ROE,DT                                                          571
     990FORMAT[1H1,12X,33HSHOCK-FRONT VELOCITY CALCULATION.,/,15X,6HROE =         572
        2F7.2,16H SLGS PER CU.FT.,1X,5HDT = F7.5,6H SEC. ,/,15X,6HSTRESS,6X       573
        3,6HSTRAIN,4X,7HSHK VEL,/,16X,5H[PSI],6X,7H[IN/IN],3X,5H[FPS],.//]        574
         DO 10 I=1,50                                                             58
```

```fortran
         READ 101,SIG[I],EPS[I]
         U[I]=SQRTF[[SIG[I]*144.]/[[EPS[I]+.000001]*ROE]]
   10 PRINT 102,SIG[I],EPS[I],U[I]
  101 FORMAT[F7.2,5X,F8.6]
  102 FORMAT[1H ,14X,F7.2,5X,F8.6,2X,F7.2]
         PRINT 88
  880FORMAT[1H1,12X,54HATTENUATION OF PEAK PARTICLE VELOCITY AND PEAK S
     2TRESS..,/,16X,5HZ[FT],7X,6HV[FPS],10X,11HSTRESS[PSI],]
         Z=0.
         STRESS=SIG[50]
         V=[[STRESS]*144.]/[[ROE]*U[50]]
         PRINT 104,Z,V,STRESS
  104 FORMAT[15X,F6.2,6X,F8.3,9X,F9.3]
         READ 103,T,P
  103 FORMAT[F8.6,5X,F7.2]
         PULS=0.
         ZL=0.
         PL=P
         READ 103,T,P
         PLL=P
         UU=VELOC[PLL]
   30 PULS=DT*[PL+P]*.5+PULS
         UBAR=[VELOC[PL]+VELOC[P]]*.5
         SS=0.
   35 Z=UBAR*DT+ZL
         V=[144.*[PULS/[ROE*Z]]]
         STRESS=ROE*V*UU*[1./144.]
         IF[ABSF[STRESS-SS]-.001] 50,50,40
   40 SS=STRESS
         UBAR=VELOC[SS]
         UU=VELOC[SS]
C
         GO TO 35
   50 PRINT 104,Z,V,STRESS
         UBAR=VELOC[STRESS]
         ZL=Z
         READ 103,T,P
         PULS=[DT*[PLL+P]]/2.+PULS
         PLL=P
         GO TO 35
         END
         FUNCTION VELOC[SIGMA]
C        PARAMETER DECK LOADED BY SUBROUTINE
         COMMON SIG[50],EPS[50],U[50]
C
         S=SIGMA
         DO 2 I=2,50
         IF[SIG[I]-S] 2,3,4
    2 CONTINUE
C
         PRINT 108
         CALL EXIT
  108 FORMAT [    23H STRESS TABLE OVERFLOW.]
    4 T1= SIG[I]-SIG[I-1]
         IF[T1] 55,55,70
   55 PRINT 105
  105 FORMAT [    26H STRESS DATA OUT OF ORDER.]
C
C
   70 T2 = U[I] - U[I-1]
```

59
61
62
63
641
642
643
644
645
646
647
648
65
66
67
68
70
71
711
761
73
74
741
75
76
77
78
781
79
790
791
80
81
811
821
83
84
841
86
87
86
85
87
88
89
90
91
92
93
94
95
96
99
100
101
102
103
104

```
      IF (T2) 72, 55, 72
   72 VELOC = U(I-1) + (S - SIG(I-1)) * T2/T1
      RETURN                                                          106
C                                                                     107
    3 VELOC=U(I)                                                      108
      RETURN                                                          109
      END                                                             110
```

```
/   3.44        0.01
    ▮           ▮
   ROE         DT

0000000000000▮0▮0000000000000000000000000000000000000000000000000000000000000000
1 2 3 4 5 6  7  8 9 10 11 12 13 14 15 16 17 18 19 20 21 22 23 24 25 26 27 28 29 30 31 32 33 34 35 36 37 38 39 40 41 42 43 44 45 46 47 48 49 50 51 52 53 54 55 56 57 58 59 60 61 62 63 64 65 66 67 68 69 70 71 72 73 74 75 76 77 78 79 80
11111111111111▮1111111111111111111111111111111111111111111111111111111111111111111
2222222222222222222222222222222222222222222222222222222222222222222222222222222222
33▮▮333333333▮33333333333333333333333333333333333333333333333333333333333333333333
4444▮▮44444444444444444444444444444444444444444444444444444444444444444444444444444
5555555555555555555555555555555555555555555555555555555555555555555555555555555555
6666666666666666666666666666666666666666666666666666666666666666666666666666666666
7777777777777777777777777777777777777777777777777777777777777777777777777777777777
888▮888888888▮8888888888888888888888888888888888888888888888888888888888888888888888
9999999999999999999999999999999999999999999999999999999999999999999999999999999999
1 2 3 4 5 6  7  8 9 10 11 12 13 14 15 16 17 18 19 20 21 22 23 24 25 26 27 28 29 30 31 32 33 34 35 36 37 38 39 40 41 42 43 44 45 46 47 48 49 50 51 52 53 54 55 56 57 58 59 60 61 62 63 64 65 66 67 68 69 70 71 72 73 74 75 76 77 78 79 80
IBM 5081
```

122

TYPICAL INPUT
CARD B

SIG (1)   EPS (1)
0.00   0.00

SIG (2)   EPS (2)
5.00   0.0027

SIG (50) EPS (50)
315.00   0.0435

TYPICAL INPUT
CARD C

0.00   315.0
T   P

```
8 8 0 8 0 0 0 0 0 0 0 0 0 0 8 0 0 8 0 0 0 0 0 0 0 0 0 0 0 0 0 0 0 0 9 0 0 0 0 0 0 0 0 0 0 0 0 0 0 0 0 0 0 0 0 0 0 0 0 0 0 0 0 8 0 0 0 0 0 0
1 2 3 4 5 6 7 8 9 10 11 12 13 14 15 16 17 18 19 20 21 22 23 24 25 26 27 28 29 30 31 32 33 34 35 36 37 38 39 40 41 42 43 44 45 46 47 48 49 50 51 52 53 54 55 56 57 58 59 60 61 62 63 64 65 66 67 68 69 70 71 72 73 74 75 76 77 78 79 80
1 1 1 1 1 1 1 1 1 1 1 1 1 1 1 1 1 1 1 1 1 1 1 1 1 1 1 1 1 1 1 1 1 1 1 1 1 1 1 1 1 1 1 1 1 1 1 1 1 1 1 1 1 1 1 1 1 1 1 1 1 1 1 1 1 1 1 1 1 1 1 1 1 1 1 1 1 1 1 1
2 2 2 2 2 2 2 2 2 2 2 2 2 2 2 2 2 2 2 2 2 2 2 2 2 2 2 2 2 2 2 2 2 2 2 2 2 2 2 2 2 2 2 2 2 2 2 2 2 2 2 2 2 2 2 2 2 2 2 2 2 2 2 2 2 2 2 2 2 2 2 2 2 2 2 2 2 2 2 2
3 3 3 3 3 3 3 3 3 3 3 3 3 3 3 3 3 3 3 3 3 3 3 3 3 3 3 3 3 3 3 3 3 3 3 3 3 3 3 3 3 3 3 3 3 3 3 3 3 3 3 3 3 3 3 3 3 3 3 3 3 3 3 3 3 3 3 3 3 3 3 3 3 3 3 3 3 3 3 3
4 4 4 4 4 4 4 4 4 4 4 4 4 4 4 4 4 4 4 4 4 4 4 4 4 4 4 4 4 4 4 4 4 4 4 4 4 4 4 4 4 4 4 4 4 4 4 4 4 4 4 4 4 4 4 4 4 4 4 4 4 4 4 4 4 4 4 4 4 4 4 4 4 4 4 4 4 4 4 4
5 5 5 5 5 5 5 5 5 5 5 5 5 5 5 5 5 5 5 5 5 5 5 5 5 5 5 5 5 5 5 5 5 5 5 5 5 5 5 5 5 5 5 5 5 5 5 5 5 5 5 5 5 5 5 5 5 5 5 5 5 5 5 5 5 5 5 5 5 5 5 5 5 5 5 5 5 5 5 5
6 6 6 6 6 6 6 6 6 6 6 6 6 6 6 6 6 6 6 6 6 6 6 6 6 6 6 6 6 6 6 6 6 6 6 6 6 6 6 6 6 6 6 6 6 6 6 6 6 6 6 6 6 6 6 6 6 6 6 6 6 6 6 6 6 6 6 6 6 6 6 6 6 6 6 6 6 6 6 6
7 7 7 7 7 7 7 7 7 7 7 7 7 7 7 7 7 7 7 7 7 7 7 7 7 7 7 7 7 7 7 7 7 7 7 7 7 7 7 7 7 7 7 7 7 7 7 7 7 7 7 7 7 7 7 7 7 7 7 7 7 7 7 7 7 7 7 7 7 7 7 7 7 7 7 7 7 7 7 7
8 8 8 8 8 8 8 8 8 8 8 8 8 8 8 8 8 8 8 8 8 8 8 8 8 8 8 8 8 8 8 8 8 8 8 8 8 8 8 8 8 8 8 8 8 8 8 8 8 8 8 8 8 8 8 8 8 8 8 8 8 8 8 8 8 8 8 8 8 8 8 8 8 8 8 8 8 8 8 8
9 9 9 9 9 9 9 9 9 9 9 9 9 9 9 9 9 9 9 9 9 9 9 9 9 9 9 9 9 9 9 9 9 9 9 9 9 9 9 9 9 9 9 9 9 9 9 9 9 9 9 9 9 9 9 9 9 9 9 9 9 9 9 9 9 9 9 9 9 9 9 9 9 9 9 9 9 9 9 9
```

0.01   220.0

0.20   0.0

TYPICAL OUTPUT

SHOCK-FRONT VELOCITY CALCULATION.

ROE =   3.44 SLGS PER CU.FT. DT = 0.01000 SEC.

STRESS [PSI]	STRAIN [IN/IN]	SHK VEL [FPS]
..0	0.000000	0.00
5.	.002700	278.37
10.	.004500	304.96
15.	.006000	323.47
2 .	.007500	334.09
25.	.009000	340.98
3 .	.010000	354.36
35.	.011200	361.67
4 .0	.012500	365.98
45.	.013600	372.15
5 .	.014500	379.92
54.38	.015700	380.06
57.46	.016400	382.96
61.	.017100	386.42
64.88	.017800	390.60
69.18	.018600	394.57
73.94	.019500	398.39
79.17	.020300	404.04
85.	.021300	408.71
91.6	.022300	414.66
99.15	.023500	420.25
5.	.024200	426.17
11 .	.025100	428.30
15.	.026000	430.28
2 .	.026700	433.74
25.	.027500	436.20
13 .	.028200	439.28
35.	.029000	441.43
4 .	.029600	444.95
5 .	.031000	450.05
6 .	.032100	456.78
7 .	.033200	462.97
8 .	.034300	468.69
9 .	.035200	475.34
.	.036200	480.90
1 .	.037000	487.42
2 .	.037700	494.24
3 .	.038500	500.07
4 .	.039100	506.89
5 .	.040000	511.49
6 .	.040500	518.39
7 .	.041100	524.39
8 .	.041800	529.53
9 .	.042100	536.98
295.	.042500	539.03
3 .	.042700	542.31
3 2.	.042900	542.84
3 5.	.043000	544.89
31 .	.043200	548.07
315.	.043500	550.56

TYPICAL OUTPUT

ATTENUATION OF PEAK PARTICLE VELOCITY AND PEAK STRESS.

Z(FT)	V(FPS)	STRESS(PSI)
. .	23.950	315.000
5.23	21.415	267.500
.16	18.497	217.698
14.84	16.010	179.043
9.35	14.111	152.208
23.76	12.715	133.942
28.1	11.637	120.670
32.39	10.746	109.941
36.6	9.989	100.643
4 .76	9.351	92.827
44.86	8.794	86.065
48.9	8.292	80.200
52.9	7.836	74.734
56.85	7.412	69.975
6 .76	7.020	65.620
64.63	6.658	61.554
68.47	6.318	57.862
72.27	5.997	54.492
76. 7	5.698	51.720
79.85	5.428	49.075
83.6	5.185	46.355

Stress Wave Propagation Through a Laterally Constrained
Column of Nonlinear Hysteretic Material

A. Description of model

The nonlinear hysteretic model was recommended by Hendron (25) on
the basis of his study of the behavior of sand under uniaxial strain
conditions. The model is rate-independent and energy dissipation is only
due to the compaction (hysteretic) characteristics of the model.

A stress-strain curve for the nonlinear hysteretic model is shown
in fig. VI-1. The initial loading curve is given by the relation

$$\sigma = A\epsilon^n \qquad\qquad \text{VI-1}$$

The unloading curve is given by the relation

$$\sigma = B(\epsilon - \epsilon_r)^n \qquad\qquad \text{VI-2}$$

where A, B, and n are constants characteristic of the medium and ϵ_r
is the residual strain. If the material is reloaded, it will follow the
curve of equation VI-2 to its previous maximum stress level, σ_{max}, cor-
responding to ϵ_{max}, and from then on the curve of equation VI-1. The
nonlinear hysteretic model is identical with the linear hysteretic model
(Chapter III) when n = 1.0.

The initial loading tangent modulus M_o for the nonlinear hysteretic
model, from equation VI-1, is given as

$$M_o = \frac{d\sigma}{d\epsilon} = An\epsilon^{n-1} \quad \text{(Tangent modulus)} \qquad\qquad \text{VI-3}$$

127
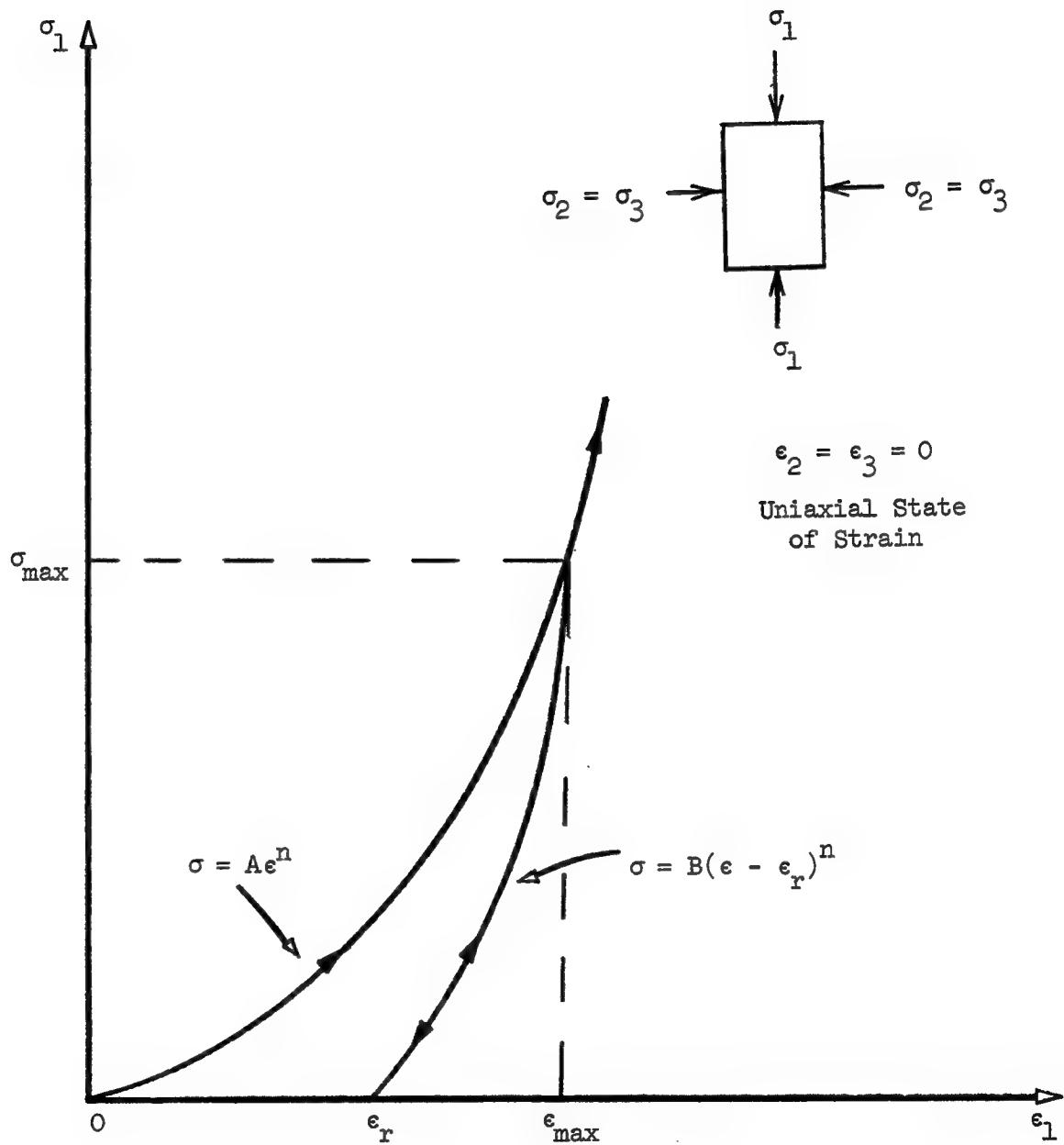
Fig. VI-1. Typical stress-strain curve
for nonlinear hysteretic model

128

The unloading/reloading tangent modulus M_1, from equation VI-2, is given by

$$M_1 = Bn(\epsilon - \epsilon_r)^{n-1} \qquad\qquad \text{VI-4}$$

For the conditions of shock wave propagation the initial loading wave velocity is determined by using the secant modulus of the material (see equation II-89). The initial loading secant modulus is given as

$$M_o = \frac{\sigma}{\epsilon} = A\epsilon^{n-1} \text{ (Secant modulus)} \qquad\qquad \text{VI-5}$$

B. Boundary load

The dynamic boundary load used for this model is a pulse characterized by a peak stress at the shock front and an exponentially decaying behavior thereafter (see fig. II-2) given by

$$P(t) = P_o e^{-t/\tau} \qquad\qquad \text{VI-6}$$

where

P_o = the peak applied pressure

t = time, the independent variable

τ = the exponential time constant (time at which the overpressure
has decayed to 0.368 P_o)

C. Solution of the problem

A numerical method developed by Heierli (26) will be used for the solution of the nonlinear hysteretic model. This procedure, often referred to as the method of impulses, assumes that (a) the applied pressure pulse is divided into a finite number of steps containing a certain amount of

129

impulse, (b) the dynamic stress-strain properties of the material are known for all conditions of loading, i.e., initial loading, unloading, and subsequent reloading and unloading, (c) each increment of stress change propagates at a velocity consistent with the secant modulus for the stress increment, (d) the impulse is conserved on an incremental basis and continuity is maintained. Using the conservation laws of mass and momentum, an expression for the change in particle velocity and stress can be obtained which, in conjunction with the propagation velocity-stress relation (obtained from the stress-strain properties of the material), can be used to determine the stress in refracted and reflected waves which propagate away from the intersection between two waves. It then becomes a bookkeeping process to compute the position of all the waves on a space-time diagram (such as the one shown in fig. III-4) as well as the state (i.e. stress and particle velocity) existing in each zone of the diagram.

D. Particle velocity-stress relation

The particle velocity-stress relation is determined from the consideration of the conservation laws of mass and momentum for a region of material subjected to a step change $\Delta\sigma$ in stress. This step change in stress, which moves from position z to $z + \Delta z$ in a time Δt, causes an abrupt change in particle velocity from $\dot{u}$ to $\dot{u} + \Delta\dot{u}$ as shown in fig. VI-2. The strain also changes from ϵ to $\epsilon + \Delta\epsilon$. Assuming that the position z is attached to the moving particle (Eulerian coordinate system), the conservation of mass for the element of fig. VI-2 yields

$$\rho\,\Delta z = (\rho + \Delta\rho)[\Delta z - \Delta\dot{u}\,\Delta t] \qquad \text{VI-7}$$

130
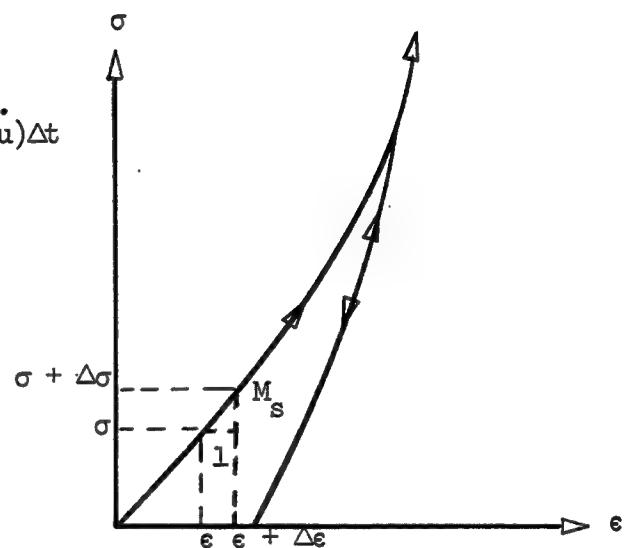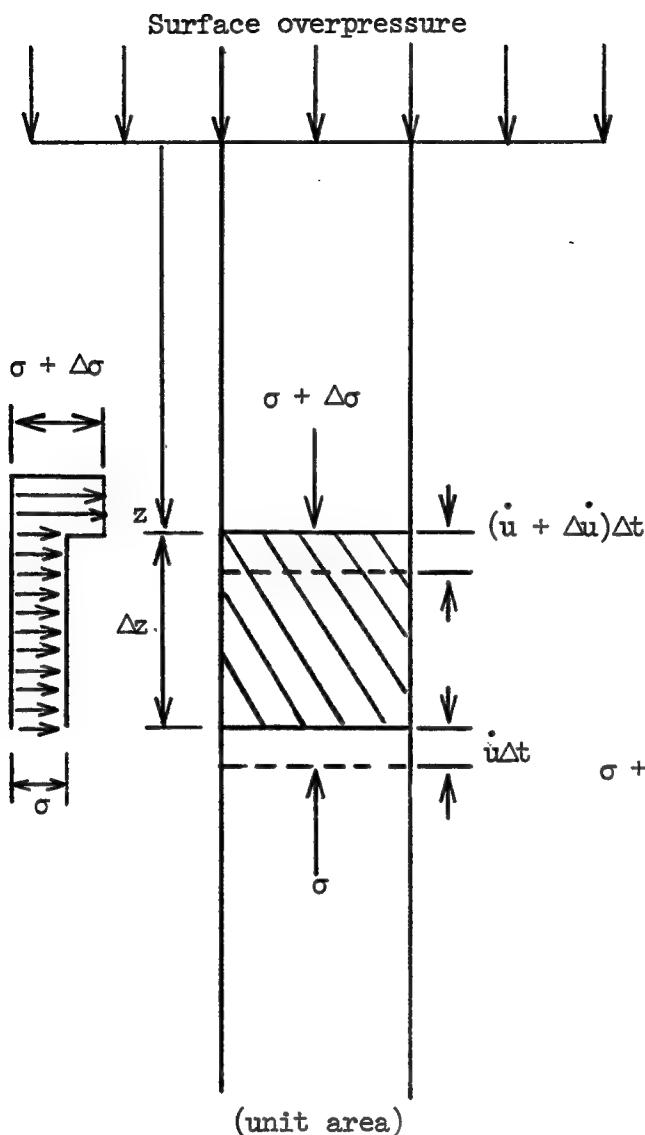
Fig. VI-2. Propagation of loading waves; relationships for
step change in stress

131

where $\Delta\rho$ is the change in density due to the step change $\Delta\sigma$ in stress. Equation VI-7 can be simplified to the following equation

$$\frac{\Delta\rho}{\rho + \Delta\rho} \Delta z = \Delta\dot{u} \, \Delta t \qquad\qquad \text{VI-8}$$

From conservation of momentum

$$\rho \, \Delta z \, \Delta\dot{u} = \Delta\sigma \, \Delta t \qquad\qquad \text{VI-9}$$

where $\rho\Delta z$ is the mass involved during the momentum transfer process and $\Delta\sigma \, \Delta t$ is the applied impulse during the time $t = \Delta t$. The absolute (Lagrangian) wave velocity C at which the step $\Delta\sigma$ travels is given by

$$C = \frac{\Delta z}{\Delta t} + \dot{u} \qquad\qquad \text{VI-10}$$

Using equation VI-10 in equation VI-9 gives

$$\Delta\sigma = \rho \, \Delta\dot{u} \, (C - \dot{u}) \qquad\qquad \text{VI-11}$$

Combining equations VI-8, VI-10, and VI-11 to eliminate $\Delta\dot{u}$ and solving for $\Delta\sigma$ gives

$$\Delta\sigma = \frac{\rho \, \Delta\rho}{\rho + \Delta\rho} \, (C - \dot{u})^2 \qquad\qquad \text{VI-12}$$

The step change $\Delta\sigma$ is assumed to be related to the strain change $\Delta\varepsilon$ by

$$\Delta\sigma = M_s \, \Delta\varepsilon \qquad\qquad \text{VI-13}$$

where M_s is the constrained secant modulus for the stress increment $\Delta\sigma$ as shown in fig. VI-2. Since one-dimensional Eulerian strain is used

$$\epsilon = 1 - \frac{\rho_i}{\rho} \qquad \text{VI-14}$$

in which ρ_i is the initial mass density of the material before propagation of any waves. Using equation VI-14, it is deduced that

$$\Delta\epsilon = \left(1 - \frac{\rho_i}{\rho + \Delta\rho} \right) - \left(1 - \frac{\rho_i}{\rho} \right)$$

$$= \frac{\rho_i \Delta\rho}{\rho(\rho + \Delta\rho)} \qquad \text{VI-15}$$

Combining equations VI-13 and VI-15 gives

$$\Delta\sigma = M_s \left[\frac{\rho_i \, \Delta\rho}{\rho(\rho + \Delta\rho)} \right] \qquad \text{VI-16}$$

Combining equations VI-12 and VI-16 gives

$$\rho(C - \dot{u}) = \pm \sqrt{M_s \rho_i} \qquad \text{VI-17}$$

where $\pm$ signs designate waves traveling in the positive and negative directions, respectively. Using equation VI-17 in equation VI-11 gives

$$\Delta\dot{u} = \pm \frac{\Delta\sigma}{\sqrt{M_s \, \rho_i}} \qquad \text{VI-18}$$

Equation VI-18 relates the change in particle velocity due to a step change in stress. The integral form of equation VI-18 is given as

$$\Delta\dot{u} = \int_{\sigma}^{\sigma + \Delta\sigma} \frac{d\sigma}{\sqrt{M_s \, \rho_i}} \qquad \text{VI-19}$$

For the boundary load considered in this problem (equation VI-6) and the loading stress-strain relation given by equation VI-1, the initial

loading stress pulse will propagate into the medium as a shock. The velocity of propagation of the initial loading stress wave is then determined from the secant modulus given by equation VI-5. In terms of stress, equation VI-5 can be written as (using equation VI-1)

$$M_s = A^{\frac{1}{n}} \, \sigma^{\frac{n-1}{n}} \qquad\qquad \text{VI-20}$$

Substitution of equation VI-20 into equation VI-18 results in the following expression for the particle velocity-stress relation for the initial loading

$$\dot{u} = \frac{\sigma^{\frac{n+1}{2n}}}{\sqrt{\rho_i}\, A^{\frac{1}{2n}}} \quad \text{(initial loading)} \qquad\qquad \text{VI-21}$$

where σ corresponds to the peak stress at the wave front ($\sigma = P_o$ at the surface). During unloading from a stress level σ to σ_{j-1}, the incremental change in particle velocity can be obtained from equation VI-19 where M_s is determined from equation VI-4. In terms of stress, equation VI-4 becomes

$$M_l = M_s = nB^{\frac{1}{n}} \, \sigma^{\frac{n-1}{n}} \qquad\qquad \text{VI-22}$$

Substituting from equation VI-22 into equation VI-19 and integrating from σ_{j-1} to σ_j, results in the following expression for the change in particle velocity due to a step change ($\sigma_j - \sigma_{j-1}$) in stress during unloading or reloading

$$\Delta\dot{u}_{j,j-1} = -\frac{\left(\sigma_{j-1}^{\frac{1+n}{2n}} - \sigma_j^{\frac{1+n}{2n}} \right)}{\sqrt{\rho_i n}\, B^{\frac{1}{2n}} \left(\frac{1+n}{2n} \right)} \quad \text{(unloading/reloading)} \qquad \text{VI-23}$$

134

E. Wave velocity-stress relation

The wave-velocity, C_o , for the initial stress wave (a shock) is determined from the secant modulus given by equation VI-5, that is,

$$C_o = \left(\frac{A\epsilon^{n-1}}{\rho_i} \right)^{1/2} \qquad\qquad \text{VI-24}$$

In terms of stress, equation VI-24 becomes

$$C_o = \left(\frac{A^{\frac{1}{n}} \sigma^{\frac{n-1}{n}}}{\rho_i} \right)^{1/2} \qquad \text{(initial loading)} \qquad \text{VI-25}$$

where, as in equation VI-21, σ corresponds to the peak stress.

The wave velocity for the unloading or reloading stress wave (from σ_j to σ_{j-1}) is determined from equation VI-2 (the unloading/reloading stress-strain relation), that is

$$C_{j,j-1} = \sqrt{\frac{(\sigma_{j-1} - \sigma_j)}{(\epsilon_{j-1} - \epsilon_j)\,\rho_i}} \qquad\qquad \text{VI-26}$$

Note that the initial mass density is used in equation VI-26; this is satisfactory when the strains are small. From equation VI-2

$$\epsilon_j = \epsilon_r + \left(\frac{\sigma_j}{B} \right)^{\frac{1}{n}}$$

$$\epsilon_{j-1} = \epsilon_r + \left(\frac{\sigma_{j-1}}{B} \right)^{\frac{1}{n}} \qquad\qquad \text{VI-27}$$

Substituting from equation VI-27 into equation VI-26 and simplifying results in the following relation

$$C_{j,j-1} = \frac{B^{\frac{1}{2n}}}{\sqrt{\rho_i}} \left(\frac{\sigma_{j-1} - \sigma_j}{\sigma_{j-1}^{\frac{1}{n}} - \sigma_j^{\frac{1}{n}}} \right)^{1/2} \qquad\qquad \text{VI-28}$$

135

The radical in equation VI-28 may be expanded (18) in terms of $\sigma_{j-1} + \sigma_j$ and $\sigma_{j-1} - \sigma_j$ to give

$$\left(\frac{\sigma_{j-1} - \sigma_j}{\sigma_{j-1}^{\frac{1}{n}} - \sigma_j^{\frac{1}{n}}}\right)^{-1/2} = \sqrt{n}\left(\frac{\sigma_j + \sigma_{j-1}}{2}\right)^{\frac{n-1}{2n}}$$

$$\left[1 - \frac{1}{12}\ 1 - \frac{1}{n}\left(2 - \frac{1}{n}\right)\left(\frac{\sigma_{j-1} - \sigma_j}{\sigma_{j-1} + \sigma_j}\right)^2 + \ldots \right] \qquad \text{VI-29}$$

If $\dfrac{\sigma_{j-1} - \sigma_j}{\sigma_{j-1} + \sigma_j} < 1/4$ the first term of equation VI-29 is sufficient to give

an accuracy of one percent. Then the wave velocity, equation VI-28, for the above conditions becomes

$$C_{j,j-1} = \frac{B^{\frac{1}{2n}}}{\sqrt{\rho_i}}\ \ n\left(\frac{\sigma_j + \sigma_{j-1}}{2}\right)^{\frac{n-1}{2n}} \quad \text{(unloading/reloading)} \qquad \text{VI-30}$$

F.   Intersection relations

Consider the space-time diagram shown in fig. VI-3. The input pressure time is approximated by a series of step changes at the appropriate times t_1, t_2, t_3, ... The first step is given as P_o at time t_o followed by a decrease in pressure equal to $\Delta P = P_o - P_1$ at time t_1. The stress in the first zone of the space-time diagram is equal to P_o (the applied pressure during the first time interval).

$$\sigma_1 = P_o \qquad\qquad\qquad \text{VI-31}$$

The particle velocity in the same zone is obtained from equation VI-21

136
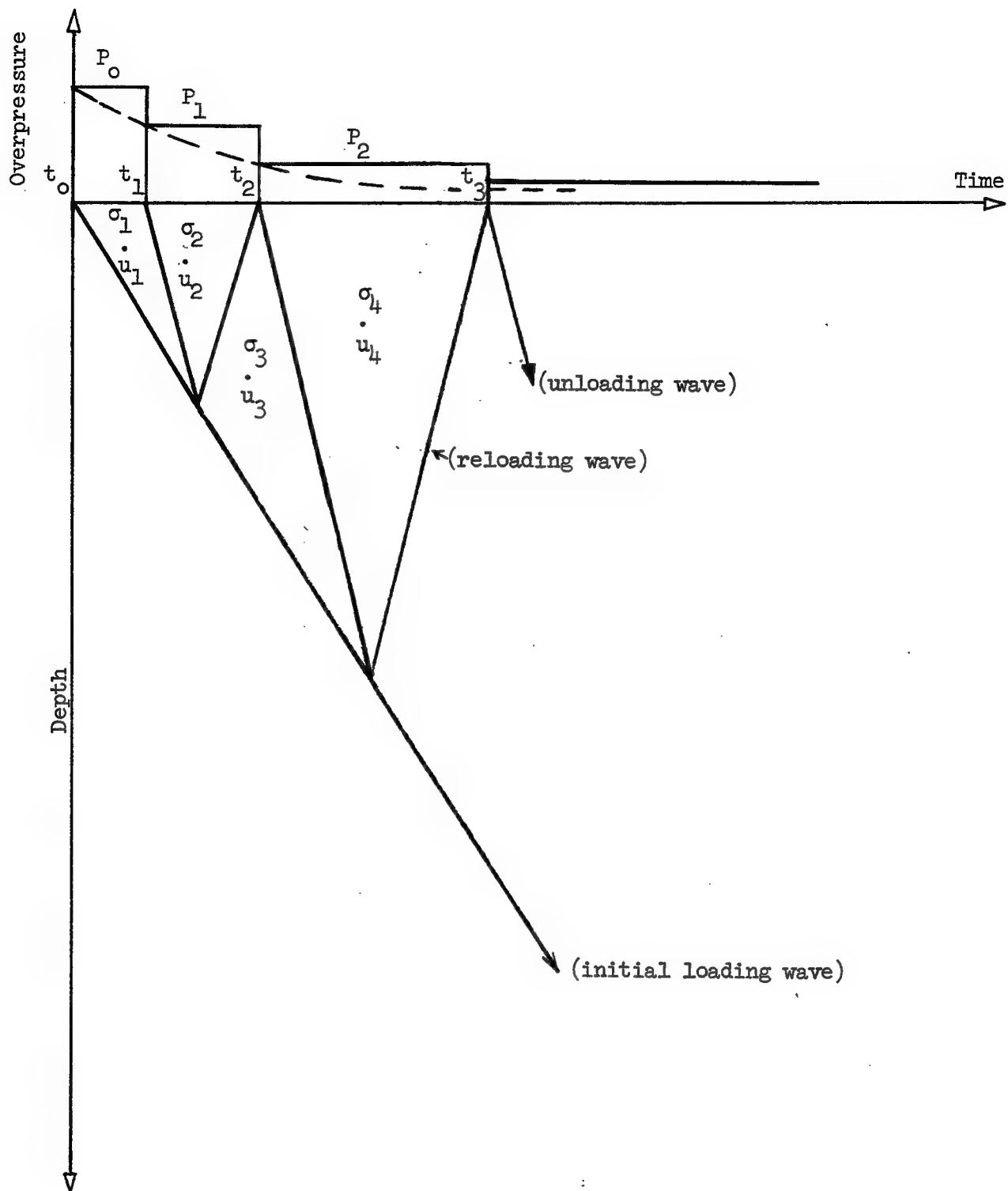
Fig. VI-3. Space-time diagram

137

which expresses the relation between stress and velocity across a shock-front

$$\dot{u}_1 = \frac{P_o^{\frac{n+1}{2n}}}{\sqrt{\rho_i} \; A^{\frac{1}{2n}}} \qquad \text{VI-32}$$

At time t_1 a decrease in pressure occurs at the surface and causes an unloading wave to travel into the medium. The stress behind this unloading front (in zone 2) is

$$\sigma_2 = P_1 \qquad \text{VI-33}$$

The particle velocity, $\dot{u}_2$, in zone 2 is determined by computing the change in velocity $\Delta \dot{u}$ due to the step change $P_o - P_1$ in stress, that is

$$\dot{u}_2 = \dot{u}_1 + \Delta \dot{u}_{12} \qquad \text{VI-34}$$

where $\Delta \dot{u}_{12}$ is determined from equation VI-23 by substituting equations VI-31 and VI-33 for σ_j and σ_{j-1} respectively

$$\Delta \dot{u}_{12} = \frac{P_1^{\frac{1+n}{2n}} - P_o^{\frac{1+n}{2n}}}{\sqrt{\rho_i n} \; B^{\frac{1}{2n}} \left(\frac{1+n}{2n} \right)} \qquad \text{VI-35}$$

The unloading stress wave, $P_o - P_1$, governed by the unloading stress-strain curve (equation VI-2), travels with a velocity determined from equation VI-30 which is higher than the initial loading wave velocity given by equation VI-25. The unloading wave therefore overtakes the loading wave and the intersection of these waves produces a reloading (reflected) wave which propagates back toward the surface and another (refracted) wave which continues on to greater depths. The region between these two wave-fronts

138

has a single stress and a single particle velocity.

The intersection equations can be derived by considering the uniqueness of particle velocity at the point of intersection. If regions above and below the interaction of the two waves are denoted by a and b , respectively, and the common region by c as shown in fig. VI-4, the particle velocities above and below the common region c are given by

$$\dot{u}_c = \dot{u}_a - \Delta\dot{u}_{ac} \quad \text{(above)} \qquad\qquad \text{VI-36}$$

and

$$\dot{u}_c = \dot{u}_b + \Delta\dot{u}_{bc} \quad \text{(below)} \qquad\qquad \text{VI-37}$$

where $\Delta\dot{u}_{ac}$ is the change in particle velocity caused by changing the stress from σ_a to σ_c and $\Delta\dot{u}_{bc}$ is similarly defined. These particle velocity increments are determined from equation VI-21 for initial loading or equation VI-23 for reloading or unloading. The stress σ_c is determined from the simultaneous solution of equations VI-36 and VI-37.

The stress σ_3 and the particle velocity $\dot{u}_3$ of the third zone in the space-time diagram in fig. VI-3 will be determined utilizing the intersection equations VI-36 and VI-37; σ_2 and $\dot{u}_2$, given by equations VI-33 and VI-34, respectively, correspond with σ_a and $\dot{u}_a$ in fig. VI-4; σ_3 and $\dot{u}_3$ correspond with σ_c and $\dot{u}_c$, and σ_b and $\dot{u}_b$ are zero because the intersection occurs at the leading edge of the shock-front. The particle velocity change $\Delta\dot{u}_{ac}$ is given by equation VI-23 and $\Delta\dot{u}_{bc}$ is given by equation VI-21. From equation VI-21

139
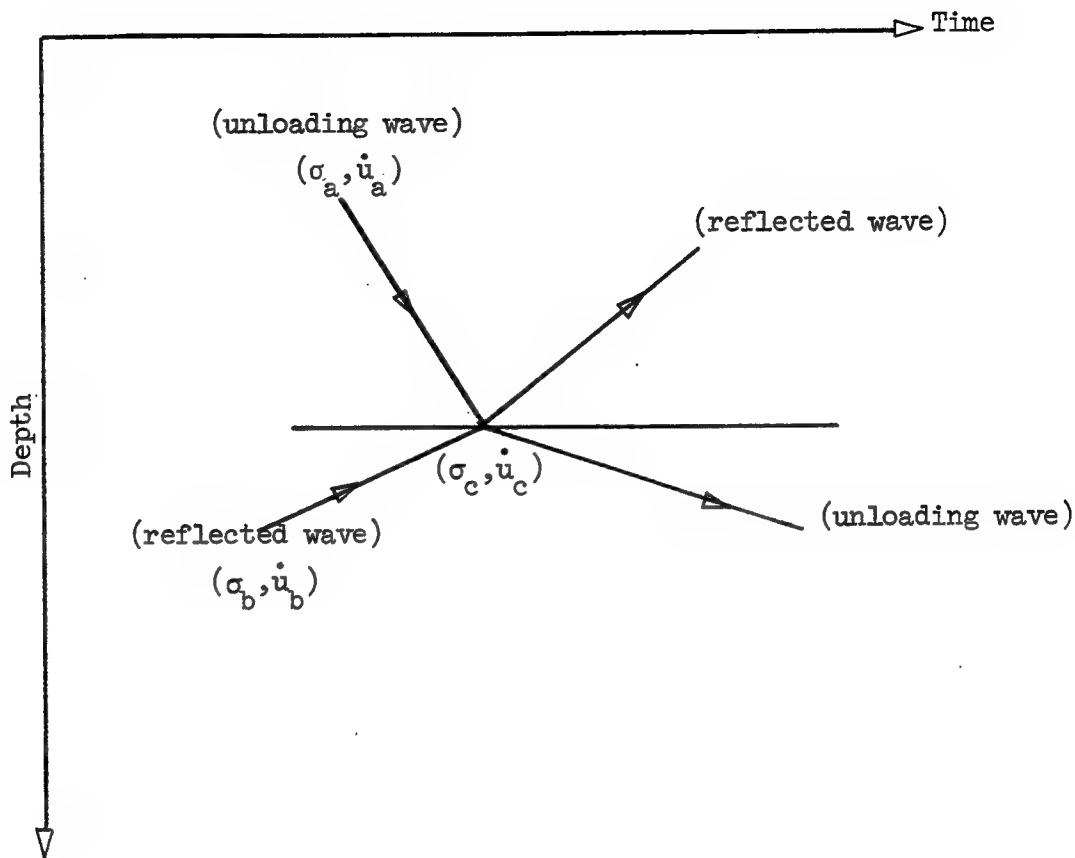
Fig. VI-4. Intersection of unloading wave with loading
wave in space time

$$\Delta \dot{u}_{bc} = \frac{\sigma_3^{\frac{n+1}{2n}}}{\sqrt{\rho_i}\ A^{\frac{1}{2n}}} \qquad\qquad \text{VI-38}$$

From equation VI-23

$$\Delta \dot{u}_{ac} = \frac{\left(\sigma_3^{\frac{1+n}{2n}} - \sigma_2^{\frac{1+n}{2n}}\right)}{\sqrt{\rho_i n}\ B^{\frac{1}{2n}}\left(\frac{1+n}{2n}\right)} \qquad\qquad \text{VI-39}$$

Substituting from equations VI-38 and VI-39 into equations VI-37 and
VI-36, respectively, and eliminating $\dot{u}_3 = \dot{u}_c$ gives

$$\frac{\sigma_3^{\frac{n+1}{2n}}}{\sqrt{\rho_i}\ A^{\frac{1}{2n}}} = \dot{u}_2 - \frac{\left(\sigma_3^{\frac{1+n}{2n}} - \sigma_2^{\frac{1+n}{2n}}\right)}{\sqrt{\rho_i n}\ B^{\frac{1}{2n}}\left(\frac{1+n}{2n}\right)} \qquad\qquad \text{VI-40}$$

Equation VI-40 can be solved for σ_3 . The particle velocity $\dot{u}_3$ can
then be determined from equation VI-38

$$\dot{u}_3 = \frac{\sigma_3^{\frac{n+1}{2n}}}{\sqrt{\rho_i}\ A^{\frac{1}{2n}}} \qquad\qquad \text{VI-41}$$

The process just demonstrated can be continued indefinitely; succes-
sively finding the stress at the surface from the boundary conditions,
computing the new velocity, taking into account the change of stress, and
then analyzing the interactions from unloading waves overtaking the initial
loading wave. To obtain more accuracy the time between t_o , t_1 , t_2 , $\ldots$
should be divided into finer divisions as shown in fig. VI-5. The

141
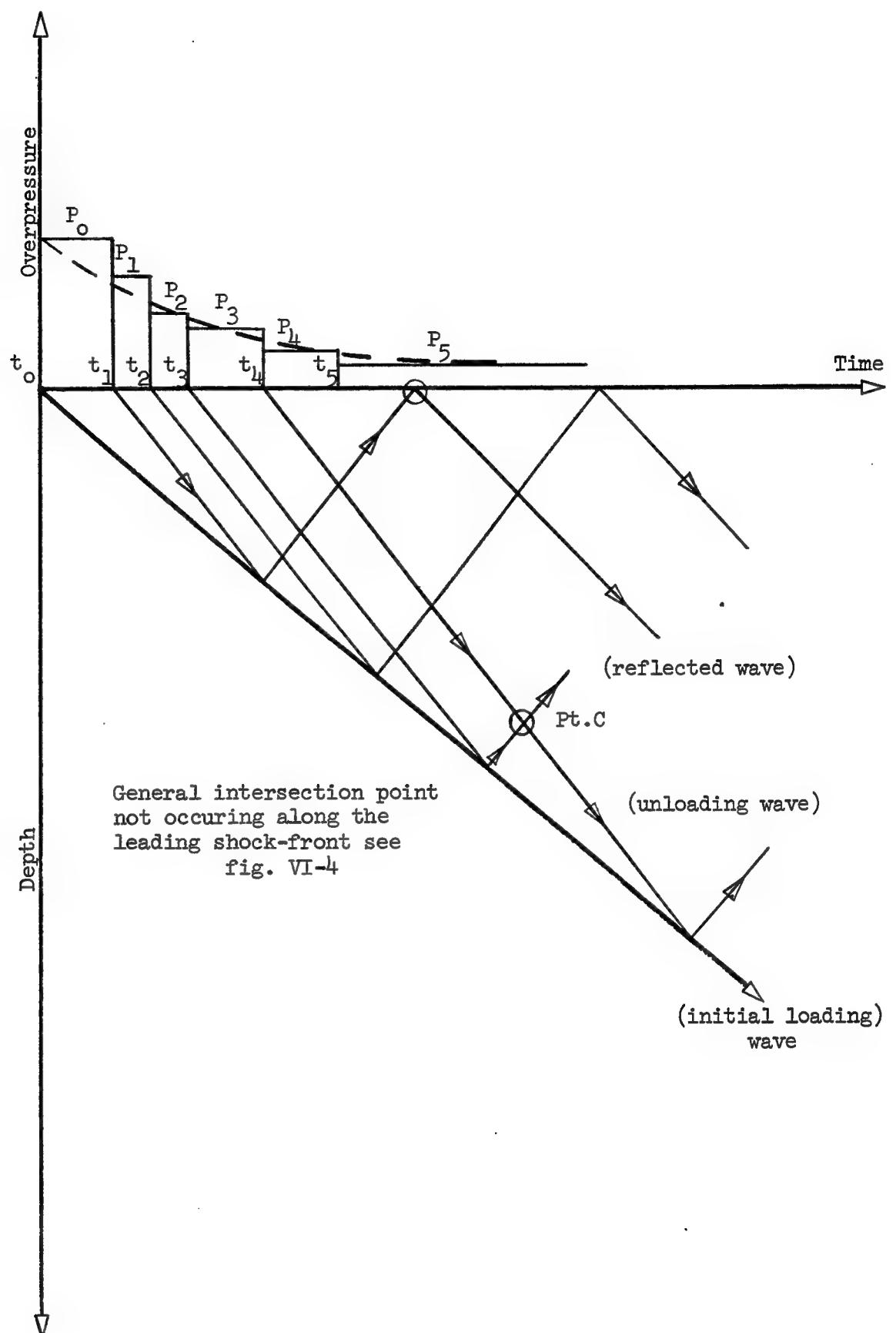
Fig. VI-5. Space-time diagram for a fine mesh

142

intersections in this case are not restricted to the simple pattern of fig. VI-3. The intersection equations for an intersection which is not along the leading shock-front are also based on equations VI-36 and VI-37. The stress σ_b and the particle velocity $\dot{u}_b$ are no longer zero and $\Delta\dot{u}_{ac}$ and $\Delta\dot{u}_{bc}$ are both determined from equation VI-23.

G. Computer program

A computer code, based on the foregoing analysis as related to the problem depicted in fig. VI-5, is available to compute the stress and particle velocity histories at selected depths in a homogeneous non-linear hysteretic medium. The code was originally written at Stanford Research Institute in ALGOL language (26) and has been translated to FORTRAN II language for a GE-225 computer with 8K memory. The mechanics of the code are described in references 18 and 26.

Output parameters are given in terms of the following nondimensional quantities

$$S = \frac{\sigma}{P_o} \qquad\qquad \text{VI-42}$$

$$T = \frac{t}{\tau} \qquad\qquad \text{VI-43}$$

$$V = \frac{\dot{u}}{\dot{u}_1} \qquad\qquad \text{VI-44}$$

$$Z = \frac{z}{\tau C_o} \qquad\qquad \text{VI-45}$$

$$\alpha = \frac{1 - \left(\frac{A}{B}\right)^{\frac{1}{2n}}}{1 + \left(\frac{A}{B}\right)^{\frac{1}{2n}}} \qquad\qquad \text{VI-46}$$

143

where S , T , V , and Z are the nondimensional stress, time, particle velocity, and depth respectively; $\dot{u}_1$ is particle velocity corresponding to the peak overpressure given by equation VI-32 and C_o is the wave velocity of a shock wave with a stress $\sigma = P_o$ determined from equation VI-25. Equation VI-46 is identical with the definition of α in equation III-25 if the tangent moduli and wave velocities are taken at one stress level. It is used here as a measure of the hysteretic energy loss.

The input variables consist of the following:

Variable	Description
NX	Number of depths of interest
ZA(N)	Specific depths of interest (ft)
B	$\frac{1-\alpha}{1+\alpha}$, α is given by the equation VI-46 (this B should not be confused with the B used in the body of the paper)
P	Stress-strain curvature parameter n (see fig. VI-1)
Q	Dummy number = 1
EPS	Acceptable error level $\approx$ 0.0005
DT	Time increment (sec), a constant
T21	Initiation time for the first unloading wave (sec), t_1 in fig. VI-5
TEND	Terminating time (sec)

The input sequence and formats are as follows:

144

Input Card	Format
(A) [NX,(ZA(N),N=1,NX)]	[I10,7F10.3,(8F10.3)]
(B) [B,P,Q,EPS,DT,T21,TEND]	(8F10.3)

The output variables are given in three groups as follows:

Group 1. Input data from card form (B) of the input variables followed by some intermediate calculations for debugging purposes.

Group 2. Input data from card form (A) of the input variables.

Group 3. Nondimensional stress (S), time (T), particle velocity (V), and depth (Z), given by equations VI-42, VI-43, VI-44, and VI-45, respectively.

A complete FORTRAN II listing of the program and an example of typical input and the resulting output is presented in Appendix VI.

APPENDIX VI

NONLINEAR HYSTERETIC MODEL

```
C       PROGRAM 41-S8-Z0-010                    29 MARCH 1968        00010
C                                                                    00020
C       NONLINEAR WAVE PROPAGATION (HYSTERETIC MODEL)                00030
C                                                                    00040
C       CONVERTED TO FORTRAN FROM ALGOL                              00050
C                                                                    00060
C                                                                    00070
C               ***** INPUT PARAMETERS *****                         00080
C                                                                    00090
C  ** NX      NUMBER OF DEPTHS OF INTEREST                           00100
C  ** ZA      LIST OF DEPTHS OF INTEREST (NX VALUES)                 00110
C                                                                    00120
C  ** B       NEWMARKS BETA PARAMETER                                00130
C  ** N       STRESS-STRAIN CURVATURE PARAMETER                      00140
C  ** M       M = N FOR NONSHOCK INPUT PRESSURE                      00150
C             M = 1.0 FOR SHOCK INPUT PRESSURE                       00160
C  ** EPS     ACCEPTABLE ERROR LEVEL                                 00170
C  ** DT      TIME INTERVAL BETWEEN START OF UNLOADING WAVES         00180
C             DURING INITIATION                                      00190
C  ** T21     INITIATION TIME FOR FIRST UNLOADING WAVE               00200
C  ** TEND    TERMINATION TIME.  WHEN AN INITIATION TIME FOR AN      00210
C             UNLOADING WAVE EXCEEDS TEND, THE PROGRAM ENDS          00220
C                                                                    00230
C                                                                    00240
C               ***** OUTPUT PARAMETERS *****                        00250
C                                                                    00260
C  ** S       NONDIMENSIONAL   STRESS                                00270
C  ** T       NONDIMENSIONAL   TIME                                  00280
C  ** V       NONDIMENSIONAL   PARTICLE VELOCITY                     0029
C  ** Z       NONDIMENSIONAL   DEPTH                                 0030
C                                                                    0031
        COMMON S(11,11),T(11,11),V(11,11),Z(11,11)
        COMMON SA(40),TA(40),VA(40),ZA(40)                           0033
        COMMON NJ,NX,JMAX                                            0034
C                                                                    0035
C                                                                    0037
C                                                                    0039
      1 FORMAT(I10,7F10.3,(8F10.3))                                  0040
      2 FORMAT(8F10.3)                                               0041
      3 FORMAT(1H1,30X,22H***** INPUT DATA *****,//,9X,1HB,11X,1HP,11X, 0042
       11HQ,10X,3HEPS,9X,2HDT,10X,3HT21,9X,4HTEND)                  0043
      4 FORMAT(1H0,10F12.5)                                          0044
   1000 FORMAT(1H0,1P8F14.6)
   1001 FORMAT(1H0,10X,18HDEPTHS OF INTEREST)
C                                                                    0045
C                                                                    0046
C***    BEGIN                                                        0047
C                                                                    0048
    100 CONTINUE                                                     0049
C                                                                    0050
C  **  READ DEPTHS OF INTEREST                                       0051
C                                                                    0052
        READ 1,NX,(ZA(N),N=1,NX)
C                                                                    0054
C***    AGAIN                                                        0055
```

```
C                                                                    0054
  101 DO 103 J=1,11
      DO 102 K=1,11
      S(J,K) = 0.0                                                   0059
      T(J,K) = 0.0                                                   0060
      V(J,K) = 0.0                                                   0061
  102 Z(J,K) = 0.0                                                   0062
  103 CONTINUE                                                       0063
C                                                                    0064
C **  READ AND PRINT INPUT PARAMETERS                                0065
C                                                                    0066
      READ 2,B,P,Q,EPS,DT,T(2,1),TEND
      PRINT 3
      PRINT 4,B,P,Q,EPS,DT,T(2,1),TEND
C                                                                    0070
C **  COMPUTE CONSTANTS                                              0071
C                                                                    0072
      VN = 0.5 + 1./(2.*P)
      CN = 0.5 - 1./(2.*P)
      SN = SQRTF(P)
      SM = SQRTF(Q)
      BSN = B/SN                                                     0077
      BSR = BSN/VN
      RM = 2.*SM/(Q+1.)
      ALP = (1-B*SM/SN)/(1+B*SM/SN)                                  0080
      PRINT 1000,VN,CN,SN,SM,BSN,BSR,RM,ALP
      S(1,1) = 1.0                                                   0081
      J = 2                                                          0082
      T(J,2) = T(J,1) + 2.*DT                                        0083
  104 IF(ABSF(T(J,2)-T(J,1))-DT)110,110,99
C                                                                    0085
C **  COMPUTE INTERSECTIONS ALONG AN UNLOADING WAVE                  0086
C                                                                    0087
   99 DO 109 K=1,J                                                   0088
C                                                                    0089
      IF(K-1)105,105,106                                             0090
  105 T(J,K) = T(2,1) + (J-2)*DT
      S(1,J) = EXPF(-ALP*T(J,1)/(1.+ALP))
      S(J,1) = EXPF(-T(J,1))
      V(J,K) = (RM-BSR)*S(1,J)**VN + BSR*S(J,1)**VN
      Z(J,1) = 0.                                                    0095
      GO TO 109                                                      0096
C                                                                    0097
  106 IF(K-J)108,107,107                                             0098
  107 S(J,K) = (V(J,K-1)+BSR*S(J,K-1)**VN)/(BSR+RM)
      V(J,K) = S(J,K)*RM
      S(J,K) = EXPF(LOGF(S(J,K))/VN)
      CU = (1./BSN)*((S(J,K-1)+S(J,K))/2.)**CN
      CL = SM*((S(J-1,K-1)+S(J,K))/2.)**CN
      T(J,K) =(Z(J-1,K-1)-Z(J,K-1)+T(J,K-1)*CU-T(J-1,K-1)*CL)/(CU-CL)  0104
      Z(J,K) = Z(J-1,K-1)+(T(J,K)-T(J-1,K-1))*CL                     0105
      GO TO 109                                                      0106
C                                                                    0107
  108 S(J,K) = 0.5*(S(J,K-1)**VN+ S(J-1,K)**VN)+ (0.5/BSR)*(V(J,K-1)-  0108
     1V(J-1,K))
      V(J,K) = V(J,K-1) - BSR*(S(J,K)-S(J,K-1)**VN)
      S(J,K) = EXPF(LOGF(S(J,K))/VN)
      CU = (SN/B)*((S(J,K-1) + S(J,K))/2.)**CN
      CL = (SN/B)*((S(J-1,K) + S(J,K))/2.)**CN
      T(J,K) = (Z(J-1,K)-Z(J,K-1)+T(J,K-1)*CU+T(J-1,K)*CL)/(CU+CL)   0114
```

```
        Z[J,K] = [T[J,K]-T[J,K-1]]*CU + Z[J,K-1]            0115
    109 PRINT 1000,J,K,S[J,K],T[J,K],V[J,K],Z[J,K],CU,CL
C                                                            0117
        J = J+1                                             0118
        T[J,2] = T[J-1,2]                                   0119
        T[J,1] = T[J-1,1]                                   0120
        GO TO 104                                           0121
C                                                            0122
    110 JMAX = J-1                                          0123
        J = JMAX                                            0124
C                                                            0125
C ** LOCATE SURFACE INTERSECTION                            0126
C                                                            0127
        DO 111 K=1,JMAX                                     0128
        S[1,K] = S[J,K]                                     0129
        T[1,K] = T[J,K]                                     0130
        V[1,K] = V[J,K]                                     0131
    111 Z[1,K] = Z[J,K]                                     0132
        J = 2                                               0133
C                                                            0134
C*** START                                                  0135
C                                                            0136
    112 IF[T[J-1,1]-TEND]114,113,113                        0137
    113 J = J-1                                             0138
        GO TO 125                                           0139
C                                                            0140
C ** COMPUTE INTERSECTIONS ALONG AN UNLOADING WAVE          0141
C                                                            0142
    114 DO 121 K=1,JMAX                                     0143
C                                                            0144
        IF[K-1]115,115,118
    115 ST = 2.*T[J-1,K+1]-T[J-1,1]                         0146
        T[J,K] = ST + 2*EPS                                 0147
        IF[ABSF[T[J,K]-ST]-EPS]117,116,116
    116 T[J,K] = ST                                         0149
        S[J,K] = EXPF[-T[J,K]]
        C = [SN/B]*[[S[J-1,K+1] + S[J,1]]/2.]**CN
        ST =[T[J,K]+T[J-1,K+1]+Z[J-1,K+1]/C]/2.             0152
    117 V[J,K] = V[J-1,K+1]+BSR*[S[J,K]**VN-S[J-1,K+1]**VN]
        Z[J,K] = 0.                                         0154
        GO TO 121                                           0155
C                                                            0156
    118 IF[K-JMAX]120,119,119                               0157
    119 S[J,K] = [V[J,K-1]+BSR*S[J,K-1]**VN]/[BSR+RM]
        V[J,K] = S[J,K]*RM
        S[J,K] = EXPF[LOGF[S[J,K]]/VN]
        CU = [1./BSN]*[[S[J,K-1]+S[J,K]]/2.]**CN
        CL = SM*[[S[J-1,K]+S[J,K]]/2.]**CN
        T[J,K] = [-Z[J,K-1]+Z[J-1,K]+CU*T[J,K-1]-CL*T[J-1,K]]/[CU-CL]   0163
        Z[J,K] = Z[J-1,K]+CL*[T[J,K]-T[J-1,K]]              0164
        GO TO 121                                           0165
C                                                            0166
    120 S[J,K] = 0.5*[S[J,K-1]**VN+S[J-1,K+1]**VN]+[0.5/BSR]*[V[J,K-1]-
       1V[J-1,K+1]]                                         0168
        V[J,K] = V[J,K-1]-BSR*[S[J,K]-S[J,K-1]**VN]
        S[J,K] = EXPF[LOGF[S[J,K]]/VN]
        CU = [SN/B]*[[S[J,K-1]+S[J,K]]/2.]**CN
        CL = [SN/B]*[[S[J-1,K+1]+S[J,K]]/2.]**CN
        T[J,K] = [Z[J-1,K+1]-Z[J,K-1]+CU*T[J,K-1]+CL*T[J-1,K+1]]/[CU+CL]  0173
        Z[J,K] = Z[J,K-1]+[T[J,K]-T[J,K-1]]*CU
```

```
C                                                                      0176
  121 PRINT 1000,J,K,S(J,K),T(J,K),V(J,K),Z(J,K),CU,CL
      IF(J-11)122,123,123
  122 J = J+1                                                          0178
      GO TO 112                                                        0179
  123 NJ = J                                                           0180
C                                                                      0181
C***  PROCEDURE INTERPOLATE AND PRINT                                  0182
C                                                                      0183
      PRINT 1001
      PRINT 1000,(ZA(N),N=1,NX)
      CALL INTERP                                                      0184
C                                                                      0185
C **  RESET INDEX TO ZERO                                              0186
C                                                                      0187
      DO 124 K=1,JMAX                                                  0188
      S(1,K) = S(J,K)                                                  0189
      T(1,K) = T(J,K)                                                  0190
      V(1,K) = V(J,K)                                                  0191
  124 Z(1,K) = Z(J,K)                                                  0192
      J = 2                                                            0193
C                                                                      0194
C***  GO TO START                                                      0195
C                                                                      0196
      GO TO 112                                                        0197
  125 NJ = J                                                           0198
      PRINT 1000,NX,NJ,JMAX
      CALL INTERP                                                      0199
C                                                                      0200
C***  GO TO AGAIN (NEXT CASE)                                          0201
C                                                                      0202
      GO TO 101                                                        0203
      CALL EXIT                                                        0204
C                                                                      0205
C***  HALT                                                             0206
C                                                                      0207
      END                                                              0208
 04172, 15352

,KP 0000000
S    0017404 0040003
T    0017022 0040006
V    0016440 0040011
Z    0016056 0040014
SA   0015736 0020050
TA   0015616 0020050
VA   0015476 0020050
ZA   0015356 0020050
NJ   0015355
NX   0015354
JMAX    0015353
/00001 0000040
/00002 0000050
/00003 0000053
/00004 0000115
/01000 0000122
/01001 0000127
/00100 0000142
N    0000017
+00001 0000021
```

```
      SUBROUTINE INTERP                                               00010
C                                                                     00020
C     PROCEDURE INTERPOLATE                                           00030
C                                                                     00040
C                                                                     00050
      COMMON S(11,11),T(11,11),V(11,11),Z(11,11)                      00060
      COMMON SA(40),TA(40),VA(40),ZA(40)                              00070
      COMMON NJ,NX,JMAX                                               00080
C                                                                     00090
    1 FORMAT(1H0,//,21X,40H***** INTERPOLATION ALONG THE WAVE *****,  00100
     1//,11HWAVE NUMBER,17X,1HS,14X,1HT,14X,1HV,14X,1HZ,/)            00110
    2 FORMAT(1H0,//,21X,39H***** INTERPOLATION BETWEEN WAVES *****,   00120
     1//,11HWAVE NUMBER,17X,1HS,14X,1HT,14X,1HV,14X,1HZ,/)            00130
    3 FORMAT(1H ,I6,14X,1P4E15.5,/,(21X,1P4E15.5))                    00140
C                                                                     00150
C                                                                     00160
      PRINT 1
      DO 208 J=1,NJ
      DO 205 N=1,NX
      IF(N-1)201,200,201
  200 IF(ZA(N)-Z(J,JMAX))202,202,208
  201 IF(ZA(N)-Z(J,JMAX))202,202,206
  202 DO 203 M=1,JMAX
      KT = M
      IF(Z(J,M)-ZA(N))203,203,204
  203 CONTINUE
  204 M = KT
      K = KT-1                                                        00260
      ST = (ZA(N)-Z(J,K))/(Z(J,M)-Z(J,K))
      SA(N) = S(J,K)+ST*(S(J,M)-S(J,K))
      TA(N) = T(J,K)+ST*(T(J,M)-T(J,K))
      VA(N) = V(J,K)+ST*(V(J,M)-V(J,K))
  205 CONTINUE
C                                                                     0032
      M = N
      GO TO 207
  206 M = N-1
  207 PRINT 3,J,(SA(N),TA(N),VA(N),ZA(N),N=1,M)
  208 CONTINUE
C                                                                     0039
      PRINT 2
      NJ1 = NJ-1
      DO 224 J=1,NJ1
      DO 221 N=1,NX
      IF(N-1)211,209,211
  209 IF(ZA(N)-Z(J,JMAX))213,213,210
  210 IF(ZA(N)-Z(J+1,JMAX))213,213,224
  211 IF(ZA(N)-Z(J,JMAX))213,213,212
  212 IF(ZA(N)-Z(J+1,JMAX))213,213,222
  213 DO 214 K=1,JMAX
      KT = K
      IF(Z(J,K)-ZA(N))214,214,215
  214 CONTINUE
  215 K = KT
      IF(K-JMAX)217,216,217
  216 IF(ZA(N)-Z(J,K))217,217,220
  217 IF(Z(J+1,K-1)-ZA(N))218,218,219
```

```
    218 KT = J+1
        M = K-1
        ST = (ZA(N)-Z(KT,M))/(Z(J,K)-Z(KT,M))
        SA(N) = S(KT,M)+ST*(S(J,K)-S(KT,M))
        TA(N) = T(KT,M)+ST*(T(J,K)-T(KT,M))
        VA(N) = V(KT,M)+ST*(V(J,K)-V(KT,M))
        GO TO 221
    219 K = K-1
    220 M = K
        ST = (ZA(N)-Z(J,K))/(Z(J+1,M)-Z(J,K))
        SA(N) = S(J,K)+ST*(S(J+1,M)-S(J,K))
        TA(N) = T(J,K)+ST*(T(J+1,M)-T(J,K))
        VA(N) = V(J,K)+ST*(V(J+1,M)-V(J,K))
    221 CONTINUE
C                                                                      0067
        M = N
        GO TO 223
    222 M = N-1
    223 PRINT 3,J,(SA(N),TA(N),VA(N),ZA(N),N=1,M)
    224 CONTINUE
C                                                                      0074
        RETURN                                                         0075
        END                                                            0076
    01475, 15352

    INTERP 0000012
S     0017404 0040003
T     0017022 0040014
V     0016440 0040017
Z     0016056 0040022
SA    0015736 0020050
TA    0015616 0020050
VA    0015476 0020050
ZA    0015356 0020050
NJ    0015355
NX    0015354
JMAX     0015353
/00001 0000045
/00002 0000112
/00003 0000156
J      0000025
+00001 0000026
N      0000027
/00201 0000230
/00200 0000210
/00202 0000250
/00208 0000572
/00206 0000535
M      0000032
KT     0000033
/00203 0000275
/00204 0000304
K      0000034
ST     0000036
/00205 0000523
/00207 0000540
NJ1 0000350
/00211 0000662
/00209 0000621
/00213 0000723
```

```
/00101 0000165
J    0000022
-00012 0000023
K    0000024
0.0 0000026
/00102 0000224
/00103 0000243
B    0000030
P    0000032
Q    0000034
EPS 0000262
DT  0000264
+00002 0000266
TEND   0000270
VN  0000272
0.5 0000274
1.  0000276
2.  0000300
CN  0000304
SN  0000310
SQRTF  0140410  EXT PROG
SM  0000412
BSN 0000414
BSR 0000416
RM  0000420
ALP 0000422
1.0 0000430
/00104 0000576
ABSF   0140432  EXT PROG
/00110 0002206
/00099 0000623
/00105 0000633
/00106 0001045
EXPF   0140434  EXT PROG
,IR 0140710  EXT PROG
0.  0000712
/00109 0002061
/00108 0001414
/00107 0001053
LOGF   0140714  EXT PROG
CU  0000716
CL  0000720
/00111 0002271
/00112 0002321
/00114 0002343
/00113 0002337
/00125 0004122
/00115 0002353
/00118 0002655
ST  0001516
/00117 0002565
/00116 0002435
C    0001520
/00121 0003666
/00120 0003250
/00119 0002663
+00011 0003164
/00122 0003756
/00123 0003762
INTERP 0103166  EXT PROG
```

```
/00124 0004071
EXIT   0104140  EXT PROG
```

31   0.0   0.02   0.04   0.06   0.08   0.1   0.2

NX   ZA (1)   ZA (2)   ZA (3)   ZA (4)   ZA (5)   ZA (6)   ZA (7)

0.4   0.6   0.8   1.0   2.0   4.0   6.0   8.0

ZA (8)   ZA (9)   ZA (10)   ZA (11)   ZA (12)   ZA (13)   ZA (14)   ZA (15)

Typical input nonlinear hysteretic model (sheet 1 of 2)

```
     10.0       12.0       14.0       16.0       18.0      20.0       22.0       24.0

    ZA (16)    ZA (17)  ZA (18)    ZA (19)    ZA (20)  ZA (21)    ZA (22)    ZA (23)
```



```
      30.       40.        50.        60.        70.       80.        90.       100.

    ZA (24)   ZA (25)    ZA (26)   ZA (27)     ZA (28)   ZA (29)    ZA (30)    ZA (31)
```


Typical input nonlinear hysteretic model (sheet 2 of 2)

156

```
0.66666666      2.        1.0       0.0001      0.0004      0.001      15.

     B          P         Q          EPS         DT         T21       TEND
```

Typical input nonlinear hysteretic model

B	P	Q	EPS	DT	T21	TEND	
0.66667	2.00000	1.00000	0.00010	0.00040	0.00100	15.00000	
7.500000E-01	2.500000E-01	1.414214E+00	1.000000E+00	4.714045E-01	6.285394E-01	1.000000E+00	3.59245&E-01
2.000000E+00	1.000000E+00	9.990005E-01	1.000000E-03	9.994551E-01	0.000000E-01	-6.289766E-49	-6.28976&E-49
2.000000E+00	2.000000E+00	9.991681E-01	1.892017E-03	9.993761E-01	1.891820E-03	2.120835E+00	9.99896nE-01
3.000000E+00	1.000000E+00	9.986010E-01	1.400000E-03	9.992373E-01	0.000000E-01	2.120835E+00	9.99896nE-01
3.000000E+00	2.000000E+00	9.987373E-01	2.092056E-03	9.991730E-01	1.467584E-03	2.120614E+00	2.12076&E+00
3.000000E+00	3.000000E+00	9.988356E-01	2.648940E-03	9.991266E-01	2.648554E-03	2.120676E+00	9.997504E-01
4.000000E+00	1.000000E+00	9.982016E-01	1.810000E-03	9.990195E-01	0.000000E-01	2.120676E+00	9.997504E-01
4.000000E+00	2.000000E+00	9.983067E-01	2.292085E-03	9.989699E-01	1.043415E-03	2.120394E+00	2.12053&E+00
4.000000E+00	3.000000E+00	9.984050E-01	2.848996E-03	9.989236E-01	2.224316E-03	2.120448E+00	2.12058&E+00
4.000000E+00	4.000000E+00	9.985032E-01	3.405929E-03	9.988772E-01	3.405291E-03	2.120500E+00	9.996672E-01
5.000000E+00	1.000000E+00	9.978024E-01	2.200000E-03	9.988018E-01	0.000000E-01	2.120500E+00	9.996672E-01
5.000000E+00	2.000000E+00	9.978763E-01	2.492104E-03	9.987669E-01	6.193122E-04	2.120174E+00	2.120307E+00
5.000000E+00	3.000000E+00	9.979745E-01	3.049043E-03	9.987206E-01	1.800145E-03	2.120219E+00	2.12036nE+00
5.000000E+00	4.000000E+00	9.980727E-01	3.606003E-03	9.986742E-01	2.981051E-03	2.120271E+00	2.120412E+00
5.000000E+00	5.000000E+00	9.981709E-01	4.162985E-03	9.986279E-01	4.162032E-03	2.120324E+00	9.99584nE-01
2.000000E+00	1.000000E+00	9.972197E-01	2.784209E-03	9.984572E-01	0.000000E-01	2.120324E+00	9.99584nE-01
2.000000E+00	2.000000E+00	9.973179E-01	3.341201E-03	9.984109E-01	1.180750E-03	2.119870E+00	2.120071E+00
2.000000E+00	3.000000E+00	9.974161E-01	3.898203E-03	9.983645E-01	2.361552E-03	2.119923E+00	2.120123E+00
2.000000E+00	4.000000E+00	9.975143E-01	4.455227E-03	9.983182E-01	3.542428E-03	2.119975E+00	2.120175E+00
2.000000E+00	5.000000E+00	9.976640E-01	5.268831E-03	9.982475E-01	5.247302E-03	2.120041E+00	9.99479nE-01
3.000000E+00	1.000000E+00	9.961094E-01	3.898192E-03	9.978407E-01	0.000000E-01	2.120041E+00	9.99479nE-01
3.000000E+00	2.000000E+00	9.962076E-01	4.455311E-03	9.977944E-01	1.180691E-03	2.119280E+00	2.11962nE+00
3.000000E+00	3.000000E+00	9.963057E-01	5.012412E-03	9.977481E-01	2.361373E-03	2.119332E+00	2.11968nE+00
3.000000E+00	4.000000E+00	9.964555E-01	5.826129E-03	9.976774E-01	4.085963E-03	2.119398E+00	2.119750E+00
3.000000E+00	5.000000E+00	9.967311E-01	7.377840E-03	9.975473E-01	7.374832E-03	2.119511E+00	9.992987E-01
4.000000E+00	1.000000E+00	9.950001E-01	5.012430E-03	9.972246E-01	0.000000E-01	2.119511E+00	9.992985E-01
4.000000E+00	2.000000E+00	9.950982E-01	5.569647E-03	9.971782E-01	1.180571E-03	2.118690E+00	2.119037E+00
4.000000E+00	3.000000E+00	9.952479E-01	6.383477E-03	9.971076E-01	2.904878E-03	2.118756E+00	2.119117E+00

4.000000E+00	4.000000E+00	9.955235E-01	7.935404E-03	-9.969775E-01	6.193207E-03	2.118869E+00	2.119264E+00
4.000000E+00	5.000000E+00	9.957989E-01	9.487854E-03	9.968475E-01	9.482873E-03	2.119016E+00	9.990640E-01
5.000000E+00	1.000000E+00	9.938919E-01	6.126865E-03	9.966088E-01	0.000000E-01	2.119016E+00	9.990640E-01
5.000000E+00	2.000000E+00	9.940415E-01	6.940847E-03	9.965381E-01	1.724105E-03	2.118113E+00	2.118475E+00
5.000000E+00	3.000000E+00	9.943170E-01	8.492989E-03	9.964881E-01	5.011895E-03	2.118227E+00	2.118627E+00
5.000000E+00	4.000000E+00	9.945924E-01	1.004566E-02	9.962781E-01	8.301021E-03	2.118373E+00	2.11876AE+00
5.000000E+00	5.000000E+00	9.948675E-01	1.159877E-02	9.961482E-01	1.159132E-02	2.118520E+00	9.88831E-01
6.000000E+00	1.000000E+00	9.922752E-01	7.754828E-03	9.957040E-01	0.000000E-01	2.118520E+00	9.88831E-01
6.000000E+00	2.000000E+00	9.925506E-01	9.307370E-03	9.955740E-01	3.287175E-03	2.117285E+00	2.117830E+00
6.000000E+00	3.000000E+00	9.928258E-01	1.086035E-02	9.954440E-01	6.575510E-03	2.117432E+00	2.117978E+00
6.000000E+00	4.000000E+00	9.931008E-01	1.241378E-02	9.953141E-01	9.865016E-03	2.117579E+00	2.118123E+00
6.000000E+00	5.000000E+00	9.935038E-01	1.468334E-02	9.951239E-01	1.467140E-02	2.117759E+00	9.985432E-01
7.000000E+00	1.000000E+00	9.891988E-01	1.085991E-02	9.939903E-01	0.000000E-01	2.117759E+00	9.985432E-01
7.000000E+00	2.000000E+00	9.894739E-01	1.241380E-02	9.938603E-01	3.287468E-03	2.115642E+00	2.116611E+00
7.000000E+00	3.000000E+00	9.897487E-01	1.396783E-02	9.937305E-01	6.575471E-03	2.115789E+00	2.116758E+00
7.000000E+00	4.000000E+00	9.901513E-01	1.623827E-02	9.935402E-01	1.137966E-02	2.115970E+00	2.116973E+00
7.000000E+00	5.000000E+00	9.909157E-01	2.056977E-02	9.931790E-01	2.054633E-02	2.116282E+00	9.980467E-01
8.000000E+00	1.000000E+00	9.861294E-01	1.396769E-02	9.922789E-01	0.000000E-01	2.116282E+00	9.980467E-01
8.000000E+00	2.000000E+00	9.864041E-01	1.552262E-02	9.921490E-01	3.287135E-03	2.113999E+00	2.11496AE+00
8.000000E+00	3.000000E+00	9.868063E-01	1.779394E-02	9.919588E-01	8.089122E-03	2.114181E+00	2.115184E+00
8.000000E+00	4.000000E+00	9.875701E-01	2.212713E-02	9.915976E-01	1.725160E-02	2.114493E+00	2.115595E+00
8.000000E+00	5.000000E+00	9.883330E-01	2.646538E-02	9.912369E-01	2.642659E-02	2.114902E+00	9.973950E-01
9.000000E+00	1.000000E+00	9.830674E-01	1.707756E-02	9.905701E-01	0.000000E-01	2.114902E+00	9.973950E-01
9.000000E+00	2.000000E+00	9.834694E-01	1.935007E-02	9.903798E-01	4.800424E-03	2.112391E+00	2.113394E+00
9.000000E+00	3.000000E+00	9.842325E-01	2.368493E-02	9.900186E-01	1.395871E-02	2.112704E+00	2.113804E+00
9.000000E+00	4.000000E+00	9.849948E-01	2.802487E-02	9.896579E-01	2.312950E-02	2.113113E+00	2.114212E+00
9.000000E+00	5.000000E+00	9.857560E-01	3.236908E-02	9.892978E-01	3.231107E-02	2.113522E+00	9.967453E-01
1.000000E+01	1.000000E+00	9.786095E-01	2.162257E-02	9.880779E-01	0.000000E-01	2.113522E+00	9.967453E-01
1.000000E+01	2.000000E+00	9.793718E-01	2.596055E-02	9.877166E-01	9.153512E-03	2.110090E+00	2.111603E+00
1.000000E+01	3.000000E+00	9.801331E-01	3.030296E-02	9.873560E-01	1.831816E-02	2.110500E+00	2.112019E+00
1.000000E+01	4.000000E+00	9.808933E-01	3.464963E-02	9.869958E-01	2.749360E-02	2.110910E+00	2.112427E+00
1.000000E+01	5.000000E+00	9.820019E-01	4.100461E-02	9.864708E-01	4.091159E-02	2.111412E+00	9.959451E-01
1.100000E+01	1.000000E+00	9.701559E-01	3.029852E-02	9.833444E-01	0.000000E-01	2.111412E+00	9.959451E-01

DEPTHS OF INTEREST

0.000100E-01 2.000000E-02 4.000000E-02 6.000000E-02 8.000000E-02 1.000000E-01 2.000000E-01 4.000000E-01

6.000100E-01 8.000000E-01 1.000000E+00 2.000000E+00 4.000000E+00 6.000000E+00 8.000000E+00 1.000000E+01

1.200000E+01 1.400000E+01 1.600000E+01 1.800000E+01 2.000000E+01 2.200000E+01 2.400000E+01 3.000000E+01

4.000100E+01 5.000000E+01 6.000000E+01 7.000000E+01 8.000000E+01 9.000000E+01 1.000000E+02

***** INTERPOLATION ALONG THE WAVE *****

WAVE NUMBER	S	T	W	Z
1	9.97802E-01	2.20000E-03	9.98802E-01	0.00000E-01
2	9.97290E-01	2.78421E-03	9.98457E-01	0.00000E-01
3	9.96109E-01	3.89819E-03	9.97841E-01	0.00000E-01
4	9.95000E-01	5.01243E-03	9.97225E-01	0.00000E-01
5	9.93892E-01	6.12687E-03	9.96609E-01	0.00000E-01
6	9.92275E-01	7.75483E-03	9.95704E-01	0.00000E-01
7	9.89199E-01	1.08599E-02	9.93990E-01	0.00000E-01
	9.90870E-01	2.03116E-02	9.93201E-01	2.00000E-02
8	9.86129E-01	1.39677E-02	9.92279E-01	0.00000E-01
	9.87799E-01	2.34267E-02	9.91490E-01	2.00000E-02
9	9.83067E-01	1.70776E-02	9.90570E-01	0.00000E-01
	9.84735E-01	2.65439E-02	9.89781E-01	2.00000E-02
10	9.78610E-01	2.16226E-02	9.88078E-01	0.00000E-01
	9.80272E-01	3.10997E-02	9.87290E-01	2.00000E-02
	9.81927E-01	4.05729E-02	9.86506E-01	4.00000E-02
11	9.70156E-01	3.02985E-02	9.83344E-01	0.00000E-01
	9.71812E-01	3.97962E-02	9.82558E-01	2.00000E-02
	9.73459E-01	4.92893E-02	9.01776E-01	4.00000E-02

***** INTERPOLATION BETWEEN WAVES *****

WAVE NUMBER	S	T	W	Z
1	9.97290E-01	2.78421E-03	9.98457E-01	0.00000E-01
2	9.96109E-01	3.89819E-03	9.97841E-01	0.00000E-01
3	9.95000E-01	5.01243E-03	9.97225E-01	0.00000E-01
4	9.93892E-01	6.12687E-03	9.96609E-01	0.00000E-01
5	9.92275E-01	7.75483E-03	9.95704E-01	0.00000E-01
6	9.89199E-01	1.08599E-02	9.93990E-01	0.00000E-01
	9.91156E-01	2.00224E-02	9.93360E-01	2.00000E-02
7	9.86129E-01	1.39677E-02	9.92279E-01	0.00000E-01
	9.90361E-01	2.08280E-02	9.92917E-01	2.00000E-02
8	9.83067E-01	1.70776E-02	9.90570E-01	0.00000E-01
	9.86366E-01	2.48848E-02	9.90691E-01	2.00000E-02
9	9.78610E-01	2.16226E-02	9.88078E-01	0.00000E-01
	9.81833E-01	2.95066E-02	9.88161E-01	2.00000E-02
	9.82400E-01	4.00893E-02	9.86770E-01	4.00000E-02
10	9.70156E-01	3.02985E-02	9.83344E-01	0.00000E-01
	9.73361E-01	3.82034E-02	9.83424E-01	2.00000E-02
	9.81047E-01	4.14368E-02	9.86037E-01	4.00000E-02

160

VII

Comparative Studies of Various Stress-Strain Models

A. Purpose

A one-dimensional wave propagation problem in a typical soil is solved herein utilizing the computer programs presented in Chapter III, V and VI for the linear hysteretic model, the nonlinear locking model and the nonlinear hysteretic model respectively, in order to compare the resulting solutions with a finite difference solution (28) of the same problem in which the "actual" stress-strain curve for the soil is used.

The stress-strain relation for the soil under consideration is shown in fig. VII-1. During the early stages of loading the stress-strain curve is concave downward indicating a "plastic" behavior of the material. However, as the stress increases further, the curve becomes concave upward indicating a "strain-hardening" behavior of the material. At stress levels higher than those indicated in fig. VII-1, the tangent modulus will generally continue to increase. During unloading the soil exhibits an extremely stiff behavior at all stress levels except near zero where a sharp breaking tail is evident. The result of a complete load cycle is a considerably large permanent strain.

The overpressure-time relation used for the comparative studies is shown in fig. VII-2 and is described by

$$P(t) = 700\ e^{-t/38} \hspace{3cm} \text{VII-1}$$

where $P(t)$ is expressed in psi and t is expressed in msec. The initial mass density of the soil is $P = 3.66$ slugs/ft^3 .

161
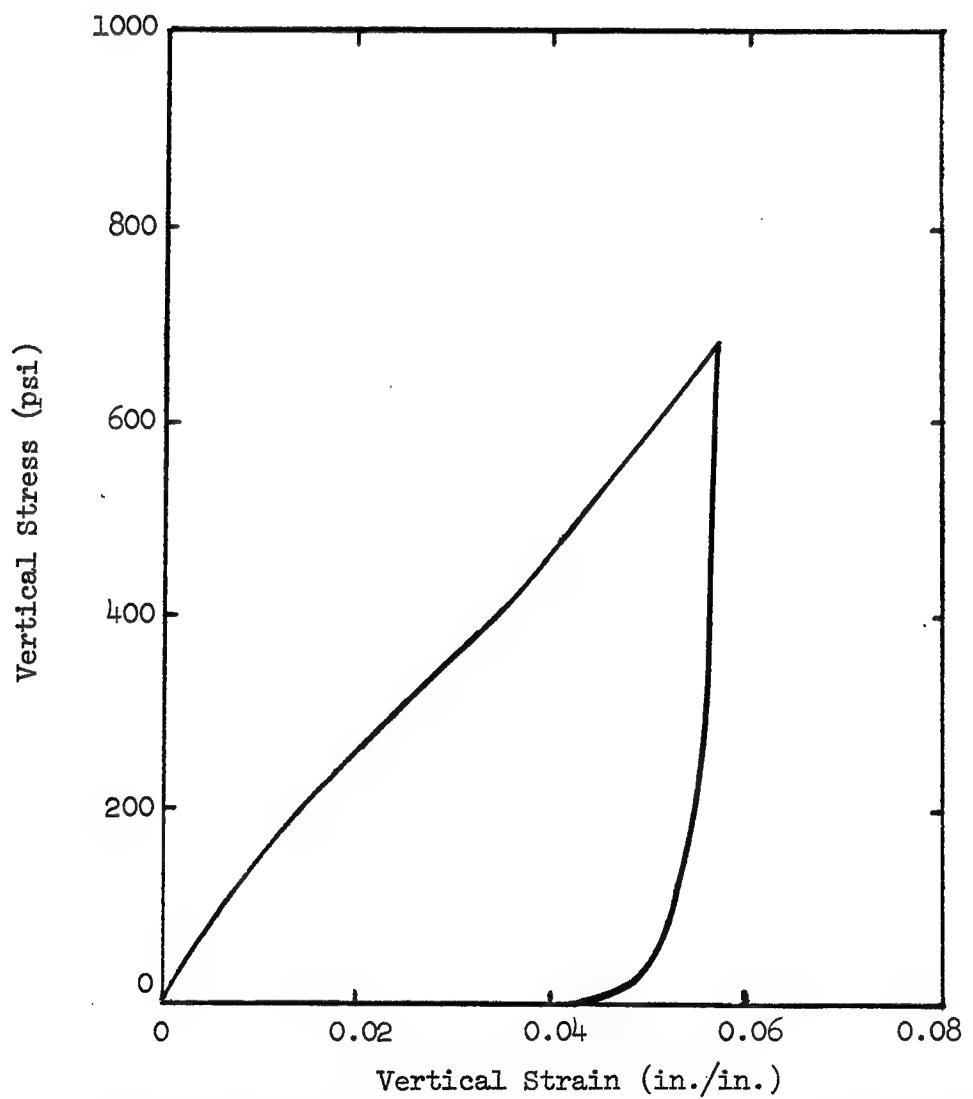
Fig. VII-1. Uniaxial strain relation of real soil used
for model comparison study.

162
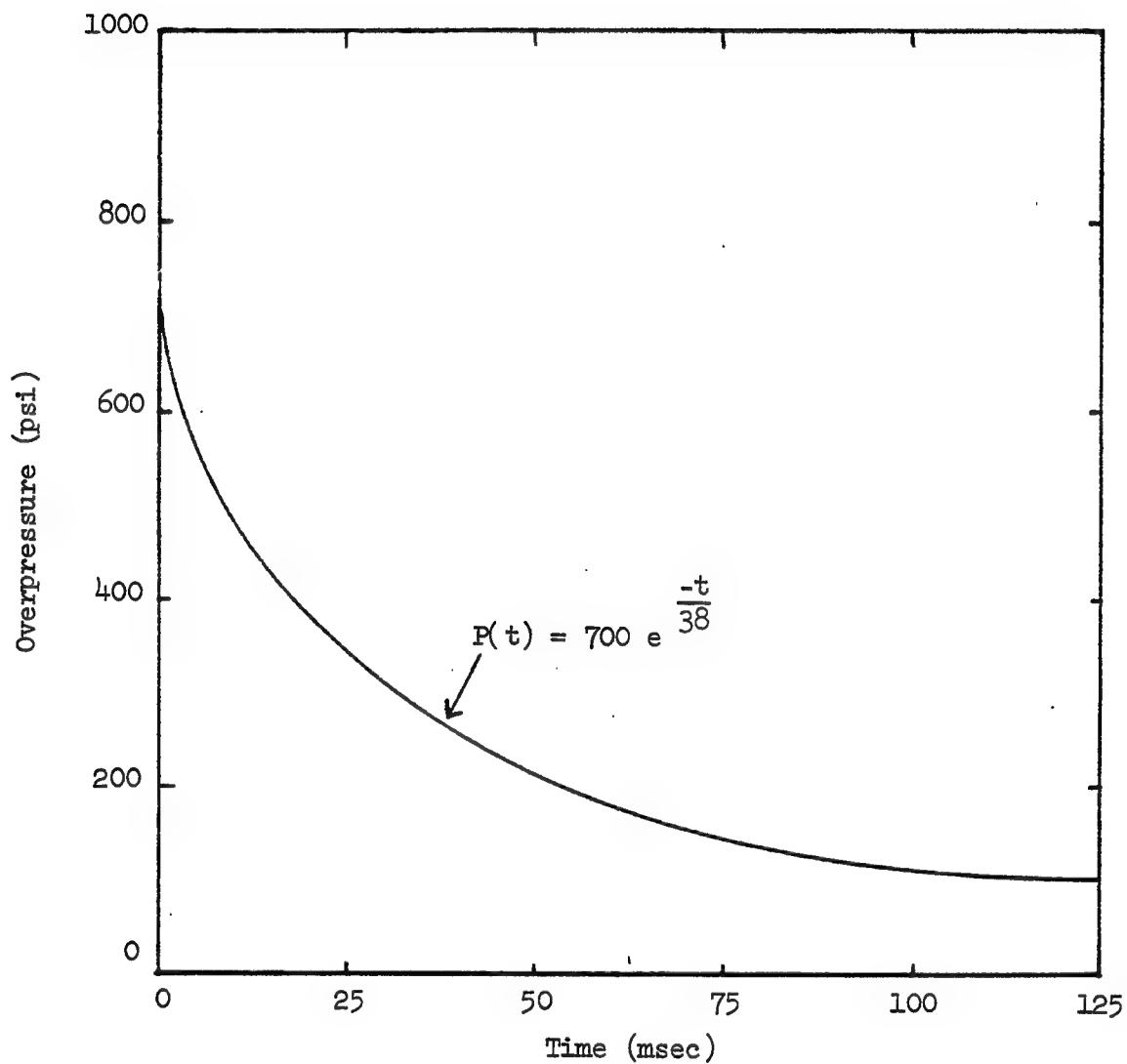
Fig. VII-2.   Overpressure-time relation for model
comparison study.

B. Approximations to the soil
    stress-strain curve with the various models

The approximations to the stress-strain curve of fig. VII-1 for the various models are shown in figs. VII-3 through VII-6. Fig. VII-3 depicts the piecewise-linear fit which was used to obtain the finite difference solution of the problem. Six straight line segments were used to represent the loading stress-strain characteristics and four straight line segments were used to represent the unloading/reloading characteristics. The comparison (shown in fig. VII-3) of the piecewise-linear fit with the actual soil relation indicates that the piecewise-linear model does indeed accurately represent the "actual" soil stress-strain relation.

Fig. VII-4 shows the nonlinear locking model approximation to the soil stress-strain curve (this model was discussed in Chapter V) and figs. VII-5 and VII-6 show the linear hysteretic model and the nonlinear hysteretic model approximations, respectively (these models were discussed in Chapters III and VI). For ease of comparison, the actual soil stress-strain relation is also shown (as a dashed line) on each of these figs. Note that all of the approximations to the loading stress-strain relation pass in common through two points on the actual curve, the zero stress level point and the 700-psi stress level point.

C. Results of the computer runs

The results of the computer runs for the various models are presented as plots of the attenuation of peak vertical stress and particle velocity with depth in figs. VII-7 and VII-8. In addition, stress-time histories at various depths are shown in fig. VII-9 for the linear hysteretic model and in figs. VII-10 and VII-11 for the piecewise-linear model. Particle
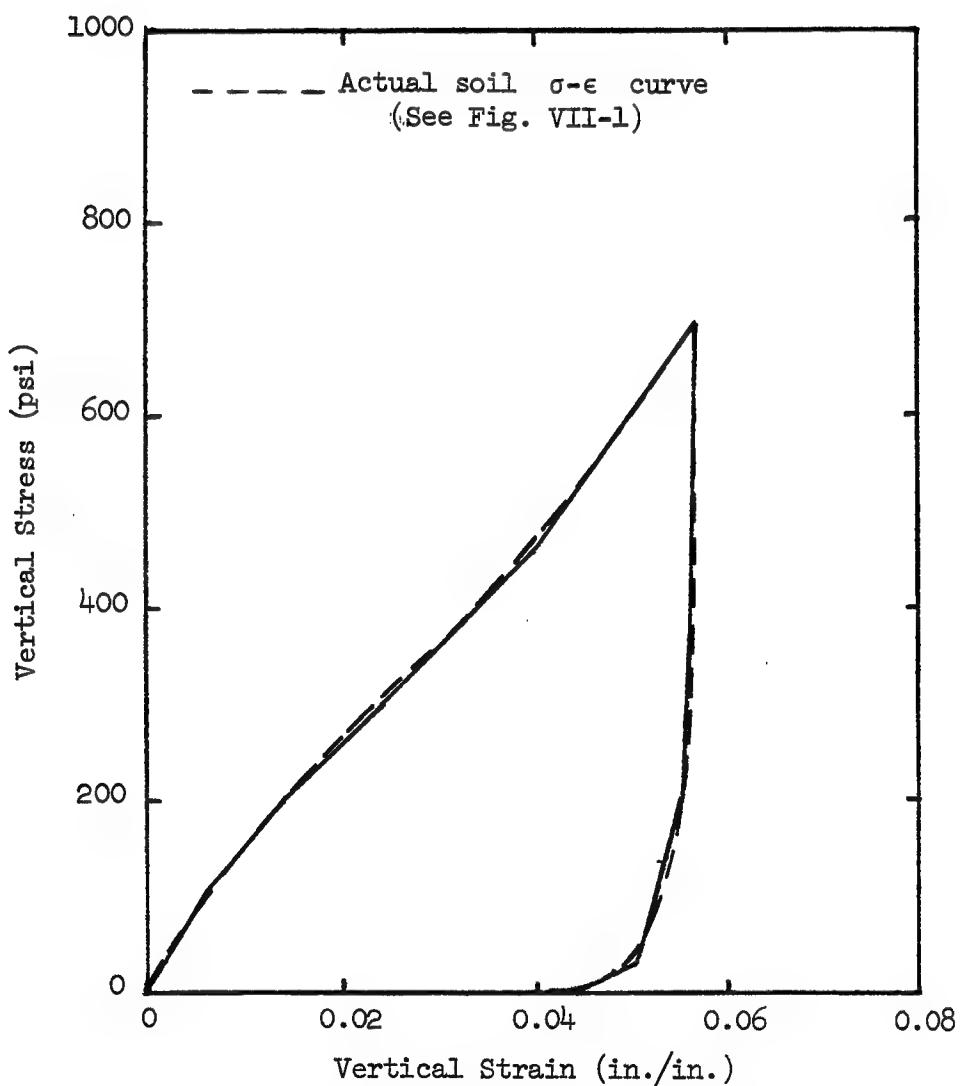
Fig. VII-3. Piecewise-linear stress-strain fit for
use with finite difference solution.

165
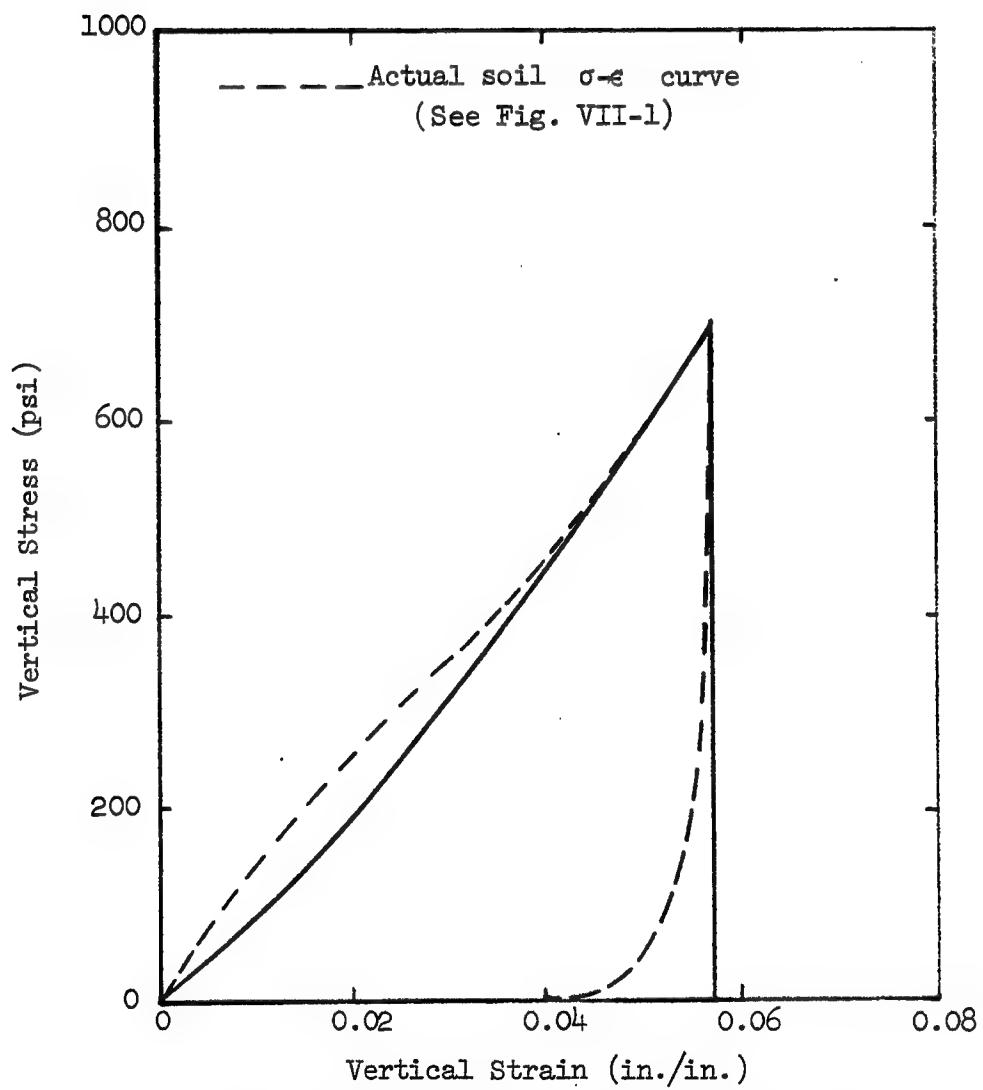
Fig. VII-4. Nonlinear locking model fit.

166
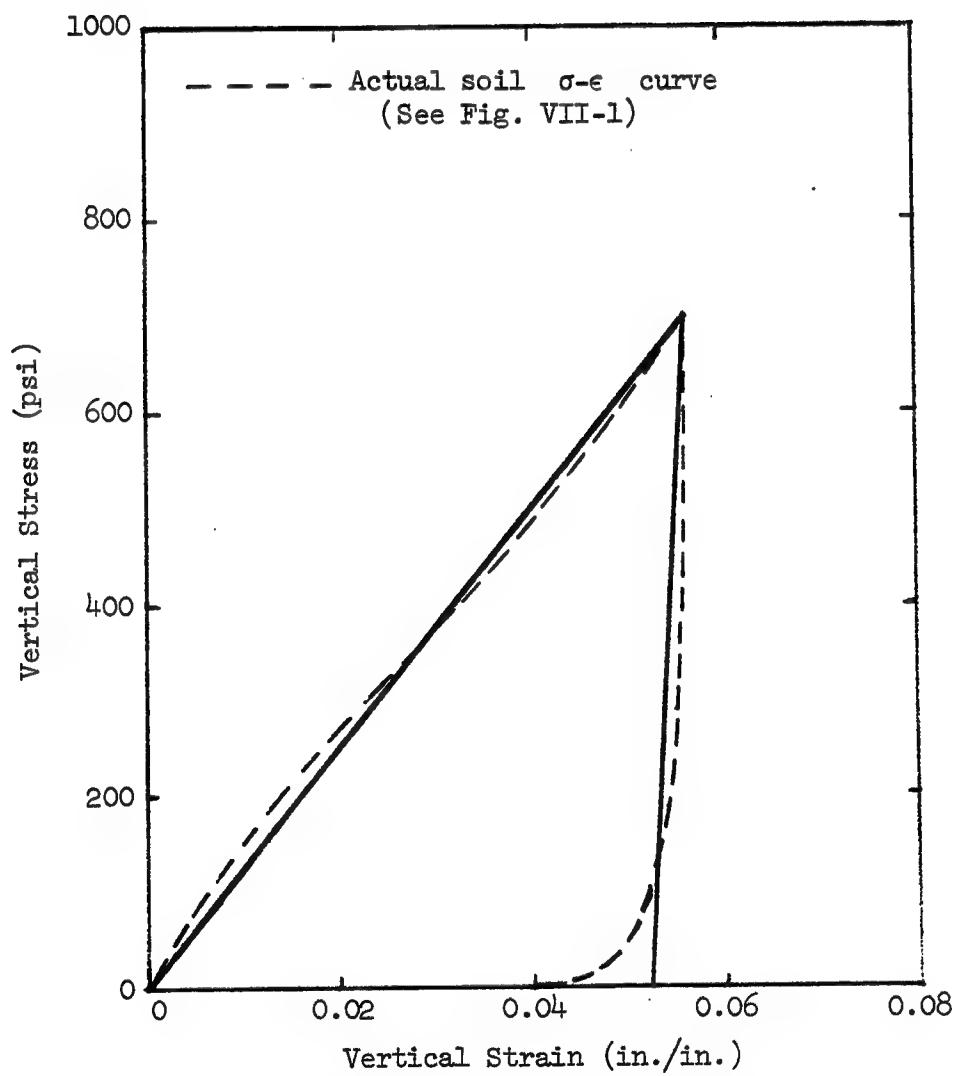
Fig. VII-5. Linear hysteretic model fit.

167
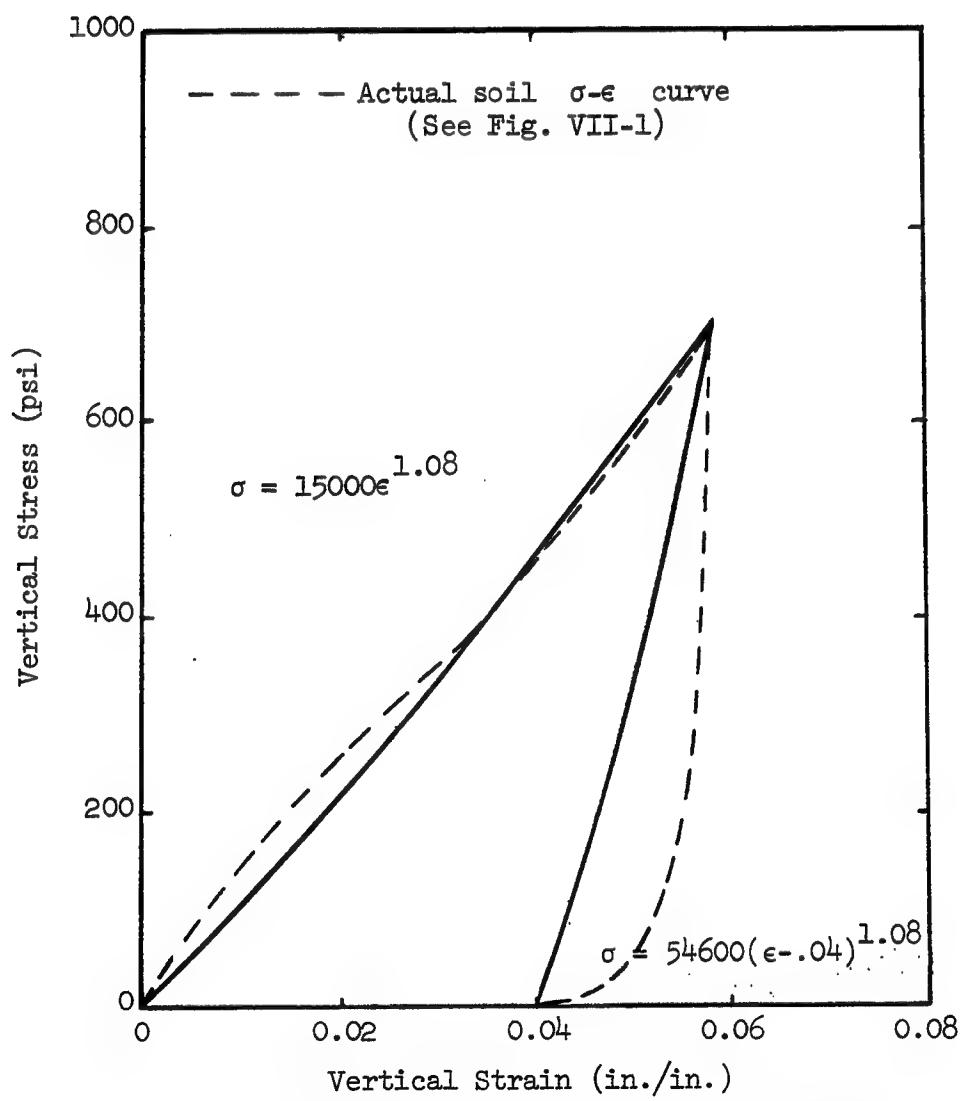
Fig. VII-6. Nonlinear hysteretic model fit.

velocity-time histories at various depths are shown in figs. VII-12 and VII-13 for the piecewise-linear model.

D. Discussion of results

    The attenuations of peak vertical stress and particle velocity with depth (figs. VII-7 and VII-8, respectively) for the various models clearly indicate that the attenuation rates are related to the hysteretic energy loss potential (area under the stress-strain curve) as well as the details of the stress-strain curve associated with each model. The piecewise-linear model (fig. VII-3) provides the highest attenuation rate of peak vertical stress and particle velocity with depth. This is partly due to the fact that the plastic behavior included in this model at the lower stress levels causes a spreading and a slowing of the wave front (i.e., an increase in rise-time and a decrease in wave velocity) as the wave propagates down the soil column (see figs. VII-10 through VII-13), and partly because the piecewise-linear model incorporates a high hysteretic energy loss potential. The spreading and slowing of the front is unique to this model; in effect, these phenomena allow unloading waves to have more influence, i.e. cause more attenuation, at a given depth. The other models all produce shocks. A shock will develop if the entire loading stress-strain relation is of the form

$$\frac{d^2\sigma}{d\epsilon^2} \geq o$$

(which is the case for the nonlinear locking and the linear and nonlinear hysteretic models).

    The nonlinear hysteretic model (fig. VII-6), having the least amount

169
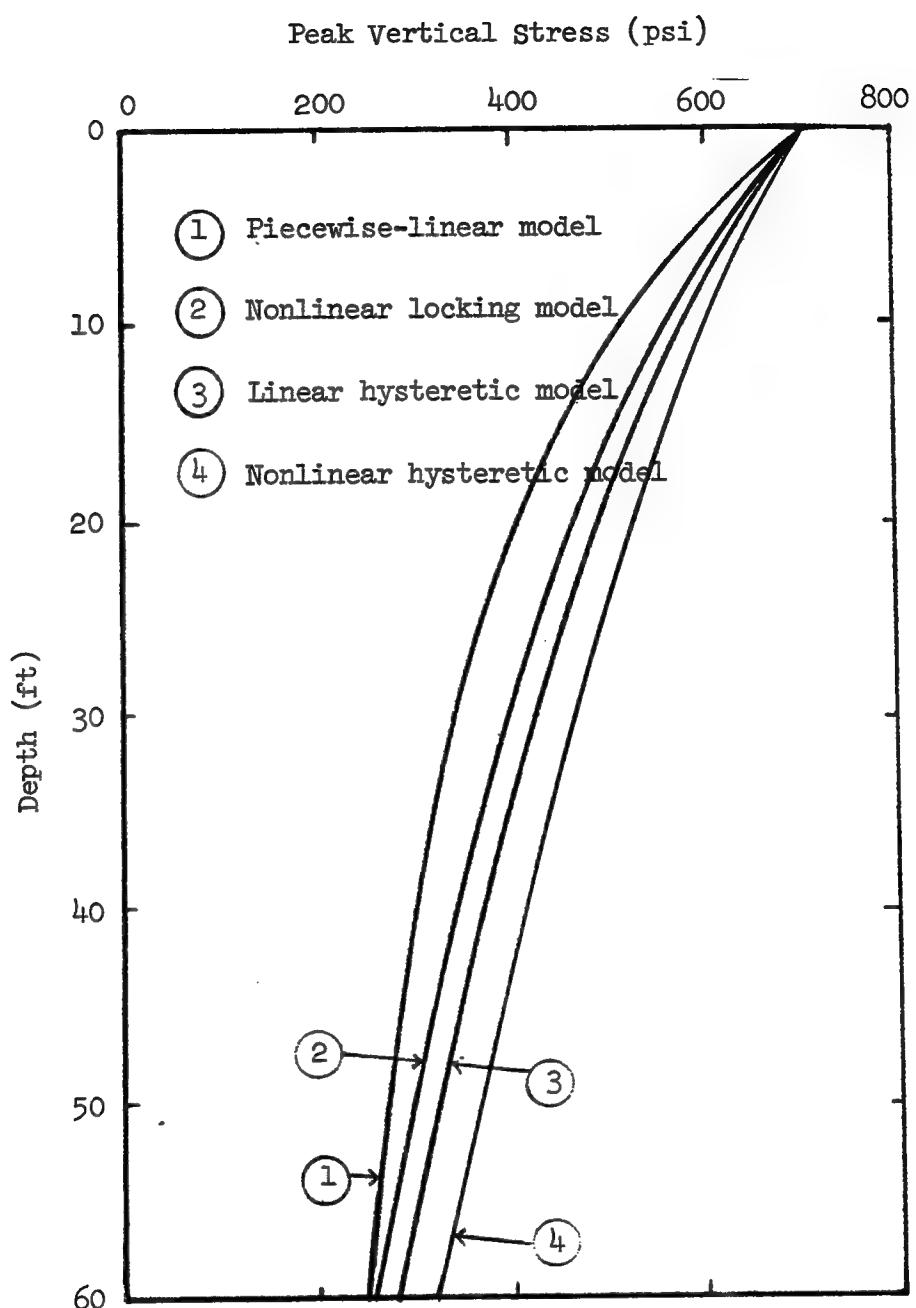
Fig. VII-7. Attenuation of peak vertical stress
with depth; various models.

170

Peak Vertical Particle Velocity (fps)
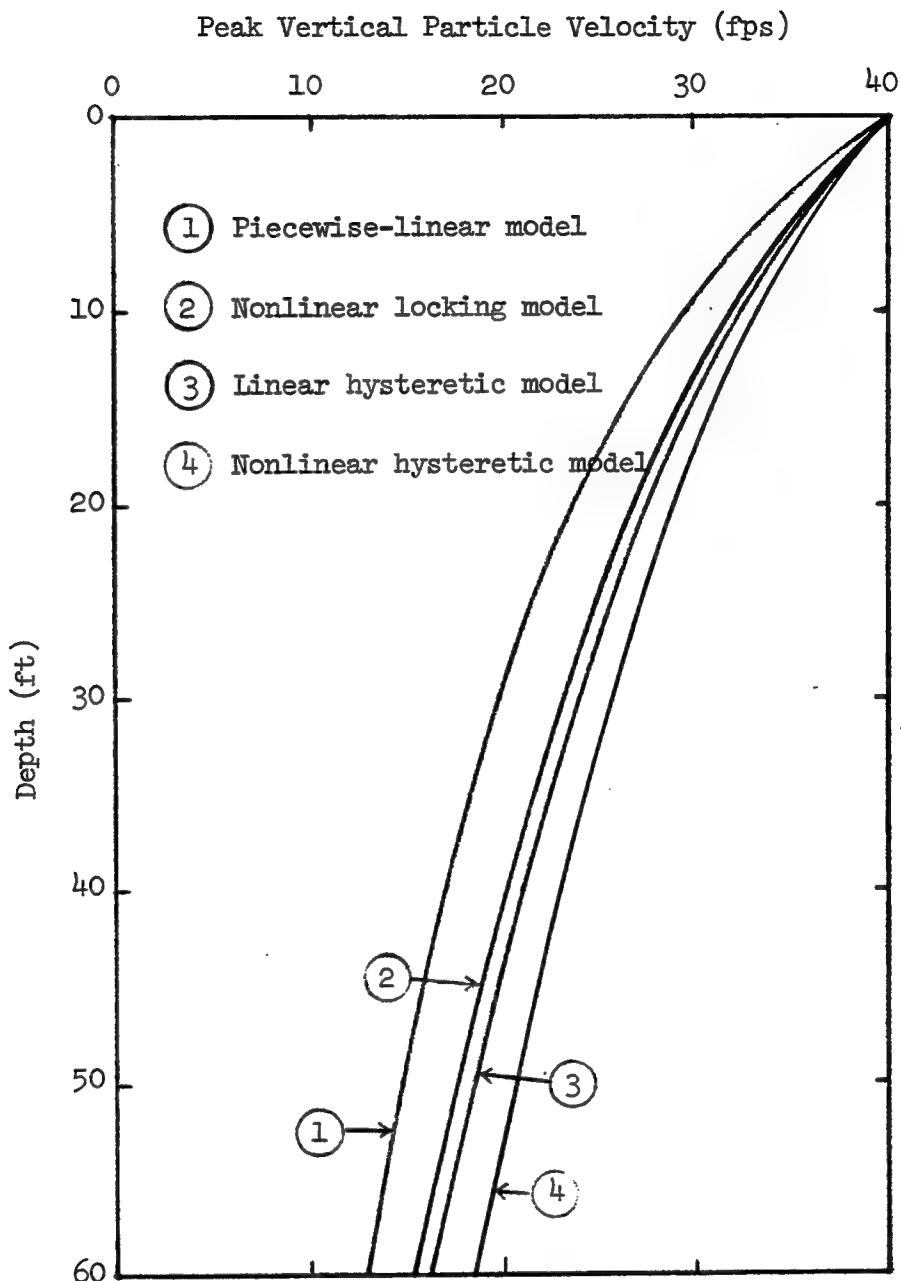
Fig. VII-8. Attenuation of peak vertical
particle velocity with depth; various
models.

171

of hysteretic energy loss potential, results in the lowest attenuation rates. The linear hysteretic (fig. VII-5) and the nonlinear locking (fig. VII-4) models, having practically the same hysteretic energy loss potentials, result in similar attenuation rates of the peak stress and particle velocity.

E. Other ground motion parameters

An interesting parameter associated with wave propagation (not explicitly studied herein), as far as the details of the stress-strain curve are concerned, is particle acceleration. For a shock-fronted overpressure pulse (fig. VII-2) the stress and particle velocity wave forms will retain a shock front if the loading stress-strain properties of the material are of the form $d^2\sigma/d\epsilon^2 \geq 0$, as was discussed in Chapter II. This "jump" discontinuity at the wave front results in an infinite value of particle acceleration. Therefore, for the nonlinear locking, nonlinear hysteretic and linear hysteretic models, the peak acceleration will be infinite at all depths. However, the piecewise-linear model cannot sustain a purely shock-fronted particle velocity or stress wave form due to the inclusion of the plastic behavior of the loading stress-strain curve at the lower stress levels (see Chapter II). This is clearly demonstrated in figs. VII-10 through VII-13 where the rise times of the stress and particle velocity wave forms can be seen to continuously increase with depth. This results in finite acceleration values and a large attenuation rate for peak acceleration. Unfortunately, accelerations obtained from finite difference solutions have only qualitative value (28); hence no computed accelerations are presented here.

172
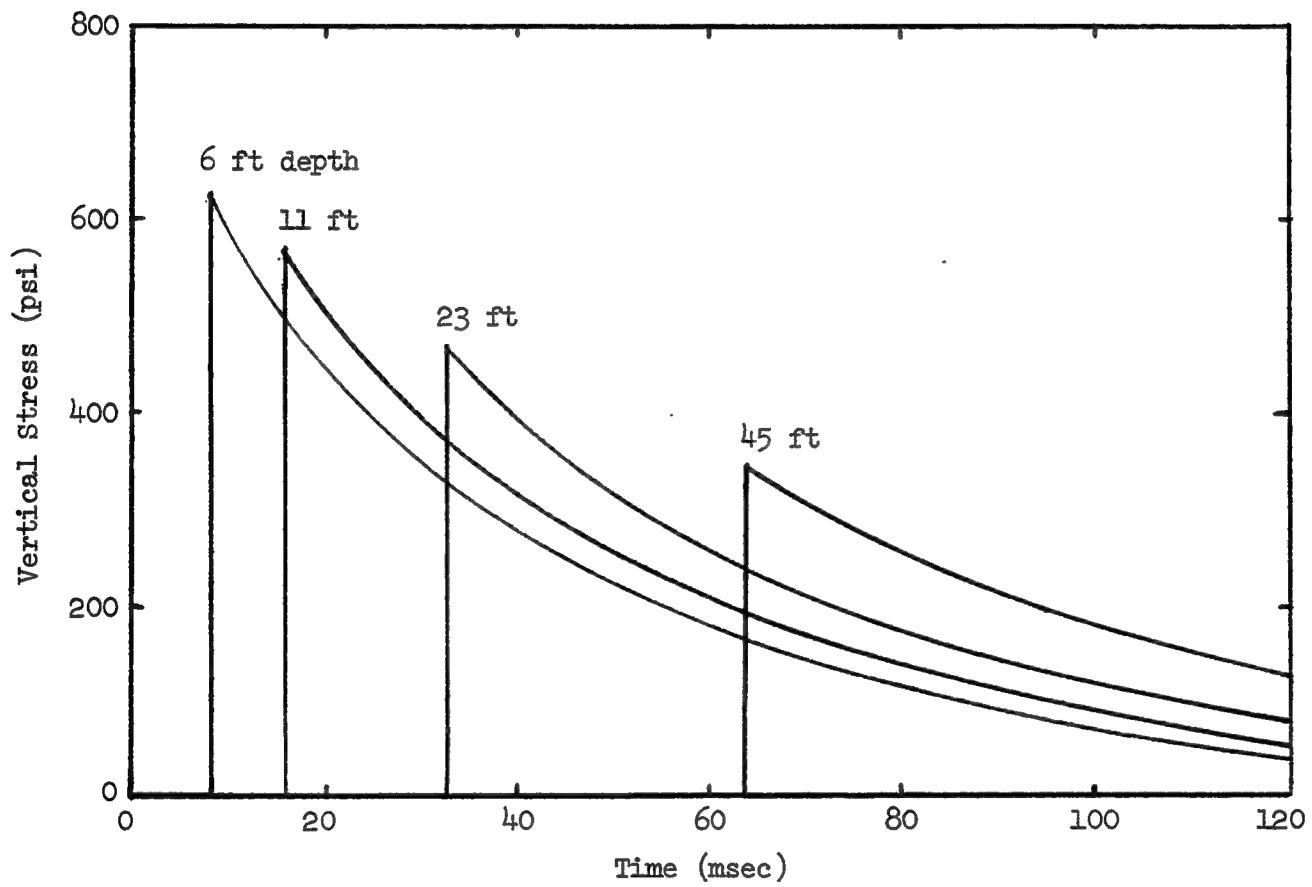
Fig. VII-9. Typical stress-time histories for several depths; linear hysteretic model.

173
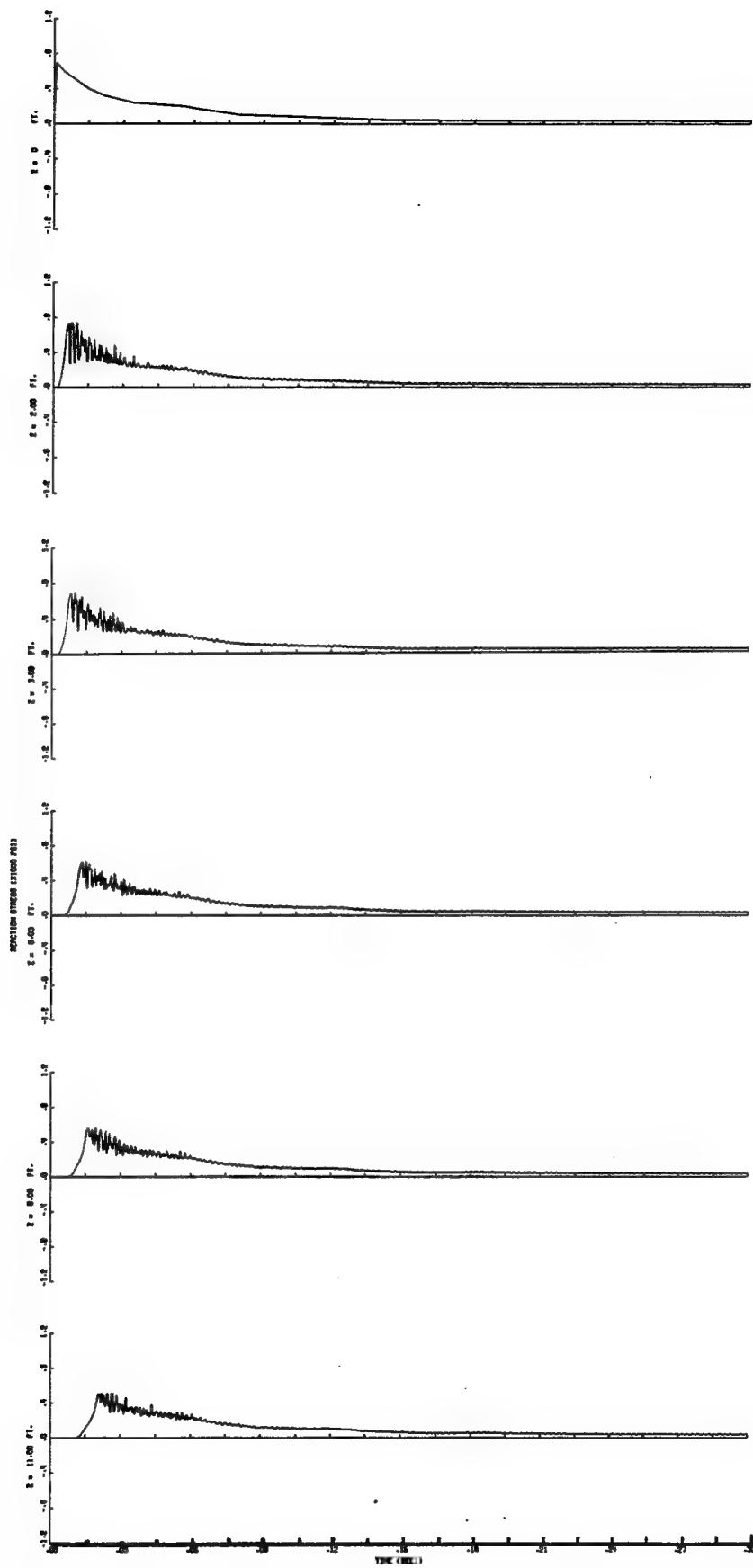
Fig. VII-10.   Typical stress-time histories for several
depths; piecewise-linear model.
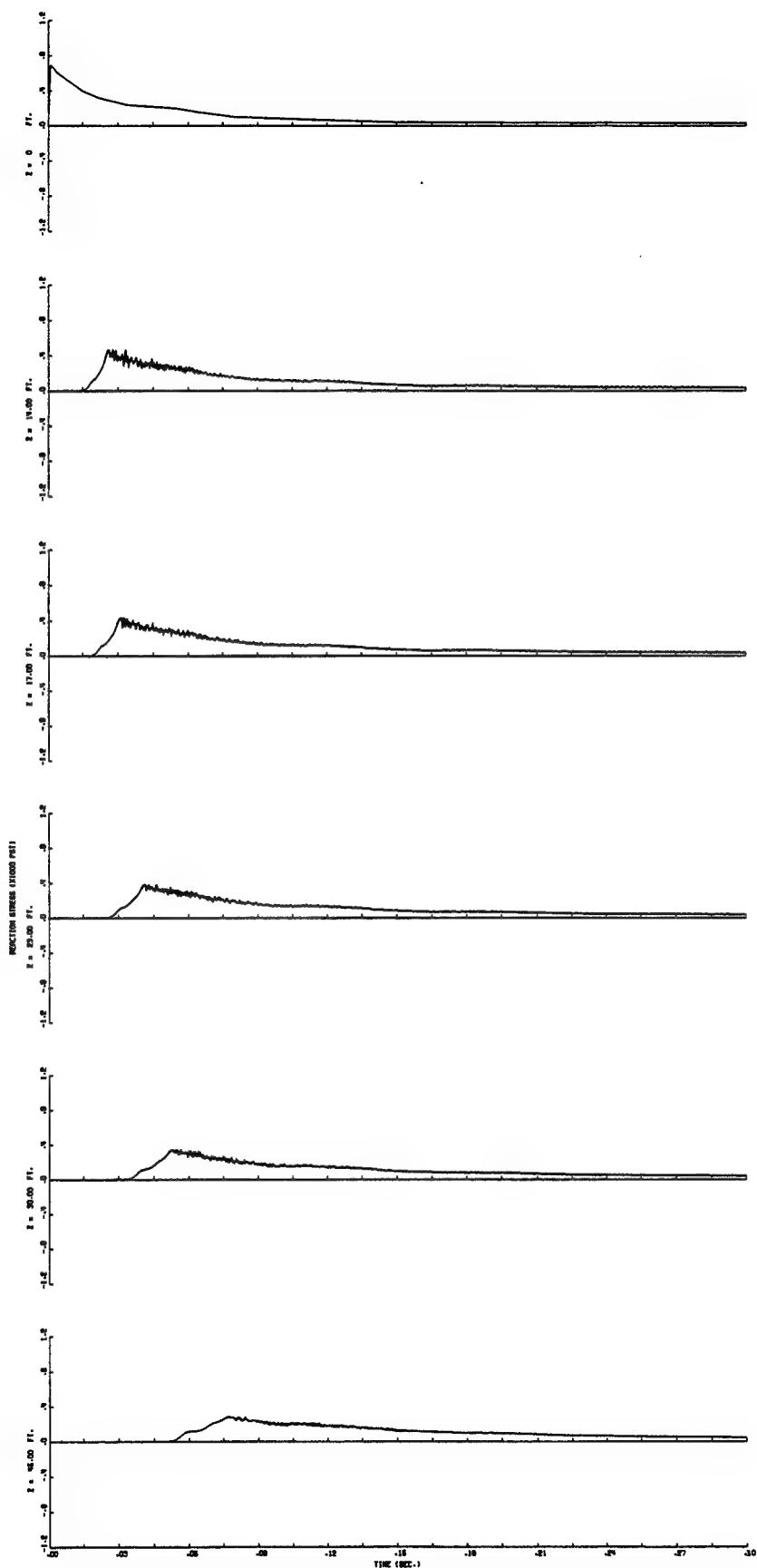
Fig. VII-11. Typical stress-time histories for
several depths; piecewise-linear model.
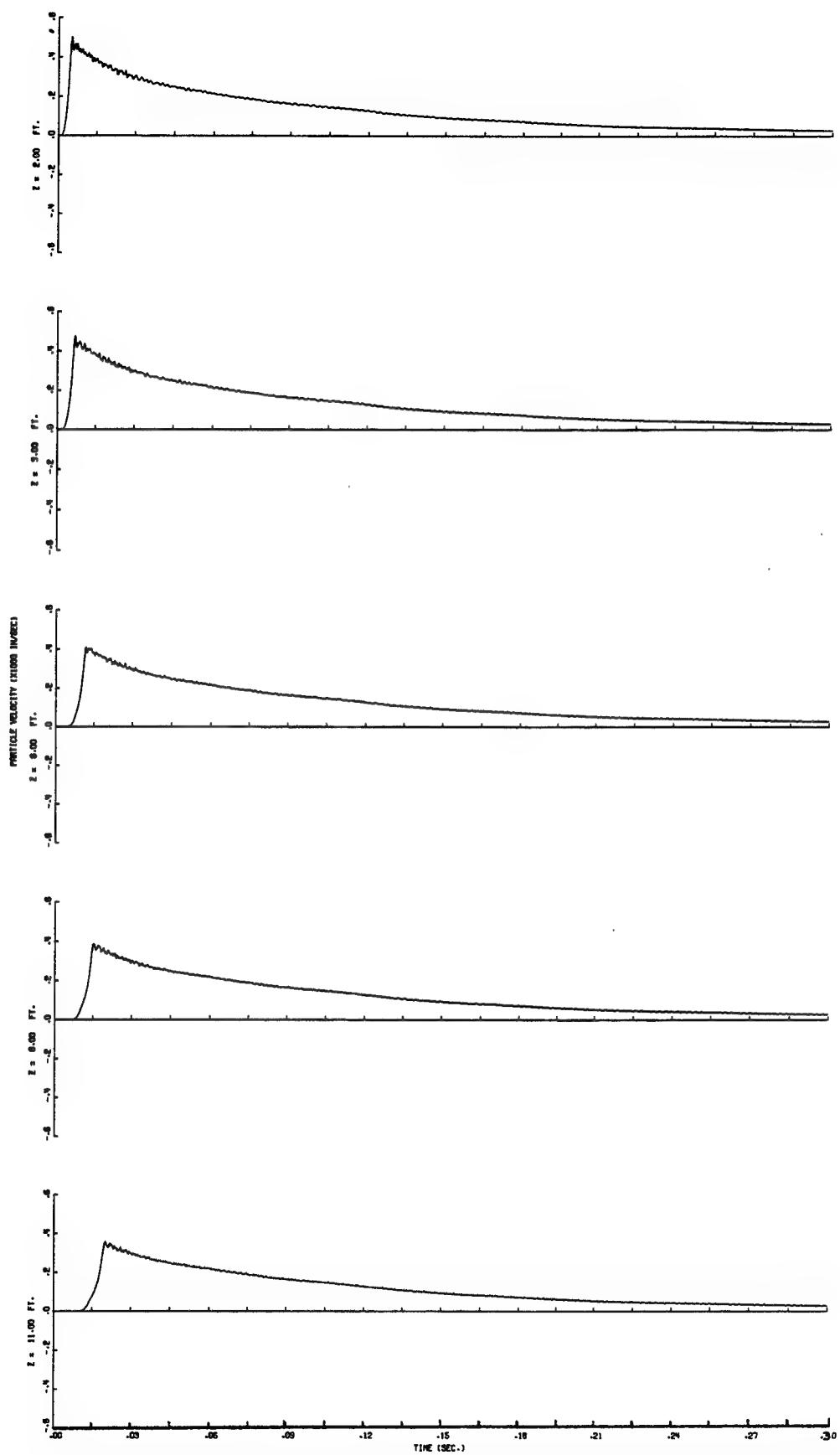
Fig. VII-12.   Typical particle velocity-time histories for
several depths; piecewise-linear model.

176
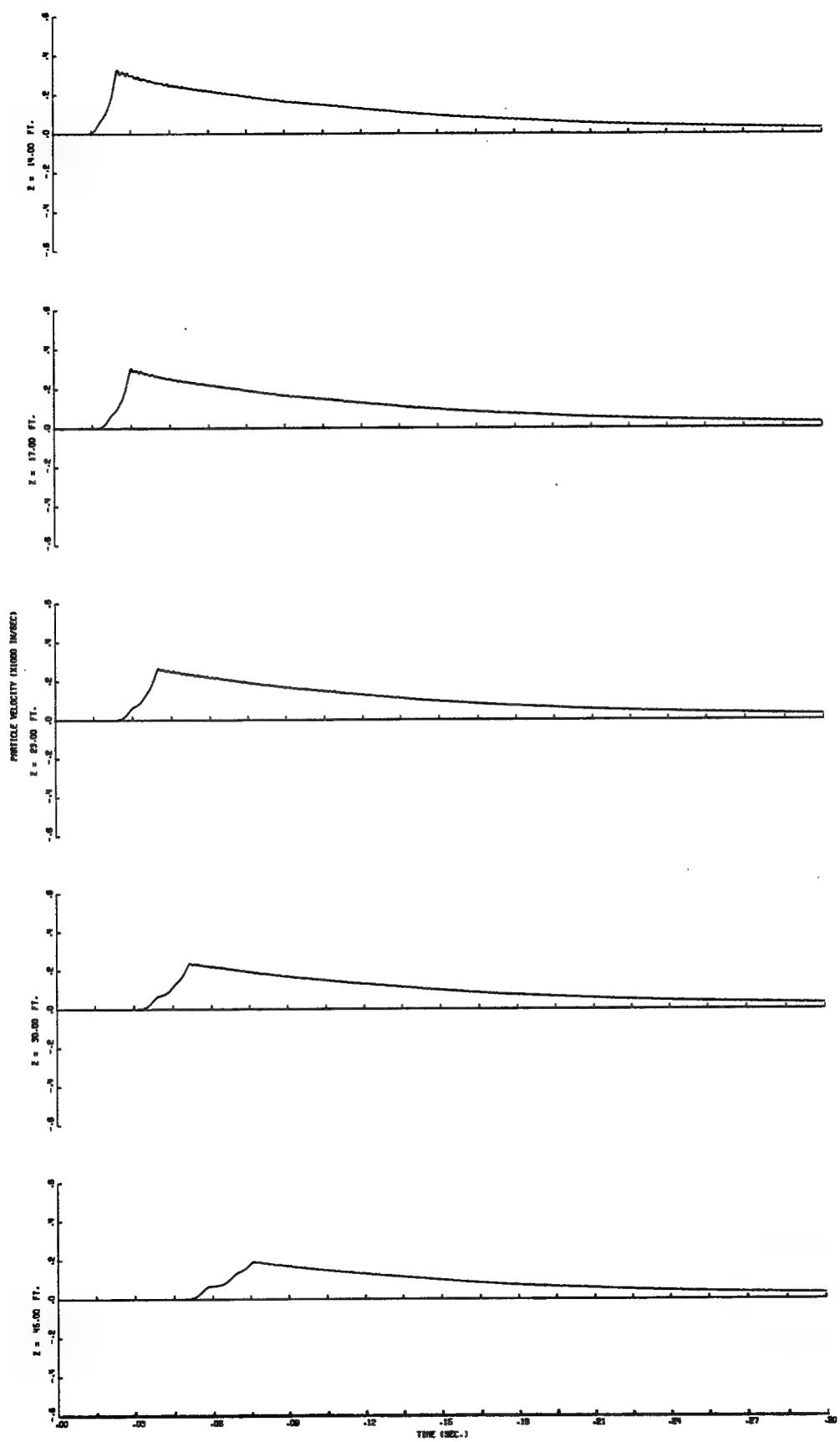
Fig. VII-13. Typical particle velocity-time histories for several depths; piecewise-linear model.

Particle displacements are not discussed herein either because the computer codes presented in Chapters III, V and VI do not calculate displacements.

F. Conclusions

Figs. VII-7 and VII-8 clearly indicate that computed wave propagation results are sensitive to the stress-strain model chosen to represent actual laboratory data. However, the variations in results exhibited by the models considered for this study are not highly significant; in fact, the "scatter" of these attenuation curves is of the same order of magnitude one would expect to see in data retrieved from actual laboratory one-dimensional wave propagation tests (29).

REFERENCES

1. Whitman, R. V., "The Behavior of Soils Under Transient Loading," _Proceedings, Fourth International Conference on Soil Mechanics and Foundation Engineering,_ Butterworths Scientific Publications, London, 1957.

2. Parkin, B. R., "Impact Wave Propagation in Columns of Sand," Research Memorandum RM-2486, Nov 1959, The Rand Corp., Santa Monica, Calif.

3. "Impact Waves in Sand, A Symposium," _Transactions, American Society of Civil Engineers,_ Vol 127, Part I, 1962.

4. Rayleigh, J. W. S., _Theory of Sound,_ Vols 1 and 2, Dover Publications, New York, 1945.

5. Kolsky, H., _Stress Waves in Solids,_ Clarendon Press, Oxford, 1953.

6. Pochhammer, L., "Uber Fortpflanzungsgeschwindigkeiten kleiner Schwingungen in einem unbegrenzten isotropen Kreiszylinder, _Journal für die reine und angewandte Mathematik,_ Vol 81, 1876, p 324.

7. Morrison, J. A., "Wave Propagation in Rods of Voigt Material and Visco-elastic Materials with Three-Parameter Models," _Quarterly of Applied Mathematics,_ Vol 14, July 1956.

8. Donnell, L. H., "Longitudinal Wave Transmission and Impact," _Transactions, American Society of Mechanical Engineers,_ Vol 52 (1), 1930.

9. Von Karman, T. and Duwez, P. E., "The Propagation of Plastic Deformation in Solids," _Journal of Applied Physics,_ Vol 21, Part 2, No. 10, Oct 1950.

10. Tayler, G. I., "The Plastic Wave in a Wire Extended by an Impact Load," British Official Report RL 329, 1942.

11. Rakhmatoolin, K. A., _Appl. Math. Mech.,_ Leningr., 9, 91, 1945.

12. White, M. P. and Griffis, Le Van, "The Permanent Strain in a Uniform Bar Due to Longitudinal Impact," _Journal of Applied Mechanics,_ Vol 14, Dec 1947.

13. Malvern, L. E., "The Propagation of Longitudinal Waves of Plastic Deformation in a Bar of Material Exhibiting a Strain-Rate Effect," _Journal of Applied Mechanics,_ Vol 18, June 1951.

14. Bland, D. R., _The Theory of Linear Viscoelasticity,_ Pergamon Press, London, 1960.

15. Churchill, R. V., _Complex Variables and Applications,_ 2d ed., McGraw-Hill, New York, 1960.

16. Salvadori, M. G., Skalak, R., and Weidlinger, P., "Waves and Shocks in Locking and Dissipative Media," _Transactions, American Society of Civil Engineers,_ Vol 126, Part I, 1961, p 305.

17. Seaman, L., "One-Dimensional Stress Wave Propagation in Soils," Project PHU-5184, Final Report, DASA 1757, Feb 1966, Stanford Research Institute, Menlo Park, Calif.

18. Seaman, L. and Whitman, R. V., "Stress Propagation in Soils," Project PHU-2917, Final Report, Part IV, DASA 1266-4, June 1964, Stanford Research Institute, Menlo Park, Calif.

19. Kondner, R. L. and Krizek, R. J., "A Rheological Investigation of the Dynamic Response Spectra of Soils; Report 2, A Response Spectra Formulation for a Cohesive Soil," Aug 1963, Technological Institute of Northwestern University; prepared for U. S. Army Engineer Waterways Experiment Station, CE, Vicksburg, Miss.

20. Whitman, R. V., "The Response of Soils to Dynamic Loading; Stress-Strain-Time Behavior of Soil in One-Dimensional Compression," Report No. R63-25, Report 17, May 1963, Department of Civil Engineering, Massachusetts Institute of Technology; prepared for U. S. Army Engineer Waterways Experiment Station, CE, Vicksburg, Miss.

21. Weidlinger, P. and Matthews, A. T., "Shock and Reflection in a Nonlinear Medium," Proceedings, American Society of Civil Engineers, Paper No. 4375 (EM-3), 1.147, June 1965.

22. Ford, L. R., Differential Equations, 2d ed., McGraw-Hill, New York 1955.

23. Zaccor, J. V., "Procedures for Prediction of Ground Shock Phenomena Based on One-Dimensional Shock Propagation Considerations, Report 1, Procedures and Applications," Contract Report No. 3-171 prepared by URS Corporation, Burlingame, California, under Contract No. DA-22-079-eng-488, U. S. Army Engineer Waterways Experiment Station, Vicksburg, Miss., April 1967.

24. Jackson, J. G., Jr., and Windham, J. E., "Soil Property Investigation for HEST Test V," Technical Report S-68-1, May 1968, U. S. Army Engineer Waterways Experiment Station, Vicksburg, Mississippi.

25. Hendron, A. J., "The Behavior of Sand in One-Dimensional Compression," Ph. D. Thesis, Department of Civil Engineering, University of Illinois, Urbana, 1963.

26. Heierly, W., "Inelastic Wave Propagation in Soil Columns," Proceedings, American Society of Civil Engineers, Paper No. 3347 (SM-6), December 1962.

27. Seaman, L., "Computer Programs for Wave Propagation Calculations," Stanford Research Institute, SRI Project 6311, Final Report, WES BP-67-1419, December 1966.

28. Zelasko, J. S. and Rohani, B., "Ground Motion Calculations and Predictions for HEST Test V," Technical Report S-68-5, July 1968, U. S. Army Engineer Waterways Experiment Station, Vicksburg, Mississippi (SECRET).

29. Zaccor, J. V., Walter, D. F., and Davis, V. W., "Procedures for Prediction of Ground Shock Phenomena Based on One-Dimensional Shock Propagation Considerations, Report 2, Experimental Study of Loading-Unloading Stress Wave Interactions in a Soil Shock Tube," Contract Report No. 3-171 prepared by URS Corporation, Burlingame, California, under Contract No. DA-22-079-eng-488, U. S. Army Engineer Waterways Experiment Station, Vicksburg, Miss., April 1967.

DISTRIBUTION LIST

DEPARTMENT OF DEFENSE

Director
Defense Threat Reduction Agency
ATTN: SWET (Dr. L. A. Wittwer)
          SWET (Mr. M. E. Giltrud)
          SWET (Maj C. A. Rutland)
          Technical Library
6801 Telegraph Road
Alexandria, VA 22310-3398

Commander
Field Command, Defense Threat Reduction Agency
ATTN: FCTT (Dr. G. Y. Baladi)
          FCTT (Dr. E. L. Tremba)
          FCT-Q (Dr. E. J. Rinehart)
1680 Texas St., SE
Kirtland AFB, NM 87117-5669

Director
Advanced Research Project Agency
ATTN: Library
3701 N. Fairfax Drive
Arlington, VA 22203-1714

Director
Defense Intelligence Agency
ATTN: Unclassified Library
Washington, DC 20340

Defense Technical Information Center
ATTN: TC (2 cys)
Cameron Station
Alexandria, VA 22314

DEPARTMENT OF THE ARMY

Commander
US Army Corps of Engineers
ATTN: CERD-ZA (Dr. L. E. Link)
          CERD-M (Dr. D. J. Leverenz)
          CERD-M (Mr. J. R. Lundien)
          CEMP-ET (Mr. Mohan Singh)
          CEMP-ET (Mr. Ray Navidi)
          CEIM-SL (2 cys)
Washington, DC 20314-1000

Commander
US Army Engineer Division, Huntsville
ATTN: CEHND-SR
P.O. Box 1600
Huntsville, AL 35807-4301

DEPARTMENT OF THE ARMY (CONTINUED)

Commander & Director
US Army Construction Engineering Research
  Laboratories
ATTN: Technical Library
P.O. Box 9005
Champaign, IL 61826-9005

Commander
US Army Engineer District, Omaha
ATTN: CENWO-ED-SH (Mr. Bruce Walton)
          CENWO-ED-SH (Mr. Tim Knight)
215 North 17th Street
Omaha, NE 68102-4978

Director
US Army Cold Regions Research and
  Engineering Laboratory
ATTN: Technical Library
72 Lyme Road
Hanover, NH 03755-1290

Commander
US Army Engineer School
ATTN: Technical Library
Fort Leonard Wood, MO 65473-5000

Commander
US Army Research Laboratory
ATTN: Technical Library
2800 Powder Mill Road
Adelphi, MD 20783-1145

Director
US Army Research Laboratory
ATTN: Technical Library
Aberdeen Proving Ground, MD 21005-5066

Commander
US Army Nuclear and Chemical Agency
ATTN: Technical Library
7500 Backlick Road, Bldg. 2073
Springfield, VA 22150

DEPARTMENT OF THE NAVY

Naval Facilities Engineering Service Center
ATTN: Technical Library
          Code 62 (Mr. R. J. Odello)
560 Center Drive
Port Hueneme, CA 93043-4328

DEPARTMENT OF THE NAVY (CONTINUED)

Naval Facilities Engineering Command
ATTN: Code 03T (Mr. M. E. Essoglou)
      Technical Library
200 Stovall Street
Alexandria, VA 22332-2300

Commander
Naval Air Warfare Center
Weapons Division
ATTN: Mr. Rex Randolf, Code 3517
China Lake, CA 93555

DEPARTMENT OF THE AIR FORCE

Air Force Institute of Technology
Air University
ATTN: Technical Library
Wright-Patterson AFB, OH 45433

Air Force Office of Scientific Research
Technical Library
Bolling AFB, DC 20332

Phillips Laboratory
ATTN: Technical Library
Kirtland AFB, NM 87117-6008

Air Force Research Laboratory
ATTN: MNQC (Mr. Dick Vickers)
      Technical Library
139 Barnes Drive, Suite 1
Tyndall AFB, FL 32403-5323

Air Force Research Laboratory
ATTN: MNAC (Mr. Dan Brubaker)
      Technical Library
101 W. Eglin Blvd., Suite 338
Eglin AFB, FL 32542-6810

DEPARTMENT OF ENERGY

Lawrence Livermore National Laboratory
ATTN: L-53 (Technical Library)
P.O. Box 808
Livermore, CA 94550-0622

Los Alamos National Laboratory
ATTN: M/S P364 (Report Library)
P.O. Box 1663
Los Alamos, NM 87545

Sandia National Laboratories
ATTN: Dept 7141 (Technical Library)
P.O. Box 5800, M/S 0899
Albuquerque, NM 87185-M/S 0899

DEPARTMENT OF DEFENSE CONTRACTORS

Dr. C. J. Higgins
Applied Research Associates, Inc.
4300 San Mateo Blvd., NE, Suite A220
Albuquerque, NM 87110

Mr. S. E. Blouin
Applied Research Associates, Inc.
Box 120A, Waterman Road
South Royalton, VT 05068

Mr. J. L. Drake
Mr. R. E. Walker
Applied Research Associates, Inc.
112 Monument Place
Vicksburg, MS 39180

Dr. John E. Higgins
Logicon, RDA
2600 Yale Blvd., SE
Albuquerque, NM 87119-9227

Mr. Ed Humphries
Science Applications International Corp.
6940 South Kings Highway
Alexandria, VA 22310

Dr. J. G. Jackson, Jr.
Logicon RDA
5024 Nailor Road
Vicksburg, MS 39180

Dr. Y. Marvin Ito
Mr. H. D. Zimmerman
Titan Research & Technology
9410 Topanga Canyon Blvd., Suite 104
Chatsworth, CA 91311-5771

Mr. Jim Rocco
Applied Research Associates, Inc.
P.O. Box 5388
Albuquerque, NM 87185

Mr. Howard S. Levine
Weidlinger Associates
4410 El Camino Real, Suite 110
Los Altos, CA 94022

REPORT DOCUMENTATION PAGE

Public reporting burden for this collection of information is estimated to average 1 hour per response, including the time for reviewing instructions, searching existing data sources, gathering and maintaining the data needed, and completing and reviewing the collection of information. Send comments regarding this burden estimate or any other aspect of this collection of information, including suggestions for reducing this burden, to Washington Headquarters Services, Directorate for Information Operations and Reports, 1215 Jefferson Davis Highway, Suite 1204, Arlington, VA 22202-4302, and to the Office of Management and Budget, Paperwork Reduction Project (0704-0188), Washington, DC 20503.

1. AGENCY USE ONLY (Leave blank)	2. REPORT DATE	3. REPORT TYPE AND DATES COVERED
	June 1999	Final report

4. TITLE AND SUBTITLE
Theoretical Studies of Stress Wave Propagation in Laterally Confined Soils

5. FUNDING NUMBERS

6. AUTHOR(S)
Behzad Rohani

7. PERFORMING ORGANIZATION NAME(S) AND ADDRESS(ES)
U.S. Army Engineer Waterways Experiment Station
3909 Halls Ferry Road
Vicksburg, MS 39180-6199

8. PERFORMING ORGANIZATION REPORT NUMBER
Miscellaneous Paper SL-99-1

9. SPONSORING/MONITORING AGENCY NAME(S) AND ADDRESS(ES)
Defense Threat Reduction Agency
6801 Telegraph Road
Alexandria, VA 22310-3398

10. SPONSORING/MONITORING AGENCY REPORT NUMBER

11. SUPPLEMENTARY NOTES
Available from National Technical Information Service, 5285 Port Royal Road, Springfield, VA 22161.

12a. DISTRIBUTION/AVAILABILITY STATEMENT
Approved for public release; distribution is unlimited.

12b. DISTRIBUTION CODE

13. ABSTRACT (Maximum 200 words)

In order to overcome the mathematical difficulties in the solution of one-dimensional stress wave propagation in soils, real soil stress-strain relationships are often idealized by various simple mathematical models. A considerable body of scientific literature on one-dimensional stress wave propagation for such models has been published in recent years by various researchers, both in the United States and abroad.

The pertinent literature applicable to one-dimensional stress wave propagation in soils are collected and studied in detail. Comparative studies are made with the various mathematical models for a wave propagation problem. Fortran computer programs for each of the analytical solutions are included as appendixes.

14. SUBJECT TERMS
Analytical solution
Ground shock
Nonlinear material response
Wave propagation

15. NUMBER OF PAGES
188

16. PRICE CODE

17. SECURITY CLASSIFICATION OF REPORT	18. SECURITY CLASSIFICATION OF THIS PAGE	19. SECURITY CLASSIFICATION OF ABSTRACT	20. LIMITATION OF ABSTRACT
UNCLASSIFIED	UNCLASSIFIED		